# THREE-PHASE FIVE LIMB TRANSFORMER RESPONSES TO GEOMAGNETICALLY INDUCED CURRENTS




THESIS BY:

TALENT TAFADZWA MURWIRA
DEPARTMENT OF ELECTRICAL ENGINEERING
UNIVERSITY OF CAPE TOWN

SUPERVISOR:
DR DAVID OYEDOKUN

Thesis submitted to the University of Cape Town in fulfilment of the academic requirements for the Master of Science degree in Electrical Engineering

# DECLARATION

I know the meaning of plagiarism and declare that all the work in the document, save for that which is properly acknowledged, is my own. This dissertation has been submitted to the Turnitin and I confirm that my supervisor has seen my report and any concerns revealed have been resolved with my supervisor.

Signature of author:

Signed by candidate

Talent Tafadzwa Murwira
Department of Electrical Engineering,
University of Cape Town,
South Africa
Date: 22 January 2021

# ABSTRACT

Geomagnetically induced currents (GIC) are quasi-DC currents that result from space weather events arising from the sun. The sun ejects hot plasma in a concept termed 'coronal mass ejections' which is directed towards the earth. This plasma interferes with the magnetic field of the magnetosphere and ionosphere, and the magnetic field is subsequently distorted. The distortions in these regions results in the variation of potential on the earth's surface and distortions in the earth's magnetic field. The potential difference between two points on the earth's surface leads to the flow of direct current (DC) of very low frequency in the range 0.001 ~ 0.1 Hz. Geomagnetically induced currents enter into the power system through grounded neutrals of power transformers. The potential effects of GIC on transformers are asymmetrical saturation, increased harmonics, noise, magnetization current, hot spot temperature rise and reactive power consumption. Transformer responses to GIC was investigated in this research focussing on a three-phase five-limb (3p5L) transformer. Practical tests and simulations were conducted on 15 kVA, 380/380 V, and 3p5L transformers. The results were extended to large power transformers in FEM using equivalent circuit parameters to show the response of grid-level transformers. A review of literature on the thresholds of GIC that can initiate damage in power transformers was also done and it was noted that small magnitudes of DC may cause saturation and harmonics to be generated in power transformers which may lead to gradual failure of power transformers conducting GIC. Two distinct methods of measuring power were used to measure reactive power consumed by the transformers under DC injection. The conventional method and the General Power Theory were used and the results show that the conventional method of measuring power underestimates reactive power consumed by transformers under the influence of DC injections. It may mislead system planners in calculating the reactive power reserves required to mitigate the effects of GIC on the power system.

# ACKNOWLEDGMENTS

First and foremost, I would like to thank the Lord Almighty for giving me the opportunity to do this Master of Science degree, without him this would have not been possible. Secondly, I would like to express my sincere gratitude to my supervisors, Dr. David Oyedokun and Prof. Komla Folly for the guidance throughout this work

A big thank you to Prof. Gaunt and Mrs. Kehinde Awodele for all your invaluable insights and experience you gladly offered at our weekly seminars. It was both your knowledge and willingness to help that gave me the energy and will power to continue.

I also thank Chris Wozniak and his team for assisting in laboratory work and all the informative suggestions and advice.

My wife Salome has been a great encouragement and comforter to me as I have worked my way steadily through this dissertation. I am deeply grateful to her.

# TABLE OF CONTENTS

# LIST OF FIGURES

# LIST OF TABLES

# LIST OF ABBREVIATIONS

| | |
|---|---|
| GIC | Geomagnetically induced currents |
| CME | Coronal mass ejection |
| FEM | Finite element method |
| GMT | Greenwich Mean Time |
| GMD | Geomagnetic disturbance |
| SAPP | Southern African power pool |
| GSU | Generator step-up |
| Var | Volt-ampere-reactive |
| 3p5L | Three phase five limb |
| SVC | Static var compensator |
| HVDC | High voltage direct current |
| UT | Universal time |
| rms | root-mean-square |
| VA | volt-ampere |
| GPT | General Power Theory |
| IEEE | Institute of Electrical and Electronic Engineers |
| IEC | International Electrotechnical Commission |
| ANSI | America National Standards Institute |
| NERC | North American Electric Reliability Cooperation |
| THD | Total harmonic distortion |
| AC | Alternating current |
| DC | Direct current |
| US | United States |
| VARIAC | Variable autotransformer |
| LV | Low voltage |
| HV | High voltage |
| e.m.f. | Electromotive force |
| CJC | Cold junction compensation |
| FEA | Finite element analysis |

| | |
|---|---|
| PDE | Partial differential equations |
| ANSYS | Analysis System |
| FDM | Finite difference method |
| BEM | Boundary element method |
| 2D | Two dimensional |
| 3D | Three dimensional |
| ETP | Electrolytic tough pitch |
| TuT | Transformer under test |
| TDD | Total demand distortion |

# CHAPTER 1: INTRODUCTION

This chapter gives a brief overview of how geomagnetic currents arise, the processes that occur from Sun to earth and how they affect the power system. The propagation of coronal mass ejections through space affects the magnetic field of the earth, giving rise to variations in potential on the Earth's surface. This potential difference results in geomagnetically induced currents (GIC) flowing and affecting transformers with grounded neutrals.

## 1.1 BACKGROUND

Geomagnetic induced currents (GIC) are quasi-DC currents with frequencies ranging from 0.001~0.1 Hz [1] that flow through the transformer neutrals into the power system network. The peak values could be as high as 200 A, lasting from several seconds to hours. The peak value ever modelled in Southern Africa is 108 A, at Alpha substation in South Africa [2]. In brief, geomagnetic induced currents are a result of solar storms. The Sun goes through 11-year solar cycles, with solar activity increasing towards the end of each cycle [3]. The last solar cycle ended in the years 2008-2009 and it was the 23$^{rd}$ solar cycle since the first recorded cycle in 1755 [4]. Although the GIC activity peaks towards the end of the cycle, they are not limited to occurring at peak times only.

The chain of events that lead to geomagnetic disturbances begins from the Sun's activities and ends when geomagnetic induced currents interfere with technological systems such as telecommunications and power systems at the Earth's surface as shown in the flux diagram in Figure 1.1.

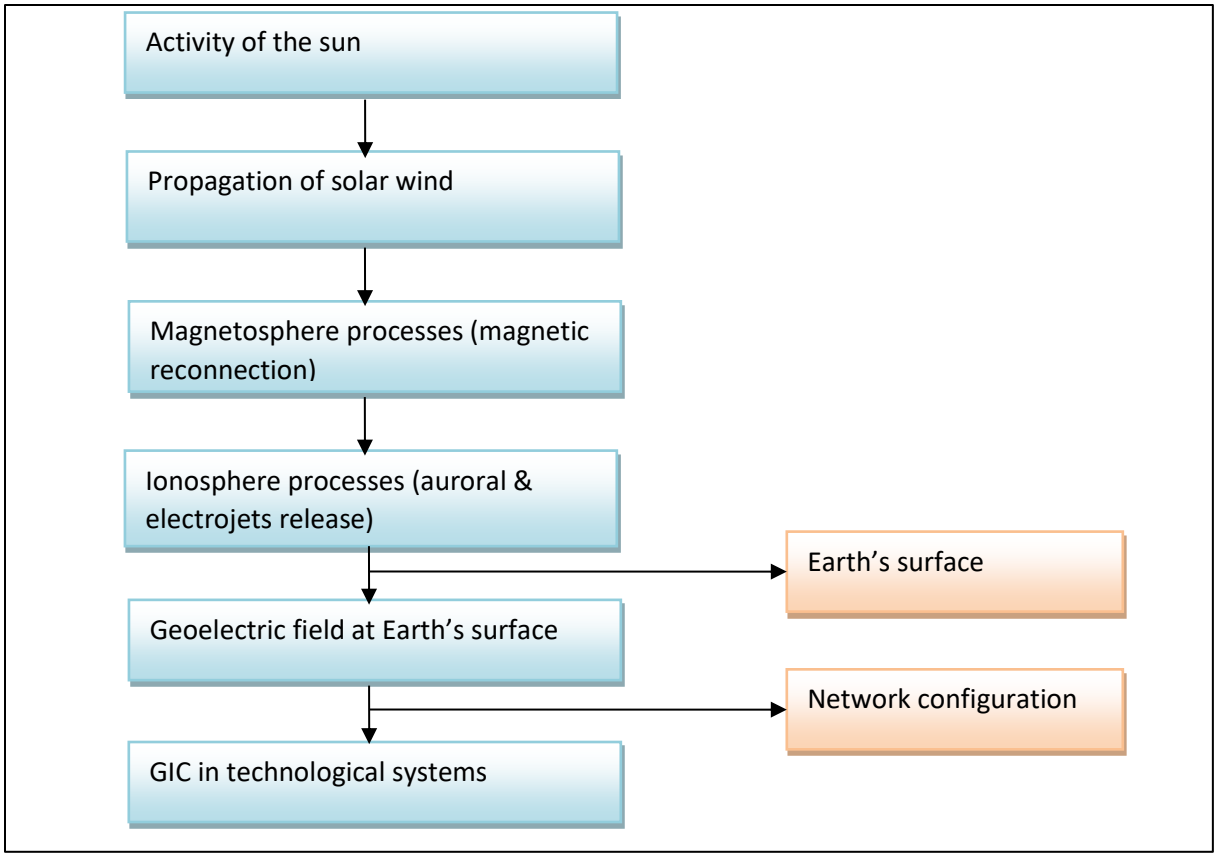


Figure 1. 1 The space flux diagram or GIC chain [3]

The hot, outer layer of the Sun is known as the corona [5]. The corona is made of hot plasma, reaching temperatures between $1x10^6$ K to $6x10^6$ K. Periodically, the Sun loses mass in the form of coronal mass ejections (CMEs). The CMEs are ejected into the space towards the earth. The occurrence of a CME is solar cycle dependent. Each directed CME hits the earth's magnetosphere and distorts its magnetic field. CMEs stretch the magnetosphere on the night-side of the earth causing it to release energy through magnetic reconnection as shown in Figure 1.2.

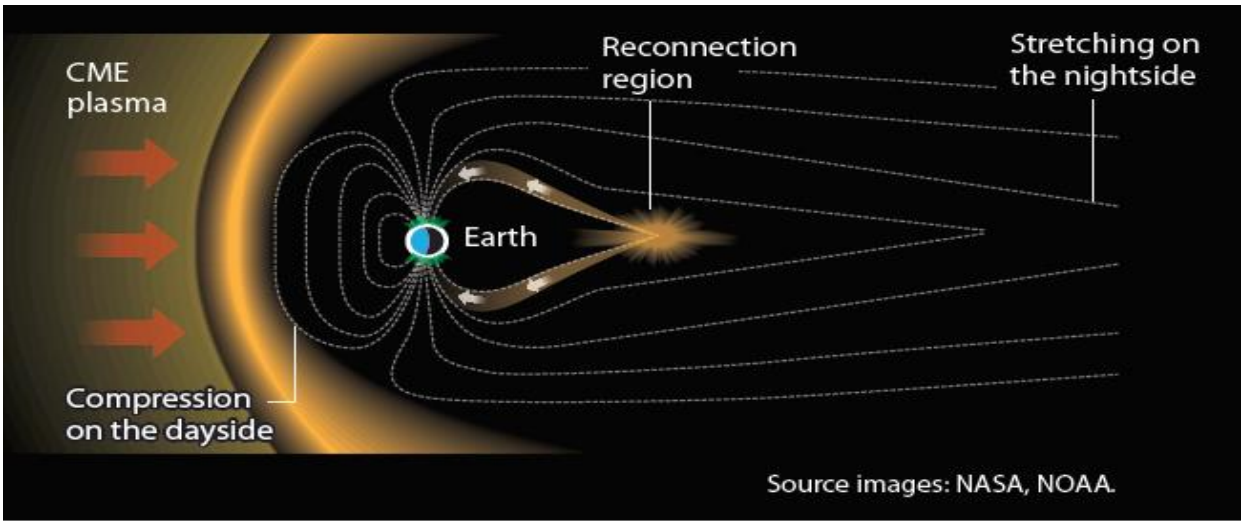


Figure 1. 2 Reconnection of the magnetosphere due to interference of coronal mass ejections (CMEs)

The perturbations in the magnetosphere have an impact on the stability of the ionosphere [6]. The dynamic changes in the magnetosphere link with the ionosphere through the ionosphere's polar regions. During the magnetosphere-ionosphere interactions, the magnetosphere's current system transfers energy to the ionospheric particles. These variations and couplings result in auroral and other electrojets in the ionosphere, which are horizontal electric currents flowing in the ionosphere [7].

The variation of the magnetosphere-ionosphere electric fields results in temporary variation of the earth's magnetic field at the earth's surface, as a result, a potential difference exists on the earth's surface. The potential difference gives rise to the flow of geomagnetic induced currents. The conductivity profile of the earth's surface determines the surface impedance which in turn determines the characteristics of the resultant geo-electric field. The magnitude of the induced electric field depends upon the rate of change of the magnetic field and the earth's conductivity. The relationship between the changing magnetic and electric fields are given by the Maxwell-Faraday equations:

$$\nabla x E = -\frac{\partial B}{\partial t} \; where \; \nabla x \; is \; the \; curl \; operator \quad (1.1)$$

$$\int_{\partial E} E.dl = -\frac{\partial}{\partial t}\iint_{\sum} B.ds \quad (1.2)$$

$$V = -\frac{\partial \lambda}{\partial t} \quad Faraday's \; Law \quad (1.3)$$

In equations 1.1, 1.2 and 1.3 E is the electric field, B is the magnetic field and V represents the electric potential difference.

Countries close to the earth's poles such as Canada, Norway, Iceland, Greenland, Finland, Sweden and Russia are more vulnerable to geomagnetic induced currents. These countries lie in the high latitude regions. The high latitude regions are more prone to GIC because the geo-electric field that gives rise to GIC is more intense. However, GIC can have impacts in low latitude regions and areas lying near the equator. The soil characteristics in a particular area can also affect the risk of a power network to GIC. The risk of geomagnetic induced currents is larger in networks located at highly resistive regions as on igneous rocks [3]. A large portion of North America has igneous rocks, and a large potential difference is induced in the local ground whenever a geomagnetic activity arises. A detailed mathematical model which confirms that a more resistive earth gives higher electric fields is given in [4].

## 1.3 OBJECTIVES

This project seeks to have an in-depth understanding of the transformer responses to geomagnetic induced currents. The work will be centred on a 3p5L core structure. In brief, the objectives of this thesis are:

- To investigate through experiments and Finite Element Method (FEM) simulations, the response of 3p5L power transformers to GIC.

- To investigate the thresholds of geomagnetic induced currents that may cause noticeable degradation to power transformers.

## 1.4 HYPOTHESIS

The study aims to prove the following hypothesis:

Tests on model transformers and extension of the results to power transformers with suitable transformer equivalent circuit and FEM simulations will improve the conventional models of the reactive power requirement in three-phase five transformers conducting GIC.

## 1.5 RESEARCH QUESTIONS

The following research questions have been set up to assess the project hypothesis:

a) How does reactive power increase in transformers saturated by the flow of GIC affect power system stability?
b) What is the role of installing GIC monitoring devices in order to fully understand the phenomenon behind the risk of quasi-DC current to transformers?
c) How does different structure of transformers affect their response to GIC?
d) What are the different levels of GIC that cause noticeable degradation in power transformers?
e) How does the reactive power consumed by a power transformer vary with respect to GIC and how important is it to evaluate reactive power correctly?
f) What is the implication of general power theory in determining reactive power absorbed by the transformer as opposed to conventional methods of calculating power?

## 1.6 DISSERTATION OVERVIEW

**Chapter 1**: This chapter is an introduction to the topic under investigation. The objectives, hypothesis and research questions are also outlined.

**Chapter 2**: This chapter provides the literature review needed to accomplish the objectives of the project and it provides literature helps in answering the research questions. An introduction to General Power Theory which forms an integral part of this research was given. Literature on ANSYS MAXWELL, a simulation software that was used in this thesis was also included.

**Chapter 3**: This chapter investigates the thresholds of GIC that initiates degradation to power transformers and brief explanations of the consequences of operating above the stipulated references.

**Chapter 4**: Provides the laboratory and simulation protocol that was used to investigate the topic and answer the research questions.

**Chapter 5**: Experimental and simulation results are presented in this chapter.

**Chapter 6**: This chapter concludes the research by providing answers to the research questions and finally concludes on the validity of the hypothesis.

# CHAPTER 2: LITERATURE REVIEW

## 2.1 INTRODUCTION

This chapter introduces details of past GIC events and the extent of damage they caused to transformers. Records of currents that flowed in transformers that were damaged by the Halloween Storm (2003) and the Hydro Quebec events are also given. In addition, a detailed explanation of the transformer electrical responses to geomagnetic induced currents, with particular reference to 3p5L transformers that form the basis of this study is reviewed.

## 2.2 HISTORICAL EVENTS

Three main events occurred since the geomagnetically induced currents were discovered. The first event being, the Carrington event (1859) discovered by the British astronomer Richard Carrington which, for the very first time in history, observed a solar flare. The second event in the history of GICs was the Hydro-Quebec event (1989). This had devastating effects on the entire Quebec power system, causing a blackout and an estimated loss amounting to $13.2 million [4]. The most recent event was the Halloween Storm (2003) that ravaged a couple of transformers in Eskom's network (South Africa), Sweden and England. This event cleared the popular belief that Africa was not prone to the geomagnetic induced currents. Severe geomagnetic disturbances leading to high GIC and chronic network disruptions are considered low probability high impact events. Such events have huge economic costs which have been studied in [8].

### 2.2.1 THE CARRINGTON EVENT (1859)

This biggest solar flare known in man's history took place on 1 September 1859 and it has been named Carrington event after the British astronomer Richard Carrington which, for the very first

time in history, observed a solar flare. On September 1, 1859, Richard Carrington observed a very intense white light flare on the surface of the sun from 11:18 to 11:23 a.m. GMT [9]. The solar flare was followed by a magnetic storm on September 1–2, 1859 at the Earth. While a Coronal mass ejection (CME) normally spends two to four days on its journey from the Sun to the Earth, it took merely 17 hours before the Earth experienced a big geomagnetic storm, probably due to a large CME. It lasted for days and the effects were many and widespread. The geomagnetic storm also caused global telegraph lines to spark, setting fire to some telegraph offices and telegraph systems all over North America and Europe went down [10].

### 2.2.2 THE HYDRO-QUEBEC EVENT (1989)

On the night of March 13, 1989 a severe geomagnetic disturbance (GMD) caused a protective relay to trip due to GIC flow. The tripped static var compensators caused a cascade of failures throughout the Quebec power grid; most notably five transmission lines from James Bay were tripped causing a loss of 9,450 MW. The total load in the grid at the time was about 21,350 MW. This led to the tripping of several protective relays, cascading failure, and resulted in the entire Quebec power grid to collapse. The whole sequence of failure events happened fast and within 75 seconds from the first capacitor tripped [11] six million people were left without power for up to nine hours during this wintry period.

## 2.3 REPORTED GIC EVENTS IN LOW LATITUDES – INCLUDING AFRICA

GIC were previously associated with areas of high latitudes and this excluded Africa in GIC studies but recent researches have proved otherwise. Results from practical measurements have shown that GIC exists in low latitudes and several transformers were damaged in South Africa and Namibia during the Halloween storm [12]. Measurements of GIC magnitudes during different geomagnetic storm phases show that values obtained in power networks located at low and middle

latitudes can reach the same levels as those observed at high latitudes. For example, [13] present GIC recordings around 15 A in a Brazilian power network during 2004, which were also recently reproduced by calculations [14]. Koen in 1999, [15] identified that the following substations are at high risk due to GIC; Alpha, Hydra, Beta, Grootvlei, Perseus, Grassridge. Figure 2.1 shows these substations and they were equipped with GIC monitoring devices on their neutrals.

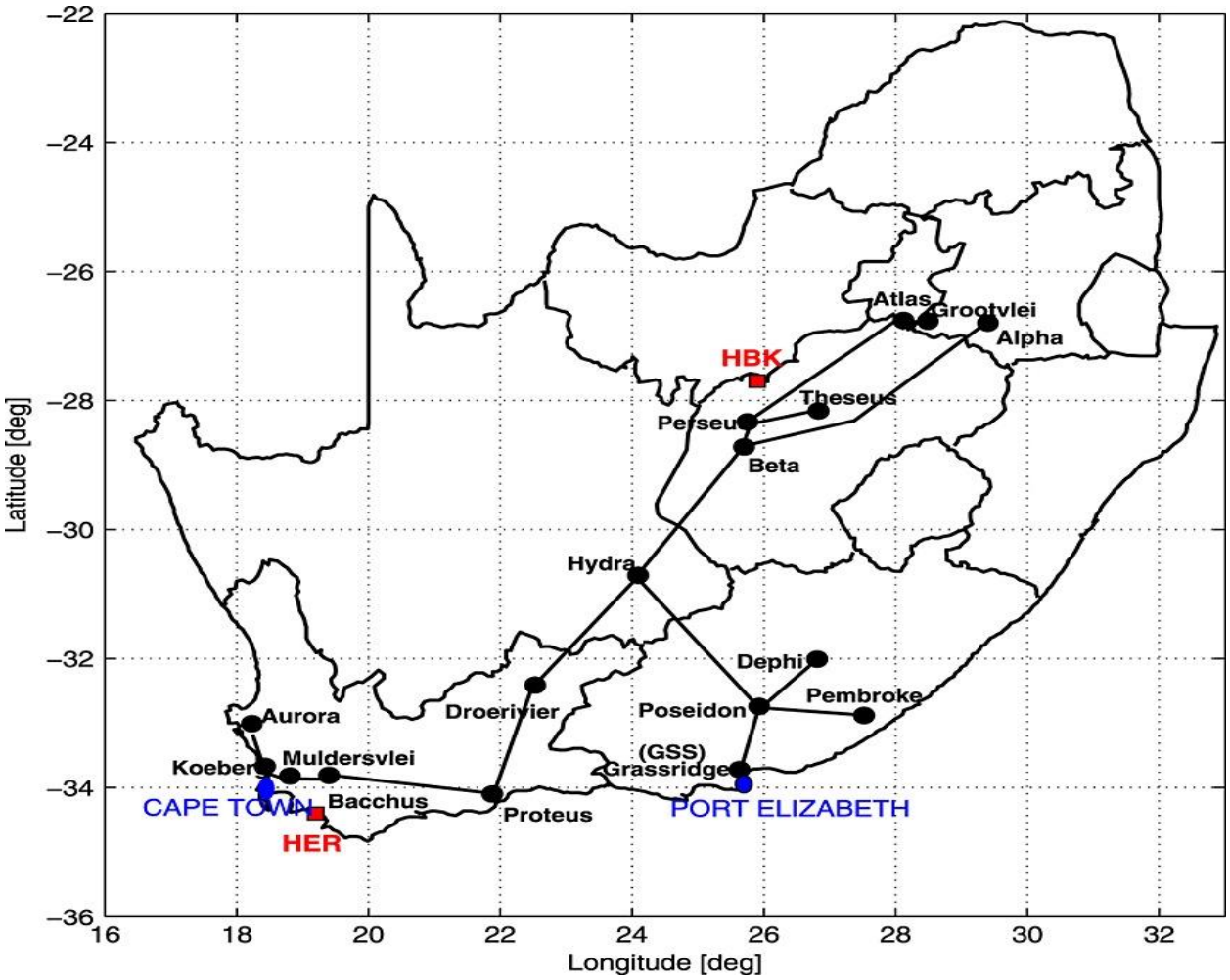


Figure 2. 1: Map showing some of the South African 400 kV substations links and the locations of the geomagnetic observatories Hermanus (HER) and Hartebeesthoek (HBK) and the Grassridge (GSS) substation that were identified as GIC prone [16]

On 31 March 2001, GIC measured on transformer neutrals at Grassridge substation reached a peak of 5 A for 1 minute. A 400/220/132 kV, 3p3L transformer at this substation saturated. Sixth harmonic current in the neutral reached a maximum of 8 A, which confirms the presence of GIC. Third-order harmonics are more dominant in GIC saturated transformers. Further evidence of GIC effects in low latitudes was obtained after the Halloween storm of 2003 that left transformers damaged in South Africa and the United Kingdom. On the 17$^{th}$ of November 2003, the transformer at Lethabo power station tripped on Buchholz protection. This showed an accumulation of gas in the Buchholz relay. There was a further severe storm on 20 November. On 23 November the Matimba #3 transformer tripped and on 19 January 2004 one of the transformers at Tutuka was taken out of service. Two more transformers at Matimba power station (#5 and #6) had to be removed from service with high levels of dissolved gases in June 2004. A second transformer at Lethabo power station tripped on Buchholz protection in November 2004. In October 2003, a generator step-up transformer (GSU) at Matimba substation failed permanently, three weeks after the Halloween storm. Ruacana power station in Namibia is one of the substations identified as GIC prone by Koen in 1999. Again, in Namibia during the Halloween storm had the same impacts as that noticed in other substations affected by GIC in South Africa. Geographically, the Ruacana substation is separated 1400km from the substations that were affected by GIC in South Africa. The substations identified to be at high risk by Koen are in the Southern African Power Pool (SAPP) and are interconnected with Ruacana. This means that they are in the same synchronous network and the effects of GIC may have the same effect on both networks. On 11 December 2003, the protection tripped a two-year old 90 MVA 330 kV GSU at Nampower's Ruacana power station in northern Namibia. One HV winding of this GSU failed permanently and the mode of failure was similar to that of transformers in South African grid.

The Halloween storm had the same impacts in the United Kingdom that sit on the same latitude as South Africa. On 20th October, 1989, the transformer neutral current varied from +5 A to -2 A at Norwich Main in East Anglia, Pembroke in Wales and Indian Queens in Cornwall for ten minutes. Two identical 400/132 kV, 240 MVA transformers at Norwich Main and Indian Queens failed, the voltage dips on the 400 kV and 275 kV systems were up to 5% and very high levels of even harmonic currents were experienced due to transformer saturation by the geomagnetic storms [17].

Literature has shown that not only transformers are at high risk of GIC. Static var compensators, insulators, surge arrestors and transformers were reported to have failed in the Hydro Quebec event [9]. Well documented reports of transformer failures in South Africa have shown that a greater number of reactors also failed due to GIC exposure [18]. Table 2.1 shows the transformers and reactors were affected by very severe storms during the period 1989 to 1994:

Table 2. 1: Transformers and reactors that failed in South Africa (1989-1994) [18]

| Date | Name | Description |
|---|---|---|
| 15 March 1989 | Poseidon-Neptune reactor | Permanent fault: inter-winding fault |
| 28 July 1990 | Beta reactor 4 | Internal fault: reactor removed on 08/09/90 |
| 24 March 1991 | No incident recorded | |
| 25 March 1991 | No incident recorded | |
| 26 March 1991 | Hydra transformer 21 | Permanent fault: reason unknown |
| 18 April 1991 | Beta reactor 4 | Neutral earthing reactor faulted |
| 18 April 1991 | Beta reactor 2 | Internal fault |
| 19 June 1991 | Hydra reactor 2 | Permanent fault, the reactor was removed |
| 14 August 1991 | Beta reactor 4 | Neutral earthing reactor faulted and was disconnected |
| 19 August 1991 | Hydra transformer 21 | Permanent fault: transformer removed |
| 25 May 1992 | Hydra transformer 3 | Transformer tripped on buchholz protection |
| 06 May 1993 | Hydra reactor 1 | Internal fault |
| 14 Dec 1993 | Beta Alpha reactor 2 | Red phase winding fault |
| 21 March 1994 | Hydra Poseidon reactor 1 | Reactor faulty and replaced |

Koen and Gaunt [19] reported reactor failures and elevated levels of dissolved gas closely associated with exposure to geomagnetic storms. A reactor at Poseidon-Neptune substation failed,

following the two days of severe geomagnetic activity on 15 March 1989. Shunt reactors are similar in many respects to power transformers, except that they generally have gapped cores. Laboratory tests at the University of Cape Town show that direct current can flow in model three-limb three-phase reactors with small gaps. The response of a reactor to GIC could be similar to the response of a three-limb transformer, with the core gap of a reactor having a similar effect to the core-tank gap of the transformer. Despite the relatively high reluctance of the magnetic path compared with a closed-core, some quasi-DC current will flow through a reactor and as for a transformer.

As with any other threats to the power system, GIC need to be detected, measured and control measures should be taken to counter their effects. Many researchers have mentioned that it is difficult to study the effects of GIC on power systems due to the lack of measuring instruments in most parts of the world. In Africa, according to reviewed literature only South Africa and Namibia have taken the first step towards installing GIC measuring devices. The substations that are currently monitored are Ruacana power station (Namibia), Alpha, Hydra, Beta, Grootvlei, Perseus, and Grassridge substation. (South Africa). These substations were identified to be at high risk, in the event of high geomagnetic activity [15]. Researchers are relying mainly on calculated values of GIC which may not give a true reflection of the real scenario. For instance, the highest GIC calculated so far in South Africa is 108A at Alpha substation. Table 2.2 summarizes the calculated values of GIC at substations in South Africa.

Table 2. 2: Substations most susceptible to GIC in South Africa (1989) [19].

| **Substation** | **Maximum calculated GIC on 13 March 1989 averaged over 1 minute** |
|---|---|
| Alpha | 108 |
| Hydra | 67 |
| Beta | 64 |
| Grootvlei | 59 |
| Perseus | 57 |
| Grassridge | 41 |

On the other hand, the highest measured value of GIC is as low as +/-9A [12]. The readings were obtained from Grassridge substation transformer neutral on 24 November 2001. The storm duration was very short. The 3p3L transformer saturated and this appears to contradict the theory that three limb, core type transformers are not susceptible to GIC saturation. Takasu et al.'s model (1994) states that 3p3L transformer is not susceptible to GIC damage [20].

## 2.4 SUSCEPTIBILITY TO GIC AMONG DIFFERENT STRUCTURES

The presence of low reluctance return paths (white arrows) increases the core's tendency to saturate during GIC induced DC bias. [10]. The susceptibility of a transformer core to GIC saturation is dependent on the presence of DC flux paths, represented by white arrows in Figure 2.2.

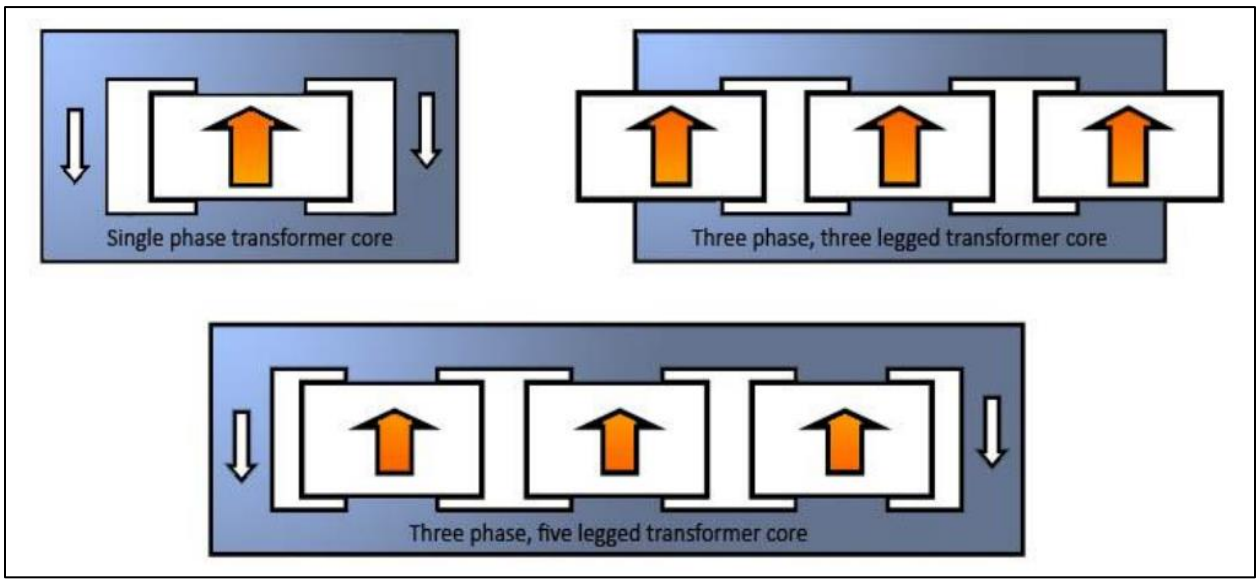


Figure 2. 2: Transformer core types. GIC Susceptibility varies between transformer core types [11]

In the case of a three-phase three-leg transformer there is no complete DC flux path in the core. In these transformers, the DC flux must leak into the transformer tank. In fact, all transformers are subject to some degree of flux leakage into the tank. Because the transformer tank is not designed as a magnetic core, the tank can be very susceptible to damage due to heating [11].

## 2.5 TRANSFORMER RESPONSES TO GIC

GIC flow in a power system causes half-cycle saturation in transformers [20]. Half-cycle saturation does not occur instantaneously and depends on the electrical characteristics of the transformer and GIC amplitude [21]. The magnetization current in a GIC saturated transformer is rich in odd and even harmonics [12]. The magnetization current is distorted because the transformer is operating in a non-linear region of the hysteresis curve. Current harmonics cause mal-operation of protective relays, heating in transformers and other equipment on the power system [22]. Figure 2.3 shows the effects of GIC on a power system

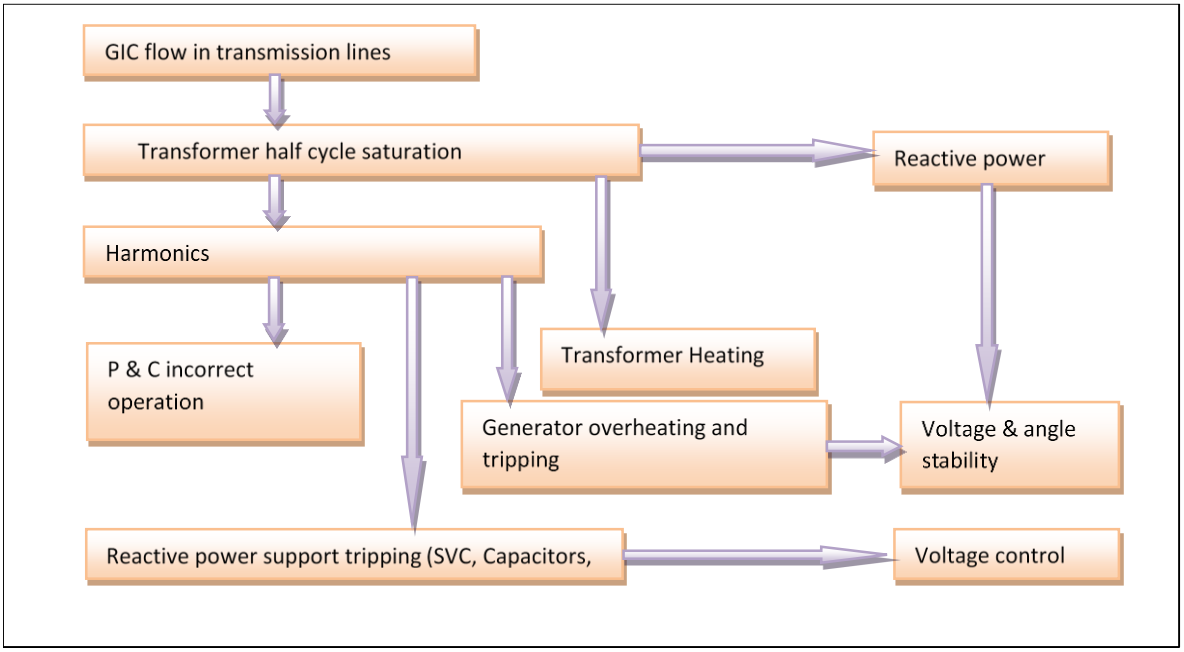


Figure 2. 3: Effects of GIC on the entire power system

In the transformer, the flow of harmonics increases the eddy currents in the transformer windings and core, causing additional heating and losses. Beyond the knee point, the core's inductance drops heavily and it approaches air-core inductance as the GIC continues to increase [23]. At air-core inductance the core's permeability reaches that of air. The drop in core inductance allows the easy flow of eddy currents exacerbating core heating. Half-cycle saturation also causes the transformer to draw more reactive power [24]. This poses stability issues on the power system. This may cause a voltage drop at the load end and frequency increase on the power system. System instability can be severely increased by tripping of reactive power support such as lines, static var compensators and capacitors as a result of harmonic currents.

In essence, when GIC flows through transformer windings, AC voltages will superimpose with DC waveforms resulting in a DC-offset, driving the transformer into saturation in the positive or negative cycle depending on the polarity of the offset. To sum up, half-cycle saturation has the following repercussions (a) increased production of harmonics (b) increase in reactive power consumption (c) increased heat production (d) increase of transformer losses (e) increase in transformer humming sound i.e. noise [25]. The severity of these effects depends on the strength of the geomagnetic disturbance. These consequences will be discussed later in the sequence below:

- Half-cycle saturation
- Thermal effects on transformers
- Harmonics generation
- Reactive power demand
- Increased noise

## 2.5.1 HALF CYCLE SATURATION

The flow of GIC causes asymmetrical saturation of transformers. This is normally termed half-cycle saturation. The superposition of the ac excitation current and the quasi-DC GIC current

causes the transformer core to saturate for a portion of each half-cycle [26]. A transition from unsaturated to saturated core represents a decrease in inductance by several orders of magnitude. The magnetizing inductance of an unsaturated transformer is large, and thus the rate of current increase is very slow until the transformer saturates. The effective core inductance variations reflect in the magnitudes of exciting current which account for the reactive power swings [27].

Figure 2.4 shows the effect of GIC on transformers. With AC excitation only, the transformer is designed to operate in the linear region of the characteristic curve - technically termed "hysteresis loop". In this region, the transformer is capable of converting primary voltage induced into secondary voltage in a linear relationship determined by the equation: $^{V_p}/_{V_s} = {}^{N_p}/_{N_s}$. On the Y-axis the corresponding excitation current under normal operation is shown and on the X-axis the normal flux which causes this excitation current is drawn.

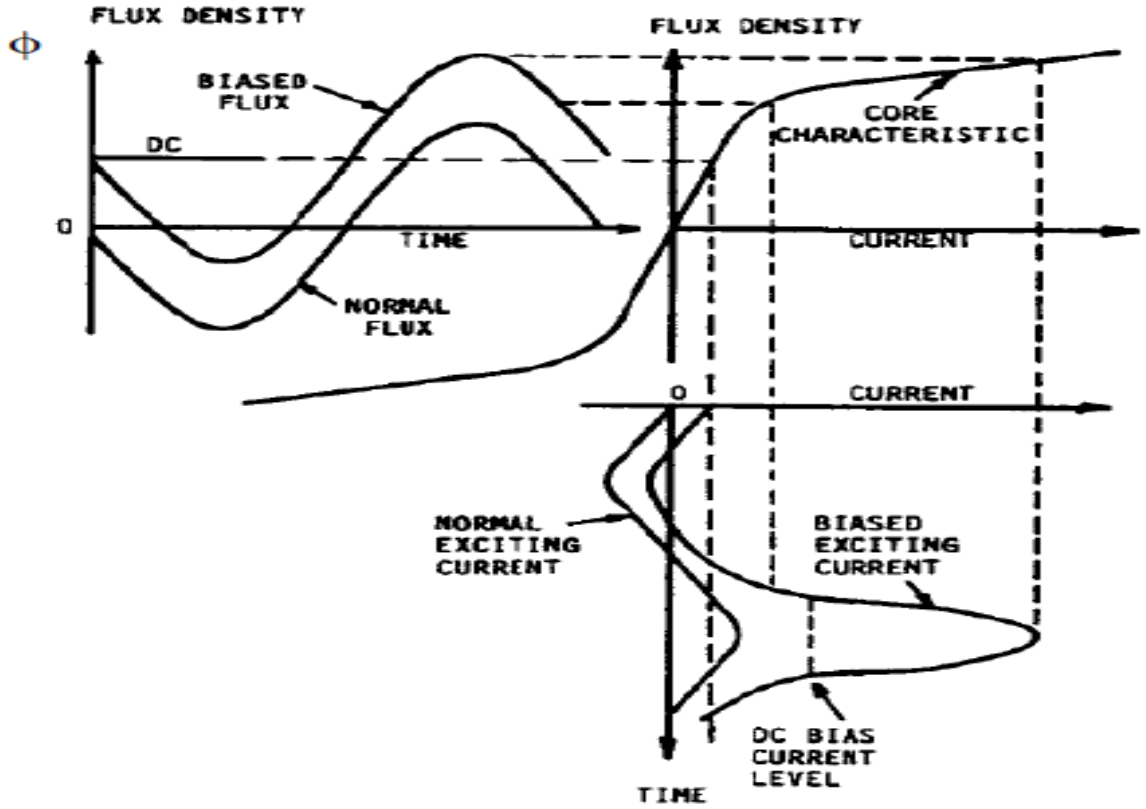


Figure 2. 4: Excitation current of a transformer as a result of DC bias [27]

The introduction of quasi-DC currents results in a biased flux that offsets vertically in a positive direction, and this results in a sharp increase in the exciting current - indicated as biased exciting current in Figure 2.4. This shift reduces the effective core impedance and causes a corresponding increase in the reactive power absorbed by the transformer core [28]. The biased exciting current lags the induced voltage by 90̊ [24]. According to the power triangle theory, if the current lags voltage then reactive power is consumed by the transformer. Moreover, this current is so huge in comparison to normal excitation current, the resultant increase in reactive power is abnormal such that compensation equipment may not supply this into the power system leading to system instability [29].

### 2.5.2 THERMAL EFFECTS ON TRANSFORMERS

The flow of GIC in transformers leads to a higher magnetizing current, which in turn produces a higher leakage flux, which also contains a lot of harmonics [26]. This leads to a significant increase in eddy and circulating current losses in both windings and structural parts of the transformer, causing heat generation and transformer losses [30, 31]. During saturation most of the excess flux flows externally to the core into the transformer tank, generating currents and localized tank wall heating spots with temperatures reaching up to 175 °C [32]. The intensity of overheating depends on the level of GIC but is also a function of various design parameters of the transformer itself. These include the saturation flux paths, cooling flow and the thermal condition or loading of the transformer. When overheating occurs, it causes the breakdown of oil and paper insulation in the hot spot regions [33]. The flux distribution under GIC is the most determinant factor in heating. The presence of a reluctance path in the 3p5L allows it to be prone to saturation more than 3p3L, hence GIC has more heating effect towards the 3p5L [34]. Repeated exposure to GIC results in long-term degradation of insulation, and because of the lack of GIC monitoring equipment, most failures are not attributed to GIC.

Figure 2.5 illustrates the thermal effects of GIC on transformers. This is a real scenario observed in Meadow Brook. The graphs show that geomagnetic induced currents of less than 60A have no

effects on oil temperature. However, tank temperature seems to increase under the same circumstances. None of the literature reviewed has stated that oil temperature increases under GIC. Nonetheless, temperature increase in the windings and structural parts have been widely reported [25]. An unfamiliar explanation of increased heating in the windings was given in [26]. R. Girgis et al, 1992 explain, "Transpositions that are provided in the windings are designed to minimize circulating currents due to flux present under normal operating conditions". With the change in flux distribution pattern, these transpositions not only become ineffective but may also aggravate the situation and result in higher circulating currents.

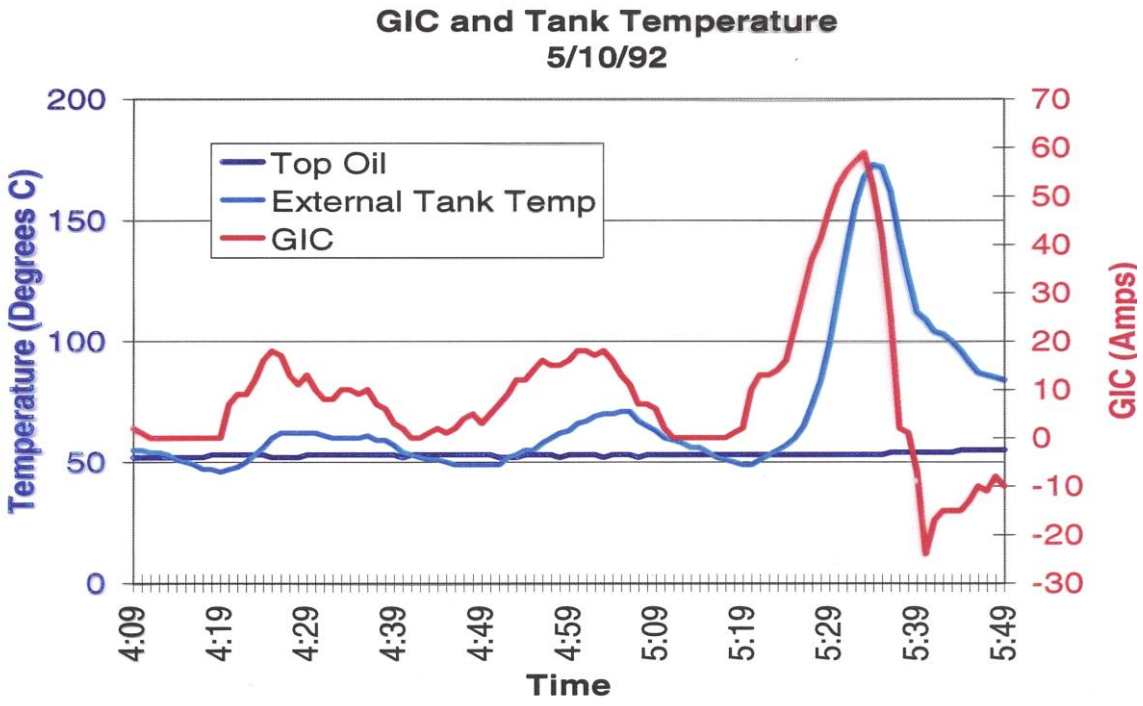


Figure 2. 5: Observed Meadow Brook transformer hotspot temperature for a minor storm on May 10, 1992 [35]

## 2.5.3 HARMONICS GENERATION

The exciting current of GIC-saturated transformers is highly distorted, and consist of harmonic components of both even and odd orders, as well as fundamental and DC components. Superimposed DC excitation will also cause the transformer to inject larger amounts of odd and even harmonics into the system thus affecting the normal operation of protective relays [36]. Spot heating is a critical threat to power transformers as a result of GIC. The extent to which harmonic currents cause spot heating, and the impact of that heating on transformer life vary depending on various factors including transformer construction and core type. The precise harmonic current spectrums depend on transformer construction type but in general the harmonic magnitude tends to decrease with increasing harmonic order. The pattern in which harmonics vary in a 3p5L shall be discussed in chapter 6.

Harmonics generated will cause mal-operation of protection and control relaying. Moreover, compensation equipment will also fail to cope with the increased harmonics generated under GIC events. This has been the scenario in 1989 when GIC caused a blackout in Canada. Consequently, when compensation equipment fails, the system will eventually collapse due to the large reactive power requirement that occurs when half-cycle saturation takes place. The harmonics injected into the system during a geomagnetic disturbance (GMD) may, as a consequence of the physical and protection impacts resulting in critical line or equipment tripping, can potentially aggravate fundamental-frequency voltage stability issues [23]. Thus, the critical concern regarding harmonics during a GMD is not their impact on power quality in the conventional sense, but rather the potential impact of the harmonics on grid security.

## 2.5.4 REACTIVE POWER DEMAND

In the saturation region of a transformer B-H curve, a small increase in magnetic flux, causes a dramatic increase in the magnetizing current – typically 10-20 times the normal excitation current

[35]. This increases the reactive power drawn by the transformer drastically. The large reactive power draws of GIC saturated transformer make the proper operation of the power system difficult and tend to lead to power system instabilities.

The magnetizing current of a power transformer increases sharply when it is subjected to geomagnetic induced current. Since the magnetizing current lags the system voltage by 90°, it creates reactive power loss in the transformer and the impacted power system [24, 35]. Under normal conditions, the transformer reactive power loss is very small. However, the several orders of magnitude increase in exciting current under half-cycle saturation also results in extreme reactive-power losses in the transformer.

The increased magnetizing current drawn by the GIC saturated transformer results in substantially greater core losses in the transformer. These core losses result in increased heating both in the transformer core and in other metallic components because of flux leakage. This heating can severely reduce the lifespan of a transformer. The tests conducted in [34, 37], show the order of increasing reactive power consumption as:

i. Three-phase three-limb
ii. Three-phase five-limb
iii. Single-phase transformers

The presence of low reluctance return paths increases the core's tendency to saturate during GIC induced DC bias, hence more reactive power absorbed [10].

### 2.5.4.1 SIGNIFICANCE OF REACTIVE POWER ON A POWER SYSTEM

When current is in phase with the voltage on a power system, real power is transmitted and when the current is out-of-phase with voltage then reactive power is generated by the system. Reactive power supports voltage in a power system, therefore the amount of reactive power determines the value of voltage in a system. An increase in reactive power consumption by a system results in voltage collapse as seen in the case of GIC flowing in power transformers, and the opposite is true. In supervised power systems, voltage control is done by regulating the amount of reactive power. Capacitors inject reactive power in a power system thereby boosting the voltage profile. Inductors on the other hand, consume reactive power thus resulting in a voltage drop. This is how voltage control is achieved.

On a transmission line, voltage is needed to transmit current to the load. Reactive power is used to build up the voltage levels necessary for active power to be transmitted. In essence, reactive power is essential to move active power through the transmission and distribution system to the customer. Reactive power is required to maintain the voltage to deliver active power through transmission lines. Finally, to understand the concept more clearly, reactive power is linked to the power factor in the sense that they both measure losses in a power system. In the event that the phase angle is not zero i.e. voltage and current are out-of-phase, the power factor is not equal to one, it shows that there are losses in the power in the power system. These losses, however, translate to reactive power drawn to support magnetic (either inductive or capacitive) needs of the system.

## 2.5.5 INCREASE IN TRANSFORMER NOISE

The noise in a transformer is a result of magnetostriction. Even under normal operation a transformer produces a humming sound as a result of magnetostriction. The degree of flux determines the amount of magnetostriction and hence, the noise level. The flow of GIC increases the flux in the core and causes the humming sound to increase [38]. This may happen for a few minutes as GIC currents continuously fluctuate and have short duration peaks. This means the flux increase momentarily, hence a short duration of increased magnetostriction. The expansion and

contraction of ferromagnetic material (magnetostriction) in saturated transformers cause noise and mechanical vibration, this may lead to mechanical failure [39]

GIC related increase in transformer noise has been reported in China [40]. Three heavy buzzing sound was heard three consecutive times for 1.5 min on 31 October, 2003. This happened at 4:20 AM, 9:20 AM and 10:20 AM. Maintenance checks were conducted on the circuit breakers, current transformers, surge arrestors and protection relays of the main transformer were made, and no abnormal condition was noticed. On 5 November 2003, the main transformer had an abnormal noise which was a little higher than usual and disappeared in about 2 minutes. In December 2004, the transformer was repaired, and it was thought that the abnormal noise was caused by the loosening of the winding underlay and insulating brackets [41]. However, the time this transformer experienced abnormal noise corresponds to high geomagnetic activities in China [42].

Another transformer at the Shanghe substation in the Jiangsu Province (China) was disturbed with unknown abnormal noise and severe vibration between March 2001 and October 2002 [39]. After joint analyses by specialists, it was concluded that the disturbance on the 750 MVA transformer, which consists of a bank of single-phase transformers, was caused by DC biasing resulting from GIC [43, 44]. Table 2.3 shows experimental results of the increase in core losses and core noise in a 750 MVA single phase transformer carried out by R. Girgis and K. Vedante.

Table 2. 3: Increase in core loss and core noise under varying GIC levels (750 MVA single-phase transformer) [25, 45]

| GIC Amp/Phase | % Core loss increase | Core noise level in dB |
|---|---|---|
| 15 | 31.1 | 27.5 |
| 20 | 34.2 | 30.0 |
| 30 | 38.9 | 33.8 |
| 40 | 42.6 | 36.9 |
| 50 | 45.5 | 39.3 |

## 2.6 DISTORTION AND UNBALANCE IN THREE PHASE SYSTEMS

In a balanced three-phase network, the voltage is purely balanced and there is no current that flows in the neutral. This system is considered to be balanced and if the load is purely resistive, the power factor is unity and no losses are incurred. However, introducing inductive and capacitive load brings the concept of reactive power and the system begins to incur some losses as the power factor changes due to phase angle difference that exists in these reactive loads. Another cause of inefficiency is an unbalanced load [46] across three phases and this results in an out-of-balance voltage drop, the resultant current returns to the source through the neutral, and there is an increase in the total losses in the supply cables. Non-linearity in the voltage and current waveforms is also known as a form of distortion and this is normally caused by transient switching, harmonic generation by power systems equipment such as generators, transformers, motors and non-linear loads. In the conventional power theory, losses caused by distortion, harmonics and unbalance are represented by the power factor which is $cos\theta$. According to Gaunt and Malengret, the reduction in the efficiency of the transfer of real power caused by distortion and unbalance can still be described by an efficiency (or power) factor, but the term no longer refers to the displacement angle between the voltage and current vectors. The concept of distorted power and reactive power was first introduced in 1979 [47] and this work was carried further developed by Gaunt and Malengret and they introduced the general power theory which extends the power triangle into a three-dimensional tetrahedral pyramid introducing distorted power and formulae to calculate power in such conditions.

In power systems, when geomagnetic induced currents are flowing the transformer becomes a source of odd and even harmonics and this introduces distortion. Therefore, considering Gaunt and Malengret's work the distorted power comes into play and there will be an underestimation of the reactive power computed using the conventional power theory. This might create problems for the utility when trying to calculate their reactive power reserves, and the reactive power compensation equipment may fail to deal with large distortions such as those caused by geomagnetic storms.

## 2.6.1 GENERAL POWER THEORY

The work performed by Malengret and Gaunt arises from more than twenty years of industrial experience and research. Based on observations and extensive research, they managed to formulate the general power theory. The work is based on the concepts of distortion and unbalance described earlier. The development of a general theory has been driven by the need for solutions to particular power systems problems [48]. Most of the time, most power systems operate with sinusoidal, balanced supplies, for which existing definitions of power are adequate. However, at other times distortion, unbalance and DC or zero sequence current components do upset systems and the conventional definitions would give misleading results. Figure 2.6 illustrates the General Power Theory, and the idea is that under distortion there is another component of reactive power $Q_A$ that requires energy storage in case of reactive loads. This was not recognized in the conventional power theory and thus the subsequent calculations may be misleading. The other symbols in the power triangle represents: Q = total non-active power, $Q_a$ is the component that can be compensated without energy storage, $Q_A$ is the component that requires energy storage for compensation, S = apparent power without any compensation, Sa is the apparent power after compensation without energy storage, and $S_A$ the apparent power after complete compensation so that $S_A$= P .

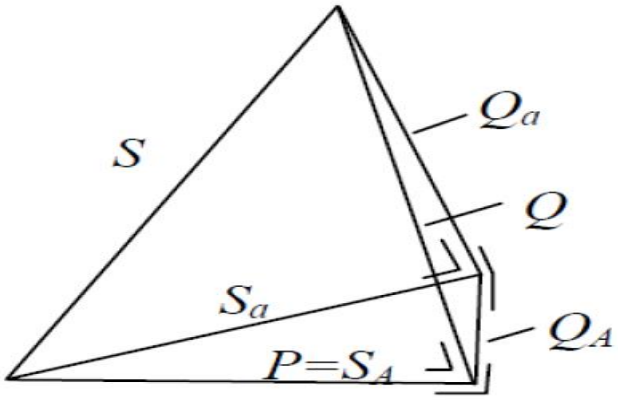


Figure 2. 6: The complete power triangle [46]

Overall the formula used to calculate the apparent power, active power and non-active power using the general power theory (GPT) is given below:

$$s^2 = P^2 + Q^2 + {Q_A}^2 \quad 2.1$$

Where S = apparent power, P= Real Power, Q= total non-active power and $Q_A$= the component of non-active power that requires energy storage for compensation.

Considering a three-phase system with a neutral, where the resistances in each phase are equal $r = r_1 = r_2 = r_3$ and the neutral resistance $r_n$ is not necessarily the same, shown in Figure 2.6. Applying Kirchhoff's law to Figure 2.7 yields:

$$i_n = -(i_1 + i_2 + i_3) \quad 2.2$$

Where $i_1, i_2, i_3$, are the phase currents and $i_n$ is the neutral current. The initial step in deriving the apparent power is to calculate the resistance-weighted square of the currents:

$$\|i'\|^2 = \left(i_1^2 + i_2^2 + i_3^2 + \frac{i_n^2 r_n}{r}\right).r \quad 2.3$$

Where $\|i'\|^2$ is the resistance weighted norm of the current. The resistance-weighted reference for the voltages for all the sample points is then calculated using equation 2.3 and from this, the weighted norm of the instantaneous voltages is calculated using equation 2.4:

$$e_{ref} = \frac{e_1+e_2+e_3}{3+\frac{r}{r_n}} \quad 2.4$$

$$\|V_2'\|^2 = \left(\left(e_1 - e_{ref}\right)^2 + \left(e_2 - e_{ref}\right)^2 + \left(e_3 - e_{ref}\right)^2 . \frac{r}{r_n}\right)/r \quad 2.5$$

The apparent power is then calculated using the resistance-weighted norms of the voltages and currents:

$$s = \|V_2'\|\|I'\| \quad 2.6$$

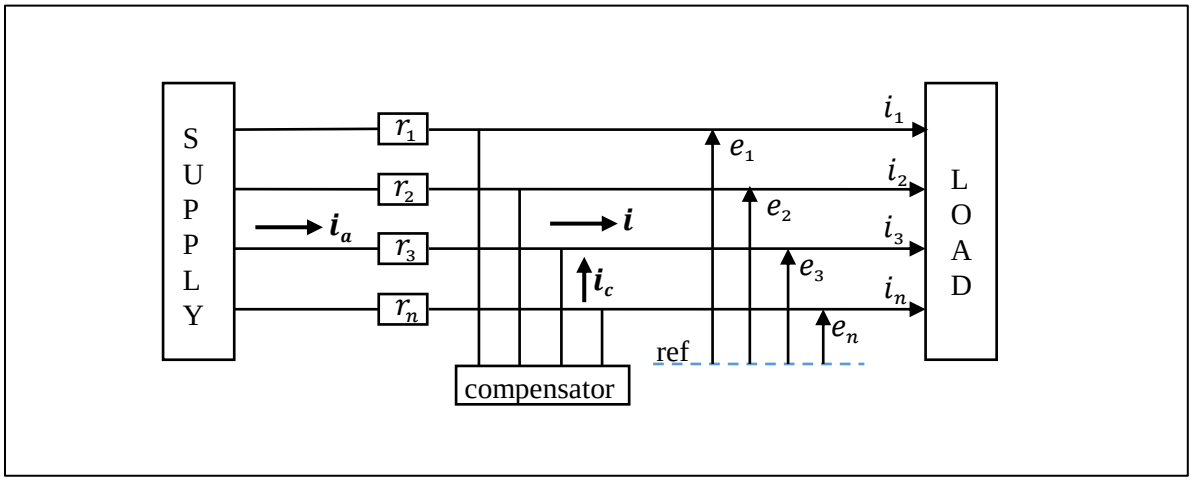


Figure 2. 7: n-wire system with resistances $r_1, r_2, r_3, \dots, r_n$, supplying load with voltages $e = \{e_1, e_2, e_3, \dots, e_n\}$, and currents, $i = \{i_1, i_2, i_3, \dots, i_n\}$, with active supply current $i_a$ and local compensator current $i_c$ [49]

The real power, P does not change and may be calculated using the conventional approach or by taking the product of the instantaneous voltages and currents. The total non-active power Q may be calculated using the Pythagorean relationship obtained from the general power pyramid.

## 2.7 FINITE ELEMENT METHOD

Finite element method (FEM) is a powerful tool to model electromagnetic devices such as the transformer. It involves the creation of a geometry and the object or geometry is broken down into small elements i.e. finite elements [46]. These elements are then represented by a set of equations, typically Maxwell's equations. The FEM software that is going to be used in this project is ANSYS MAXWELL. The differential form of Maxwell's equations are written as:

$$\nabla \times H = J + \frac{\partial D}{\partial t} \quad 2.7$$

$$\nabla \times E = -\frac{\partial B}{dt} \quad 2.8$$

$$\nabla \cdot B = 0 \quad 2.9$$

$$\nabla \cdot D = \rho \quad 2.9$$

Where B and H are the magnetic flux density and the magnetic field intensity respectively. D and E are the electric flux density and electric field intensity respectively. J is the current density and ρ is the resistivity of the material. Figure 2.8 represents the methods of computing electromagnetic problems.

Finite element method is a numerical technique for finding approximate solutions to boundary value problems. FEM can be used for solving differential equations in many disciplines like, electromagnetics, magnetostatics, thermal conduction, structural mechanics, transient, fluid dynamics and acoustic [50]. The finite difference method (FDM) is another numerical technique frequently used to obtain approximate solutions of problems governed by differential equations. The finite difference method is based on the definition of the derivative of a function f(x) that is [51]:

$$\frac{df(x)}{dx} = \lim_{\Delta x \to 0} \frac{f(x+\Delta x) - f(x)}{\Delta x} \quad 2.10$$

where: $x$ is the independent variable.

From differential equation theory, it is known that the solution of a first-order differential equation contains one constant of integration. The constant of integration must be determined such that one given condition (a boundary condition or initial condition) is satisfied. The reason why these boundary conditions are set when analyzing electromagnetic problems using either FEM or FDM.

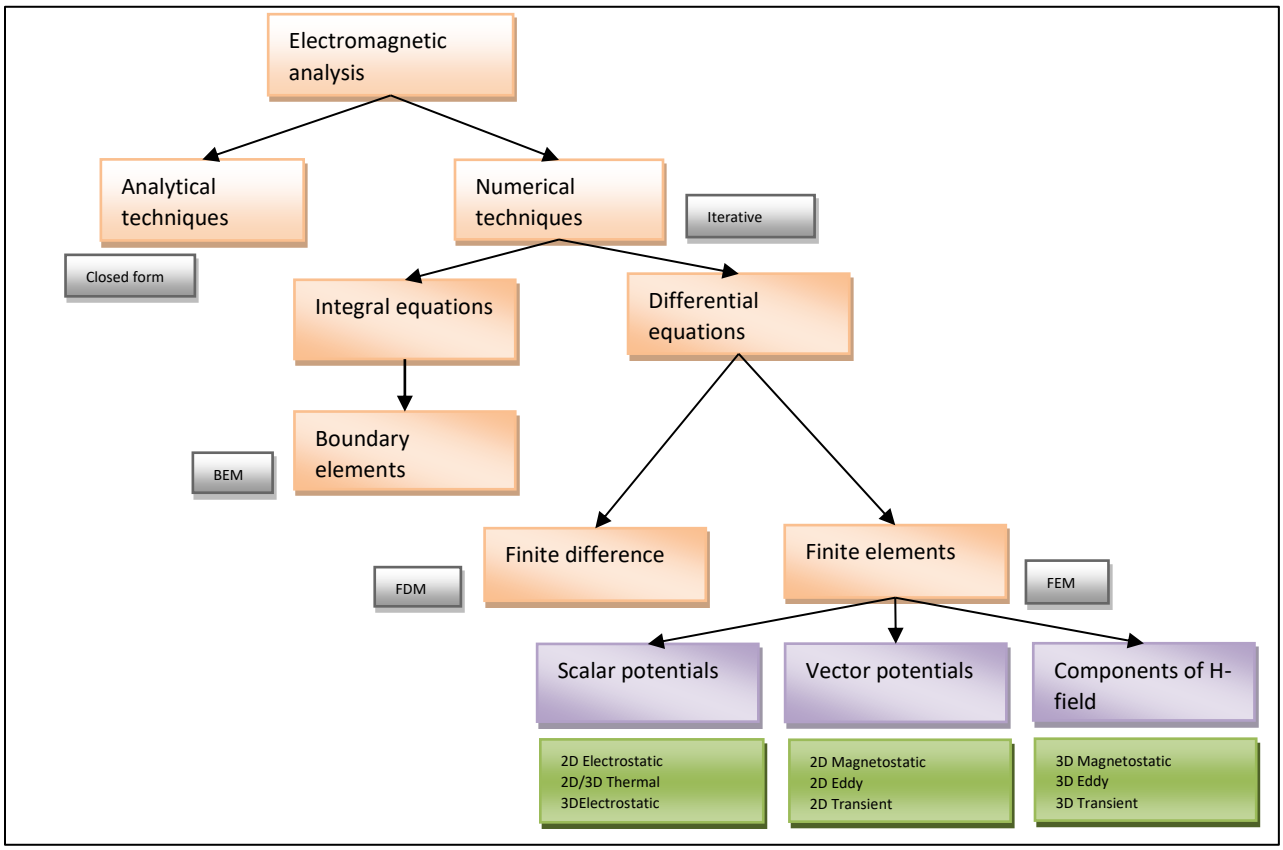


Figure 2. 8: Flowchart of the Finite Element Method [52]

The most descriptive way to contrast the two methods is to note that the FDM models the differential equation(s) of the problem and uses numerical integration to obtain the solution at discrete points. On the other hand, FEM models the entire domain of the problem and uses known

physical principles to develop algebraic equations describing the approximate solutions. Thus, the finite difference method models differential equations while the finite element method can be said to more closely model the physical problem at hand [51].

## 2.8 GENERAL GUIDE TO FEM SIMULATIONS

In general, FEM uses specific formulae and mathematical models of the different problems under study and the basic steps for solving them are: creating the geometry, generating a mesh, validation and retrieving the solution and post-process. Finite element method is performed in three stages: pre-processing, solution setup (processing) and post-processing. Pre-processing is building a finite element model and generating a mesh; processing uses the related equations and iterative algorithm to obtain results; post-processing is the collection and the processing of results. Figure 2.9 gives a good view of the simulation steps in the finite element method.

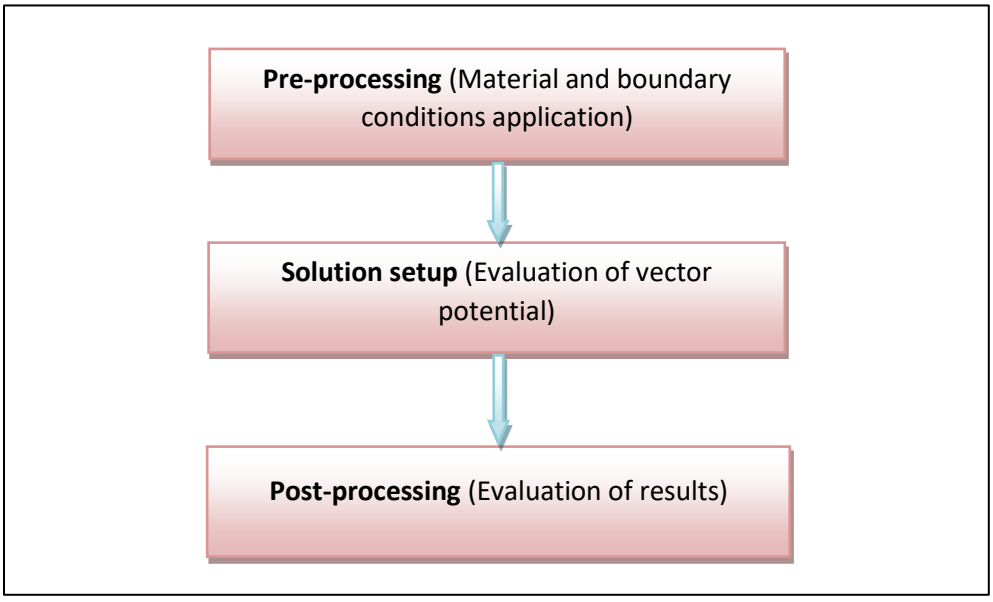


Figure 2. 9: A general representation of simulation steps in finite element method

### 2.8.1 PROCESSING

This is the most critical step that defines the model. It includes:

- Defining the geometric domain of the problem.
- Defining the solution type.
- Assigning the material properties of the elements.
- Defining the element connectivity (mesh the model).
- Define the physical constraints (boundary conditions).
- Assigning other variables that define the problem e.g. equipment rating.

### 2.8.2 POSTPROCESSING

Analysis and evaluation of the solution results is referred to as post-processing. Postprocessor software contains sophisticated routines used for sorting, printing, and plotting selected results from a finite element solution. Examples of operations that can be accomplished include:

- Core loss measurement
- Flux analysis
- Thermal analysis
- Excitation characteristics, etcetera

While solution data can be manipulated in many ways in post-processing, the most important objective is to apply sound engineering judgment in determining whether the solution results are physically reasonable. Therefore, it is important to compare these results with some practically measured results.

## 2.8.3 SOLUTION

Figure 2.10 illustrates the flowchart of the algorithm used in finite element analysis of a power transformer. During the solution setup phase, finite element software assembles the governing algebraic equations in matrix form and computes the unknown values of the primary field variable(s). The computed values are then used by back substitution to compute additional, derived variables.

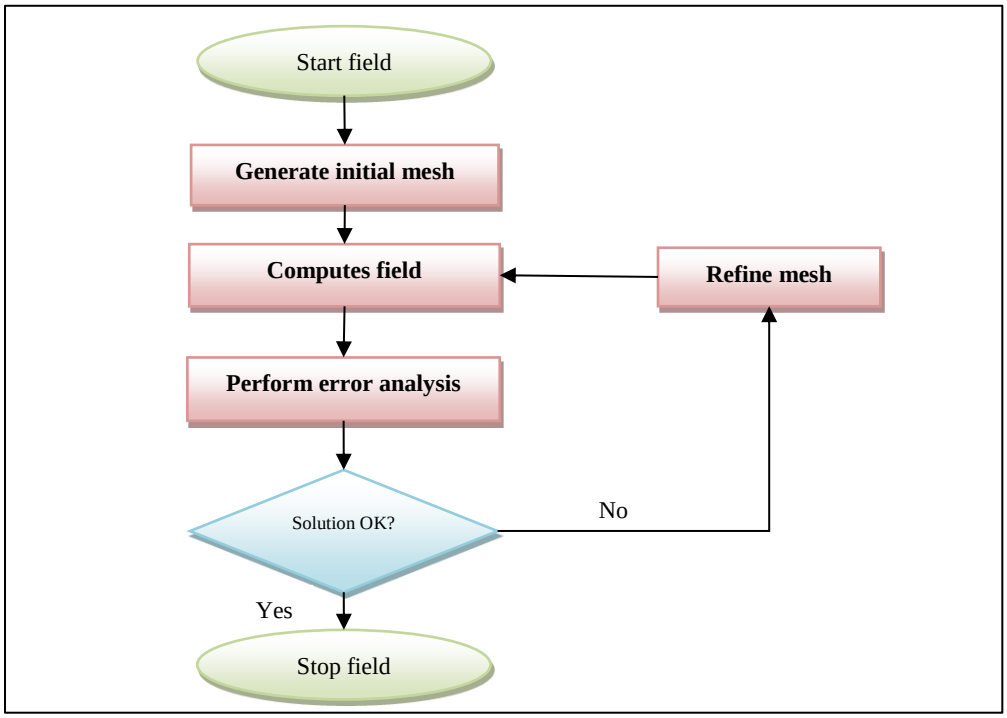


Figure 2. 10: The flowchart of the algorithm for finite element analysis [53]

## 2.9 CONCLUSION

As discussed, the impacts of geomagnetic induced currents on transformers are: half-cycle saturation, reactive power increase, harmonics generation, thermal effects, and erratic noise increase. As a result, insulation degradation due to heating, hotspots, transformer tank destruction, increase in core losses, and noise in transformers may occur in the affected transformer. Half-cycle saturation in transformers has ripple effects on the entire power system. The effects are: protection and control mal-operation, voltage and load angle instability, reactive power loss, reactive power compensation equipment mal-functioning and harmonics generation. If proper planning is not available before GIC events, transformers can be destroyed and a possible blackout can happen depending on the magnitude of GIC. The chapter also provides a brief background of the General Power Theory and its applications. Finally, the Finite Element Method which is a particular technique that is going to be used for simulation of GIC in power transformers has been described.

# CHAPTER 3: THRESHOLDS OF GIC INITIATING DAMAGE IN POWER TRANSFORMERS

## 3.1 INTRODUCTION

Earlier chapters have described the effects of geomagnetic induced currents on transformers and the power system. This chapter will investigate the thresholds of GIC that initiates degradation to power transformers with particular reference to the 3p5L core structure and brief explanations of the consequences of operating above the stipulated references. Case studies will form the basis of this chapter and the laboratory experiments that I have carried out. A quick look at the standards formed by reputable organizations such as IEEE, IEC, ANSI, NERC and METATECH has guided the researcher to arrive make valuable conclusions.

## 3.2 DEFINITION OF DAMAGE

According to this research damage: refers to the noticeable degradation, any form of mal-operation that will cause harm to the operation of the transformer taking into account internationally recognized standards (IEEE, IEC). A brief explanation of the temperature and voltage limits as defined in internationally recognized standards shall be covered in this section:

1. Temperature thresholds:

Table 3.1 identifies the temperature thresholds under base GIC, which assumes a continuous steady flow of a defined value of GIC. Sources of continuous DC to the power system may be HVDC links, electric arc converters and geomagnetic events. GIC data shows that GIC peak amplitudes may only last for periods between 1 to 5 minutes, therefore short duration GIC events thresholds would apply in this case. The purpose of these recommended temperature limits is to provide reasonable values for the rate of loss of life of the solid insulation used in the transformer and also prevent gas bubbles in the oil.

Table 3. 1: Maximum allowable temperatures on transformers [54]

| **Component** | **GIC type** | | |
|---|---|---|---|
| | **Base GIC** | **Short duration GIC events** | |
| | **IEEE/IEC** | **IEEE C57.91** | **IEC 60076** |
| Cellulose insulation | 140 ˚C | 180 ˚C | 160 ˚C |
| Structural parts | 160 ˚C | 200 ˚C | 180 ˚C |
| Top oil | 110 ˚C | 110 ˚C | 110 ˚C |

The ANSI guide specifies that the initial value of the strength of insulating paper is reduced by as much as 50% after 300 h (lifetime) of use at 170 °C. At 115 ˚C, the paper has a lifetime of 20,000 h [55]

2. Voltage limits: the operating voltage should be within +/-10%. The transformer is designed to operate at the knee point of the magnetization curve and if the voltages exceed the prescribed limits in the positive direction, the transformer may saturate leading to problems that arise due to saturation described in chapter 2.
3. Harmonics: Total harmonic distortion measures

Table 3.2 shows the percentages of the voltage total harmonic distortion (THD) as described in IEEE Std. 519. For large power transformers, the IEEE limit Voltage THD limit is 1.5% [56]

Table 3. 2: Percentage Voltage THD, for low voltage transformers [57]

| | Special applications | General system | Dedicated system |
|---|---|---|---|
| Voltage THD | 3% | 5% | 10% |

## 3.3 CURRENT THRESHOLD STUDIES

The effects of GIC on power transformers have been researched for decades and it seems that most people seem to agree upon certain behaviors exhibited such as asymmetrical saturation, harmonics generation and their impacts on the entire power system. However, there is a huge variance on the thresholds of GIC that are being proposed by various research groups. For instance, NERC proposed a threshold of 75 A/phase while METATECH consider a threshold of 90 A/phase. At the same time, study by Q. Qui, R. Girgis et al on a 750 MVA, 765/345/35.5 kV, single-phase transformer proposed a standard of 155 A/phase after extensive practical experiments. Setting a single threshold value seems not quite a noble idea. Transformer parts respond differently under GIC, for example oil temperature, core and tank temperature vary differently with GIC. Rather specifying that this is a threshold for oil temperature, winding temperature, etc. could separate the focus on the studies of GIC thresholds and the standards will speak to a certain kind of degradation. After taking into account all possible mechanisms that could lead to failure in a transformer, then an overall threshold can be set. This study tries to separate these aspects and come up with thresholds for safe levels of temperature, harmonics and reactive power absorption of the transformer.

### A. NERC

According to North American Electric Reliability Cooperation (NERC), voltage stability collapse of power systems exposed to extreme GMD events is of the greatest concern in North America, and the risk of transformer damage is negligible for GICs below 75 A/Phase (225 A in the neutral). NERC hence proposed that transformers exposed to such levels of GIC should be assessed for damage, with the assumption that GIC magnitudes below this value offer some minimal effect [58]. The later statement meant close examination such as performing dissolved gas analysis must be performed prior to a GMD that exposes to a transformer to such a quasi-DC current. Table 3.3 shows the experimental results to test the thresholds of GIC that can affect power transformers. The tests were conducted on single-phase power transformers.

Table 3. 3: Maximum temperatures on single phase transformer tested by NERC [59]

| Effective GIC (A/Phase) | Metallic Hotspot Temperature (˚C) | Effective GIC (A/Phase) | Metallic Hotspot Temperature (˚C) |
|---|---|---|---|
| 0 | 80 | 140 | 172 |
| 10 | 106 | 150 | 180 |
| 20 | 116 | 160 | 187 |
| 30 | 125 | 170 | 194 |
| 40 | 132 | 180 | 200 |
| 50 | 138 | 190 | 208 |
| 60 | 143 | 200 | 214 |
| 70 | 147 | 210 | 221 |
| 75 | 150 | 220 | 224 |
| 80 | 152 | 230 | 228 |
| 90 | 156 | 240 | 233 |
| 100 | 159 | 250 | 239 |
| 110 | 163 | 260 | 245 |
| 120 | 165 | 270 | 251 |
| 130 | 168 | 280 | 257 |

NERC used single-phase transformers to determine the 75 A/Phase threshold, but for the purpose of TPL-007-1 is applicable to all types of transformer construction [59]. The use of single-phase transformers was justified because it is a well-known fact that the single-phase transformer is the most susceptible transformer structure. The 75 A/Phase threshold selected represents a 70 ˚C incremental temperature rise from an initial of 80 ˚C and it is well below the 180 ˚C and 200 ˚C short time duration thresholds set by IEC and IEEE respectively.

## B. METATECH

The United States National Academy of Sciences noticed inconsistencies and uncertainty in GIC events. Citing such inconsistencies, they could not give a single value of GIC as thresholds of GIC initiating damage. Instead, the provided two values and these values were 30 A/phase and 90 A/phase DC, where 90 A/phase was passed. The METATECH document [60] made assessments on the number of high voltage transformers that would be more at risk when the two different thresholds are considered, where it was found that the lower GIC level would increase the damage by a factor of two or more [60].

## C. AMERICAN ELECTRIC POWER

The American Electric Power (AEP) performed tests on a 750 MVA, 765/345/35.5 kV, 1-phase, auto-transformer [61]. The tests were aimed at identifying thresholds of GIC that can damage transformers. They found that the test transformer could withstand 155 A/Phase for 30 minutes without the need for reducing their load while limiting the rate of loss of life of insulation to less than 1% and at the same time reducing the risk of forming gas bubbles in the oil. However, transformer tests in this paper confirm that there are significant increases in core noise, core losses, and load losses below 155A/Phase and that the transformer would saturate for values of GIC greater than or equal to 30 A/Phase. Similar to NERC, their capability was arrived at taking account of hotspots temperature capability, ignoring that the transformer would have saturated at GIC values slightly above 30 A/Phase. It is known that the transformer would be generating harmonics that could cause mal-operation of protective relaying equipment, SVC tripping among other effects. In addition, a saturated transformer draws enormous amounts of reactive power which may lead to voltage instability issues in the network.

## 3.4 TEMPERATURE THRESHOLDS

In literature it was established that the flow of GIC, cause a considerable increase in transformer temperature. The flow of GIC causes half-cycle saturation and this results in increased flux flowing in the core. High flux concentration leads to eddy currents and the resulting increased core losses [62]. Stray flux also riches the tank and some parts of the transformer such as flitch plates, tie plates, core bolts and joints leading to increased hotspots in these parts. Oil in the transformer acts as an insulator and coolant. Thus, the heat produced in the core, tank and other metallic parts is transferred to the oil by conduction. This causes the oil temperature to rise slowly, and significantly high temperatures will cause partial discharging and gas bubbles to be produced in the oil. This degrades the transformer oil, causes carbonization and some lumps of carbon may be deposited in the oil. Carbon partially conducts electricity and the insulating properties of oil soon dropdown. If oil maintenance by filtering or complete recycling is not done the transformer may be damaged permanently.

Practically the thermal GIC capability of a transformer has to consider the maximum allowed temperature in the windings, core and other structural parts. When carrying out these capability tests it is vital to consider the combined effect of AC and DC flowing in the transformer. Therefore, the analysis used to reach on some threshold values in this section will consider the thresholds set by IEEE, IEC for temperature in the oil, windings, cellulose or paper insulation and other hotspots. These temperature thresholds are given in IEEE Std C57.91 and IEC 60076 standards for base GIC and short duration GIC events. The IEEE Std C57.91 clearly states, the purpose of these recommended temperature limits is to provide reasonable values for the rate of loss of life of the solid insulation used in the transformer and also prevent gas bubbles in the oil.

It is a common practice in industry to set the protection system to operate slightly below these standards to allow for factory errors, deviations in required maintenance programs and to prolong the life of transformers as these are high-cost devices.

### 3.4.1 HOTSPOTS

Figure 3.1 shows the simulation of the impact of GIC on a single-phase transformer. Simulations performed in [63] show that, the IEEE Std. C57.91 emergency loading hot spot threshold of 200 °C for metallic hot spot heating is not exceeded in this example. The peak temperature is 186 °C.

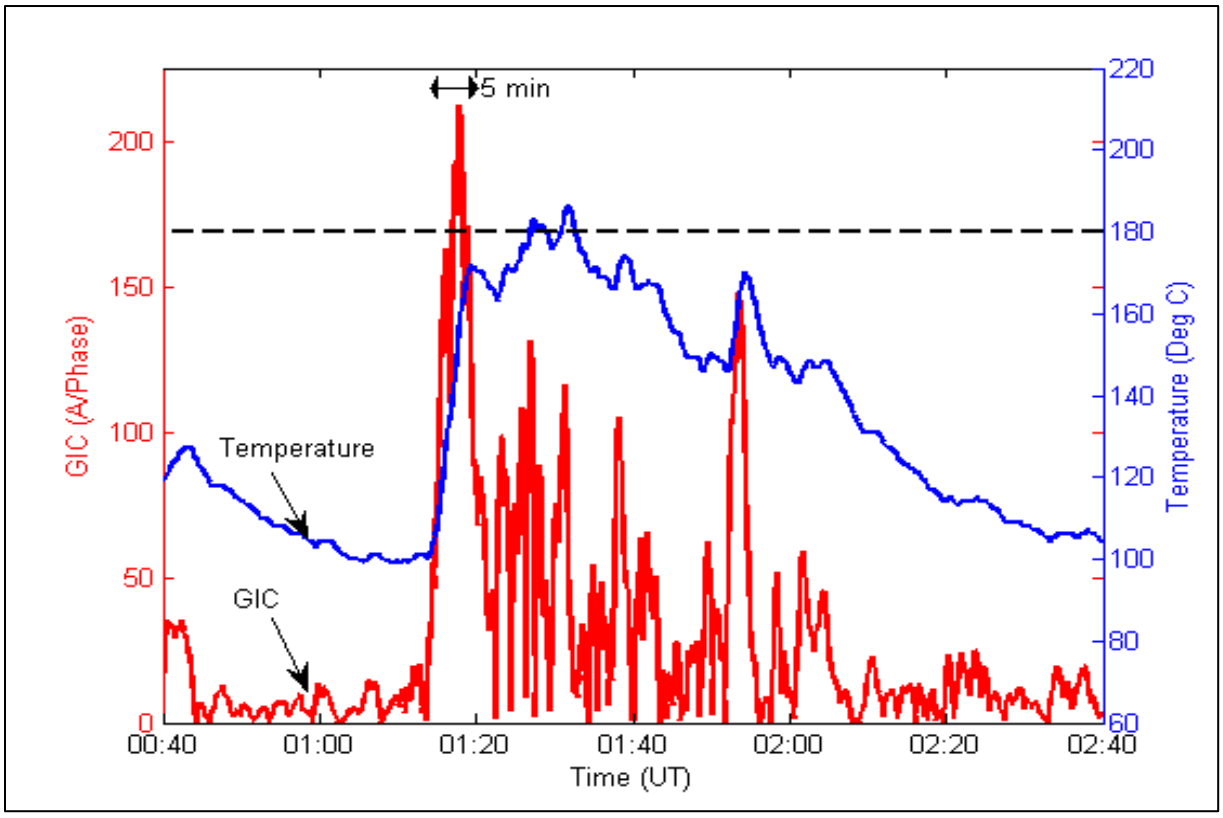


Figure 3. 1: Metallic hot spot temperature for a GIC waveshape derived from the March 1989 GMD event [63]

The manufacturers can provide guidance on individual transformer capability, which are lower than the IEEE threshold. The IEC standard however has set the temperature threshold to 180 ˚C, this would mean that a GIC current of 210 A/phase would cause the hotspot temperature to be exceeded for 5 minutes. This is too high a value compared to the threshold set by NERC on

hotspots. However, if a conservative threshold of 160 °C were used to account for the age and condition of the transformer, then the full load limits would be exceeded for approximately 22 minutes.

### 3.4.2 OIL AND TANK TEMPERATURE

Figure 2.4 illustrates the temperature variations of top oil temperature and tank temperature that were taken at Meadow Brook substation after a minor storm in 1992. The results show an insignificant increase in top oil temperature while the tank temperature increased sharply as the GIC current peaks. From this short term duration, one can say GIC have little effect on the oil temperate. However, studies show that metallic hotspots may cause the oil to lose its integrity although the overall temperature of the oil may not rise significantly in a GMD event. Again, as the core saturates due to DC bias, some of the ac core flux will stray outside the core and into the tank creating localized additional losses and heating. However, because of the short duration of the high peak GIC pulses, the increase in temperature has less impact on the overall integrity of the transformer [64].

### 3.4.3 WINDING HOTSPOTS

An extract of a 60 minutes duration of GIC, from the 1989 geomagnetic disturbance is given in Figure 3.3. The transformers evaluated were the single-phase, 250 MVA GSU in the Hydro Quebec network. Analysis using real geomagnetic data gives a true representation of what could happen in a real GMD scenario. It is noticeable that the temperature rise of the winding hot-spot, due to the base GIC of 10 A, is negligible [64].

As the GIC started to rise beyond 10 A, the winding hot-spot temperature started to rise acutely till a temperature of 117 ˚C was reached corresponding to a peak GIC current of 100 A. The

maximum temperature reached with 100 A GIC is way below the temperature IEC and IEEE thresholds of 180 ˚C and 200 ˚C respectively.

Despite the winding hot-spot temperature not reaching the threshold, it is interesting to note that the transformer may fail due to the voltage fluctuations that occur as a result of a GIC event of similar nature. In conclusion, such magnitudes of excursions of the winding hot-spot temperatures for short-duration GIC magnitudes should not cause any damage to the windings or any significant loss of life of the winding insulation.

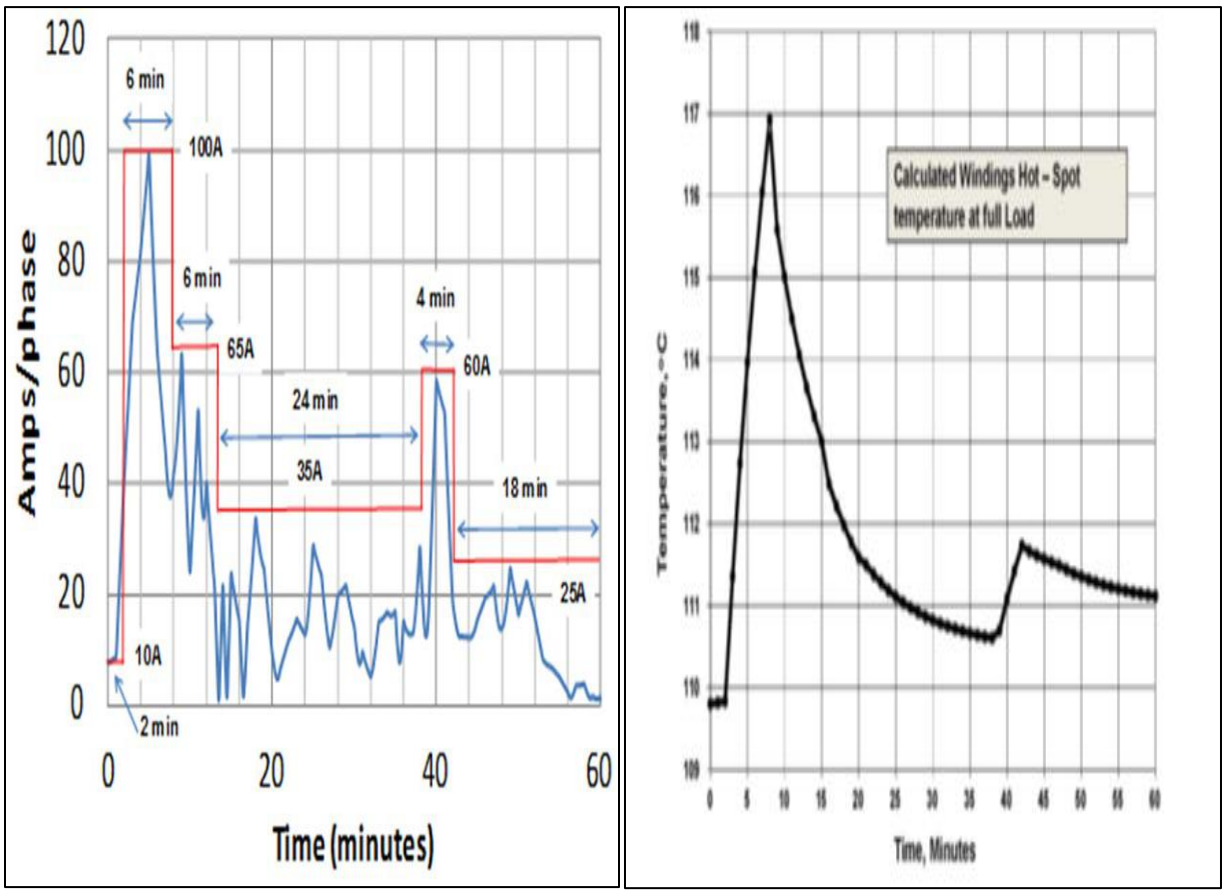


Figure 3. 2: GIC variation and calculated winding temperature from 1989 GMD event in Canada [64]

Windings prove to be very robust and unaffected by high levels of GIC even up to 200 A/Phase. Figure 3.4 shows that even after 30 minutes of DC bias, the maximum temperature of the winding will reach 121 ˚C. The results were extracted from experiments carried out by Qui and Girgis. Another set of results from Siemens confirm that the maximum temperature would rise to approximately 122 ˚C with a DC bias of 200 A/Phase (Figure 3.5).

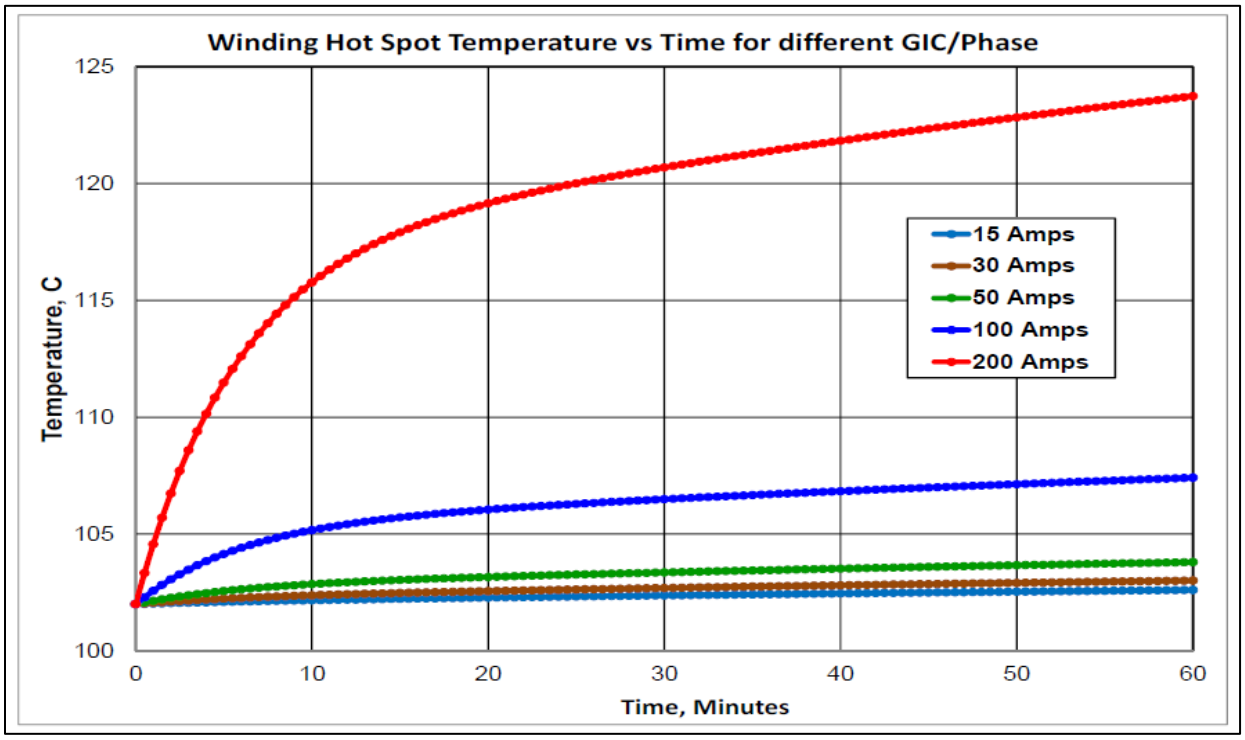


Figure 3. 3: Winding temperature rise 750 MVA, 765/345/35.5 kV, 1-phase, auto-transformer [61]

Figure 3.5 shows that the temperature of the tie plate on single-phase passes the IEEE limit at 80 A/Phase of GIC while that of 3p5L passes the limit at 150 A/Phase of GIC. Hence looking at these values, the NERC threshold looks reasonable on hotspots and applicable, since it correlates with most studies that took place independently. For the purpose of general transformer thresholds the worst affected shall be used.

The high-peak magnetizing current pulse, associated with GIC asymmetrical saturation produces correspondingly high levels of leakage flux that is also rich in higher-order harmonics. This leakage flux impinges on the tie-plates causing high localized eddy losses. This component of losses increases approximately linearly with the level of DC. The combination of these two loss components causes the higher temperatures in the tie-plates.

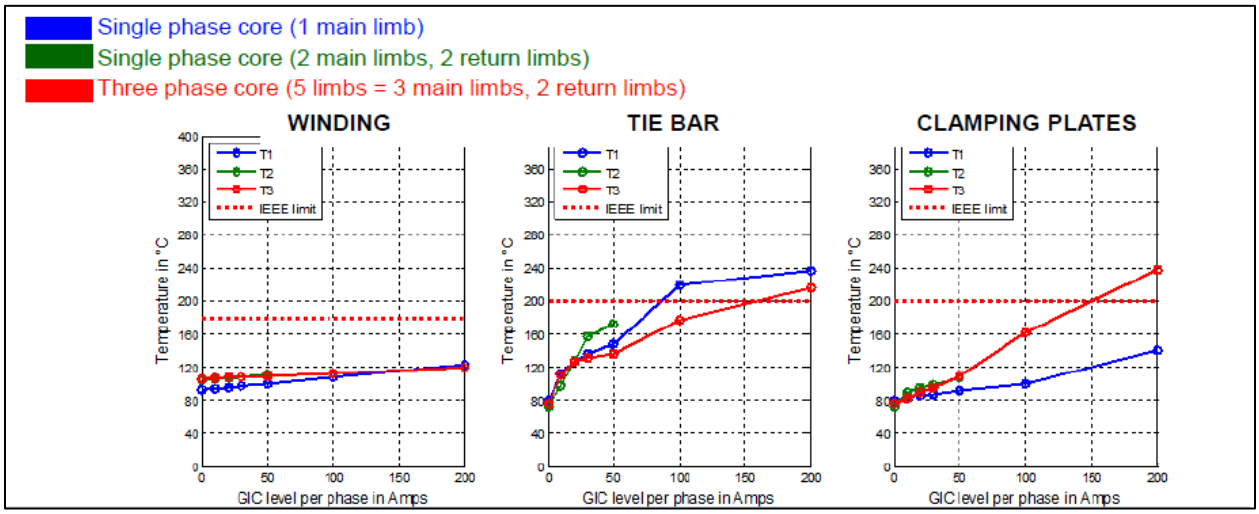


Figure 3. 4: Hotspot temperature on windings, tie plates and clamping plates [65]

## 3.5 HARMONICS

A better indication of the severity of the disturbance is the THD level of the voltage [24]. Hydro-Quebec utilizes a form of harmonic distortion level measurement by comparing successive voltage peaks to detect an unbalanced voltage. Typically, the THD for voltage is 2.5% on most power systems, but has been measured as high as 30% during severe GIC events. The THD is a measure of the harmonic content of a given voltage or current waveform. IEEE set the THD level, after consulting equipment manufacturers on the level of harmonics that certain loads can tolerate. Apparently, the maximum allowable THD decreases as the voltage of a system becomes high. For

systems operating above 500 kV the IEEE 519 Std. [57] specifies the THD is 1.5% for 3 seconds, while lower voltages may operate at a limit of 5% [59].

Studies done by Dong 2001, [37] correlate with R. Walling 2014 [23] and they have proved that currents below 10 A in neutral, causes the voltage THD to go beyond the IEEE limit for large transformers which is set at 1.5% [64]. This shows a major flaw in the NERC, METATECH and Qui and Girgis way of identifying the thresholds. It is clear that harmonics are also essential to consider when trying to come up with thresholds. Extending the graph to extrapolate the real margin of GIC corresponding to a value of 1.5% $V_{THD}$ for 400 MVA, 500 kV GSU in Figure 3.6 shows that 2 A GIC may cause a considerable amount of harmonics generation in large power transformers. This result correlates well with the result published in [12, 17, 19] that transformers failed in South Africa and Britain after they were exposed to GIC currents of similar magnitudes.

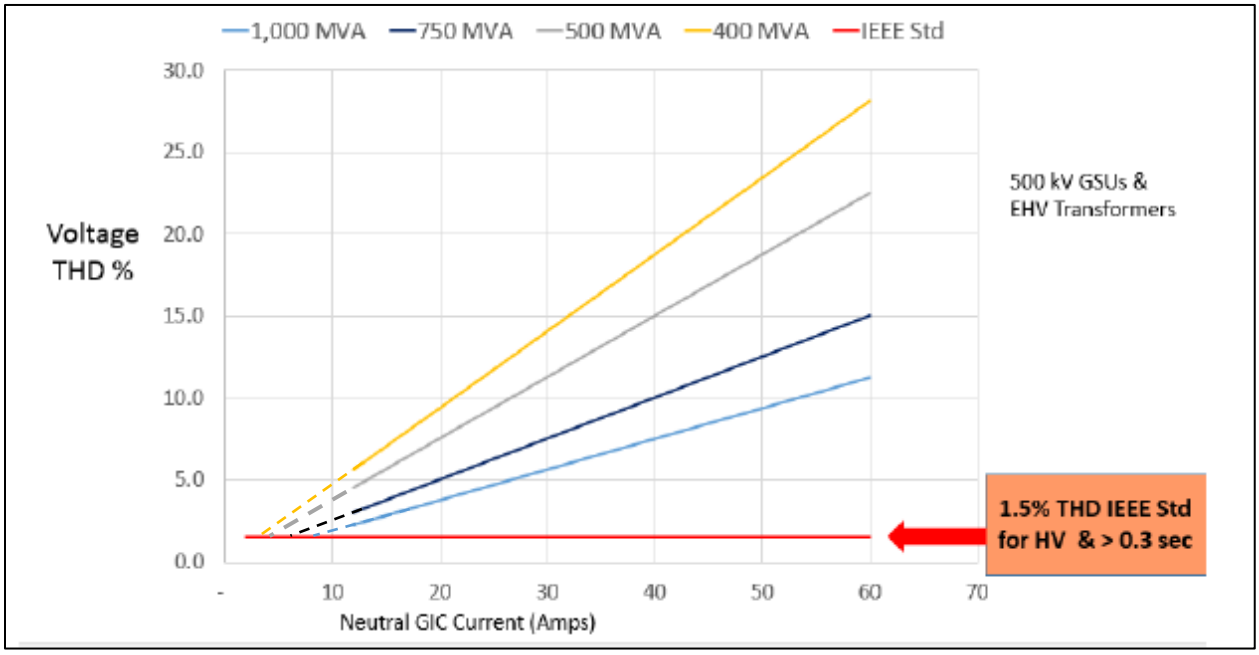


Figure 3. 5: Voltage total harmonic distortion ($V_{THD}$) as a function of GIC for GSU transformers operating at 500 kV and above [29]

The study of harmonic effects to generators in [67] showed that the generator capability limit can be exceeded at moderate GIC levels, e.g. 50 A/phase, and the rotor damage is likely during a severe GMD event. The studies show that negative sequence currents due to harmonics cause heating that may damage the generators. In addition, the study suggests that IEEE standards C50.12 and C50.13 require modifications to take into account the even harmonics of the generator current during a GMD event which is underestimated.

## 3.6 SATURATION

There is well-documented evidence that power transformers may saturate at GIC levels as low as 1-2 A [33]. Therefore, it is not worthwhile to rely on the thresholds that have been set by NERC, METATECH and AEP. The flaws identified earlier that their mechanism of identifying the thresholds did not identify all the mechanisms that would lead to transformer failure as a result of GIC. Saturation is undesirable in the transformer operation. Therefore, thresholds that lead to transformer saturation are worthwhile investigating. Post-event analysis of a transformer that failed at Grassridge substation in South Africa [19], show that saturation occurred with GIC currents that reached approximately 5 A (1 min avg.). Figure 3.7 shows the GIC profile that was measured a three-phase, three-limb, 400/132 kV, 500 MVA at Grassridge substation on 31 March 2001. Sixth harmonic currents were also noticed and these are normally produced by transformers saturated with GIC. This result confirms that a very small GIC flow is adequate to saturate the core.

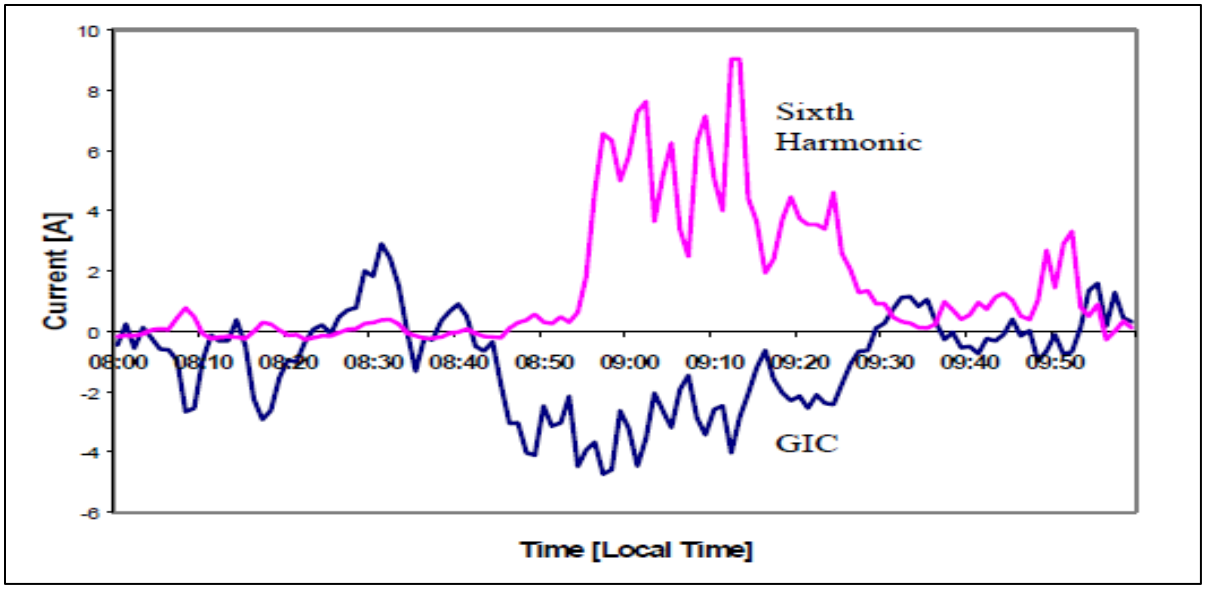


Figure 3. 6: The GIC and 6th harmonic in transformers measured in 2001 [19]

Moreover, the transformer at Grassridge was a 3p3L transformer that most researchers say are more robust and less affected by GIC. As is well documented, the presence of even a small amount of GIC (3-4 A per phase or less) will cause half-cycle saturation in a large transformer [35]. On 20th October, 1989, the transformer neutral current varied from +5 A to -2 A at Norwich Main in East Anglia, Pembroke in Wales, and Indian Queens in Cornwall for ten minutes. Two identical 400/132 kV, 240 MVA transformers at Norwich Main and Indian Queens failed, the voltage dips on the 400 kV and 275 kV systems were up to 5%; and very high levels of even harmonic currents were experienced due to transformer saturation by the geomagnetic storms [17]. The measurements of GICs and harmonics indicate that saturation occurred more than once in a three-limb three-phase transformer with GICs as low as 2 A/phase [12].

## 3.7 CONCLUSION

The chapter examined case studies of the effects of geomagnetically induced currents to transformers with the aim of getting thresholds of GIC that initiates damage in transformers. Three separate researchers have identified different thresholds, although their assessment criteria were the same. The transformers used in the researches were all single-phase transformer. The range of thresholds from these sources lies between 75 A/Phase and 155 A/Phase. In this research, it was identified that the assessment criteria used by these researches missed critical detail that leads to damage in transformers. Saturation and harmonic effects were not taken into account. Bringing in harmonics and saturation suggests that the real safe margin could lie between (1 to 5) A/Phase GIC, since GIC around 3 A/Phase causes saturation and the 1.5% Vthd to be exceeded, and transformers also saturate within low values of GIC (1 to 5) A/Phase. There is enough evidence from measurements and simulations that shows transformers saturating at low values of GIC. Among these is the saturation of the transformer at Grassridge substation and transformers in the United Kingdom that saturated and harmonics measured show an increase in triplen harmonics that are present in GIC events.

# CHAPTER 4: LABORATORY PROTOCOL AND SIMULATION PROTOCOL

## 4.1 INTRODUCTION

This chapter is dedicated to developing a laboratory and simulation protocol to investigate the response of a 3p5L transformer to geomagnetically induced currents. Bench-scale transformers are normally used to investigate the effects of GICs on transformers. In this study a slightly large transformer was used because core and coil material are of the same grade as that used in manufacturing large power transformers. The joint design should be similar to that of large power transformers such that the results are applicable in the real world. A relatively large power transformers may help in determining the thresholds of GIC initiating degradation in power transformers.

## 4.2 EXPERIMENTAL SETUP

In practice geomagnetically induced currents flow in the earth and enter the transformer neutral via grounded neutrals of transformers and they flow through transmission lines to the next substation and out again through grounded neutrals of star vector group transformers. The consequences of geomagnetic storms elaborated on the power system emanate from the transformer as discussed in the literature review. A complete replica of the real scenario would be to connect to transformers as given in Figure 4.1.

The use of two transformers was necessitated by the fact that the transformer under test needed a supply of 400 V and I was doing the tests in a workshop where 11 kV supply was not available for me to use a 11000/400 V transformer. Therefore, source transformer number 1 had to be 400/11000 V then the second transformer was 11000/400 V.

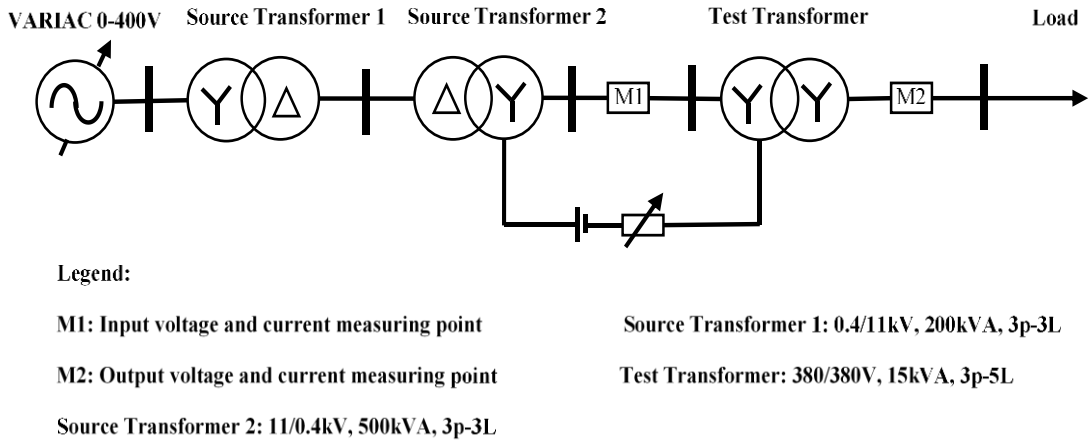


Figure 4. 1: Test system for transformer response to geomagnetically induced currents (GIC)

## 4.3 TEST EQUIPMENT

In order to carry out the tests effectively, without damaging the transformer and to extract reliable results, the following equipment was used for this project:

- DC Source: The DC supply circuit consisted of a 12 V, 100 Ah, rechargeable lead-acid battery and a variable resistor to change DC values.
- Power Meter: A high precision and wide bandwidth, IEC-l992 compliant Yokogawa WT1800 digital power meter was used for reactive power, voltage, current, and harmonics measurements.
- Load: A three-phase resistor bank load of 500 W per phase and 4 kVA per phase variable inductors.
- Source transformer 1: 0.4/11 kV, 200 kVA, 3p3L
- Source transformer 2: 11/0.4 kV, 500 kVA, 3p3L

- Transformer under test: 380/380 V, 15 kVA, 3p5L
- Variable load supply: A 3 phase (0-400 V), 60 A VARIAC.

## 4.4 TEST PROTOCOL

This laboratory protocol is designed to determine the step by step procedure to be followed when carrying out the intended tests and to determine the safe magnitude of DC injections that are going to be used without damaging the transformer. The test shall comprise of a source transformer and a transformer under test. The selection of the source transformer was such that the source transformer shall be significantly larger than the transformer under test so that the DC injection levels based on the load transformer characteristics would have a negligible effect on its magnetization characteristics. The following procedure shall be strictly adhered to:

- Initially the harmonics in the supply voltage shall be checked for compliance with IEEE Std. 579-19 which states that, harmonic content must not exceed a total harmonic distortion (THD) of 5%.
- Check if the supply voltage is balanced, otherwise unbalanced sources results in distortions that may inherently cause the transformer reactive power to increase. This may distort the reactive power analysis of this research project.
- Properly connect the transformer step-up as in Figure 4.1 and ensure that all connections are tight. Loose connections may cause heating of connections and subsequently burning cable insulation.
- Determine the short circuit and open circuit parameters of the transformer
- Carry out open circuit tests on the load transformer and determine the magnetization current. It is the current that corresponds to the knee point voltage.
- Use the magnetization current to calculate the per unit values of GIC currents that are safe to inject without causing permanent damage to the transformer.

## 4.5 TRANSFORMER RESPONSE TESTING

### 4.5.1 FLUX MAPPING

The magnetic field around the transformer core changes drastically when GIC currents are flowing within the transformer. In addition, leakage flux increases to the extent of flowing in the region where it is not supposed to such as the tank, tie plates and bolts, causing extensive hotspots in these regions. Thus, it is necessary to monitor that flux. The method employed in this thesis is the use of search coils. A search coil is a device that makes use of electromagnetic induction for measuring the strength of a varying magnetic field, for instance a wire made into a coil and tied around the core. Suppose a current (I) flows in a coil of N turns, a voltage E is induced in that coil, according to Faraday's law. The transformer equation can be used to determine the relationship between the voltage measured and the flux.

$$E = 4.44\phi_m f N \quad (4.1)$$

Where:

E = the induced voltage, $N$ = the number of turns, $f$ = the frequency and $\phi_m$ = the peak flux in the core.

The flux in the coil related to the flux density, $B_m$ and core area, $A_c$ as:

$$\phi_m = B_m A_c \quad (4.2)$$

Substituting 4.2 in 4.1 yields:

$$E = 4.44 B_m A_c f N \quad (4.3)$$

When a search coil is placed inside a changing magnetic field perpendicular to the coil, a varying e.m.f. will be induced across the ends of the coil. From equation 4.3 it is evident that the maximum induced e.m.f. is proportional to the maximum field strength. Therefore, by measuring the amplitude of the induced e.m.f. using a multimeter, the magnetic field strength can be obtained. Search coils of two turns shall be used, on the 3p5L transformer as shown in Figure 4.2:

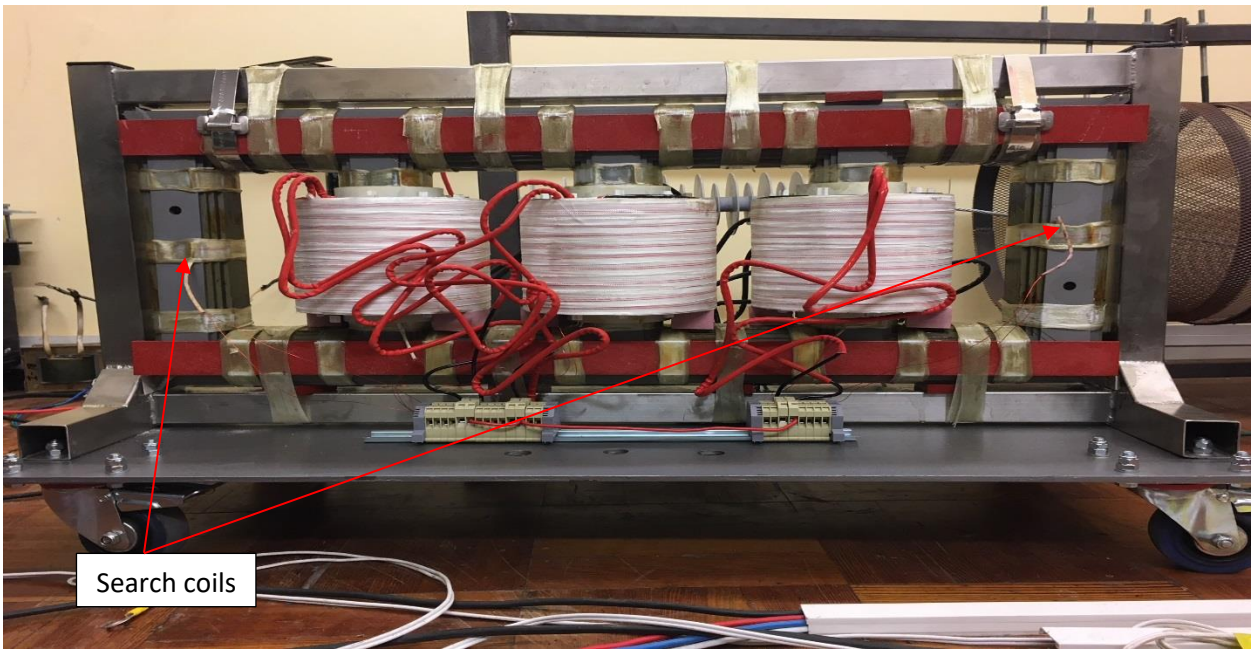


Figure 4. 2: Search coils positioned around the limbs and yoke of a 3p5L, 15 kVA transformer.

The search coil uses a 0.5 mm diameter insulated wire conductor. The designed volts per turn e.m.f. of the cores is 1.5671 V. Hence, the search coils should read 3.134 V at rated voltage (380 V). This voltage corresponds to the designed flux of 1.7 T of the transformer.

## 4.5.2 REACTIVE POWER AND HARMONICS MEASUREMENT

Voltages and currents were measured by an IEC76-1 (1976) compliant Yokogawa WT1800 Digital Power Meter. The meter is capable of performing online measurements and also has a facility whereby the instantaneous values of the voltage and current waveforms can be recorded and stored for post-processing. Fast Fourier Transforms are done up to the 10th harmonic (500 Hz). Samples can be taken over two and a half cycles within a resolution of 1002 readings (20.04 kHz), more than satisfying the Nyquist criterion. The neutral current could easily be calculated by application of Kirchhoff's laws during post-processing.

## 4.6 3p5L TRANSFORMER DUALITY TOPOLOGICAL MODEL

Figure 4.3 shows a duality topological model for a 3p5L transformer. Topological transformer models are now widely used because they reproduce phase-to-phase magnetic coupling as well as different operating conditions of the legs and yokes in saturation [68].

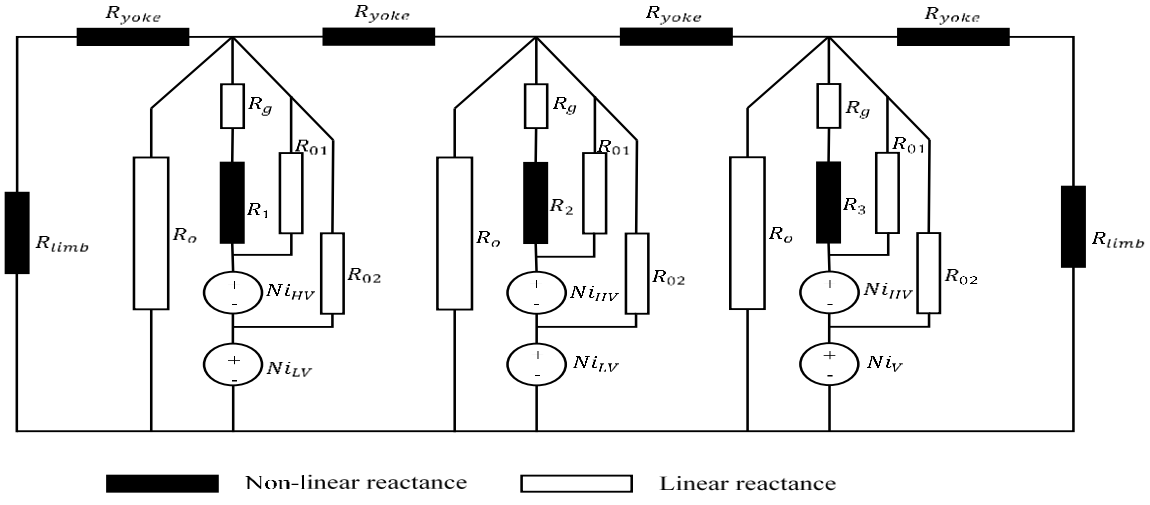


Figure 4. 3: Duality topological model for a 3p5L transformer [69, 71]

Topological models correctly represent transformer operation in regimes with high flux densities in the core [69]. A topological model focusses on representing the transformer magnetic fluxes in the core and those flowing within the windings (leakage fluxes), nonetheless, the flux in non-magnetic paths like air gaps is not considered [70]. One key aspect of the duality topological model is that the presence of the transformer tank can be effectively accounted for by linear inductances representing the paths of the off-core fluxes from yoke to yoke [69].

The duality topological model for 3p5L transformers have been developed in [69, 71]. The models were not different but one of the authors neglected the air gap reluctances and that will lead to a slight difference in the accuracy of the model. I used information from both papers to develop the duality topological model for a two winding, 3p5L transformer shown in Figure 4.4. In the model, the meaning of the symbols used is given below:

$R_o$ = the path of flux flowing from yoke to yoke through the surrounding non-magnetic medium i.e. "air".

$R_{01}\ and\ R_{02}$ = the equivalent leakage channels from HV-LV.

$R_g$ = the air gap reluctance at core joints

$R_1$, $R_2$, $R_3$ = the reluctance of the limbs in the phases

$R_{limb}$ = the reluctance of the return limbs

$R_{yoke}$ = the reluctance of the yokes

$Ni_{HV}$ and $Ni_{LV}$ = the sources of the magneto-motive force

The air gap reluctance $R_g = l_g/\mu_0 S_{leg}$ represents the reluctance of the air gaps at the core joints, which are related to the legs with the cross-section $S_{leg}$ and air gap length $l_g$ [72]. The reluctance of a core depends on the composition of the material and its physical dimension and is similar in concept to electrical resistance [72]. The magneto-motive force ($mmf$) is related to the reluctance ($R$), according to the following expression:

$$mmf\ (Ni) = \varphi R \qquad 4.4$$

The value of reluctance $R_{01} = \omega N_1^2 / X_{01}$ , which characterizes the channel between the core and outer (HV) winding. Similarly, $R_{02} = \omega N_2^2 / X_{02}$ refers to the channel between the core and the LV winding reluctance.

## 4.7 SIMULATION PROTOCOL

### 4.7.1 CREATING A GEOMETRY

A model is created based on real transformer dimensions and Figure 4.4 shows a geometry for the 3p5L transformer that I created using ANSYS MAXWELL FEM package. The units of measurement are chosen so that the dimensions represent the actual model. The core and the windings created are assigned a material.

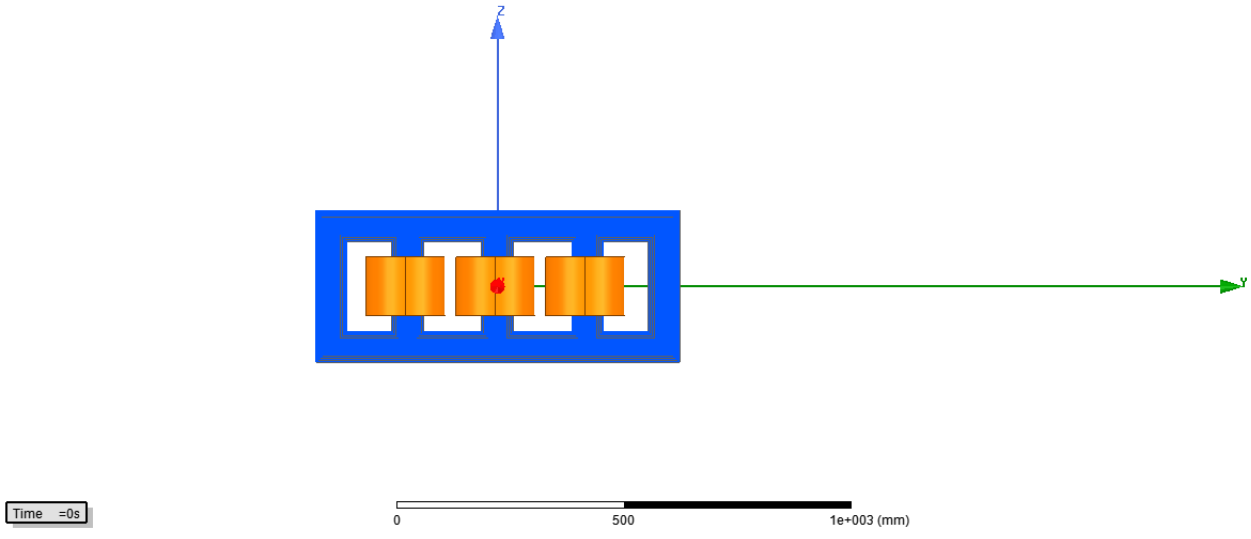


Figure 4. 4: 3p5L transformer model in FEM

When the windings are created and assigned a material (copper windings used in this project), the next step is to assign excitations and adding them to a particular winding (A, B, C). The AC voltages in each winding are specified using the following equations that specify the magnitude and phase difference between the phases.

- Winding A: Vpeak*(1-exp(-50*time))*sin(2*pi*50*time)
- Winding B: Vpeak*(1-exp(-50*time))*sin(2*pi*50*time+(2/3*pi))
- Winding C: Vpeak*(1-exp(-50*time))*sin(2*pi*50*time+(4/3*pi))

## 4.7.2 DEFINE CORE AND WINDING MATERIAL

ANSYS MAXWELL software allows the user to add customized material, and input the B-H curve and core loss data of the transformer. The designed magnetic flux density of the 3p5L transformer is 1.703 T and the B-H curve of the core material (M-5 grade steel) that has been used in FEM simulations is shown in Figure 4.5.

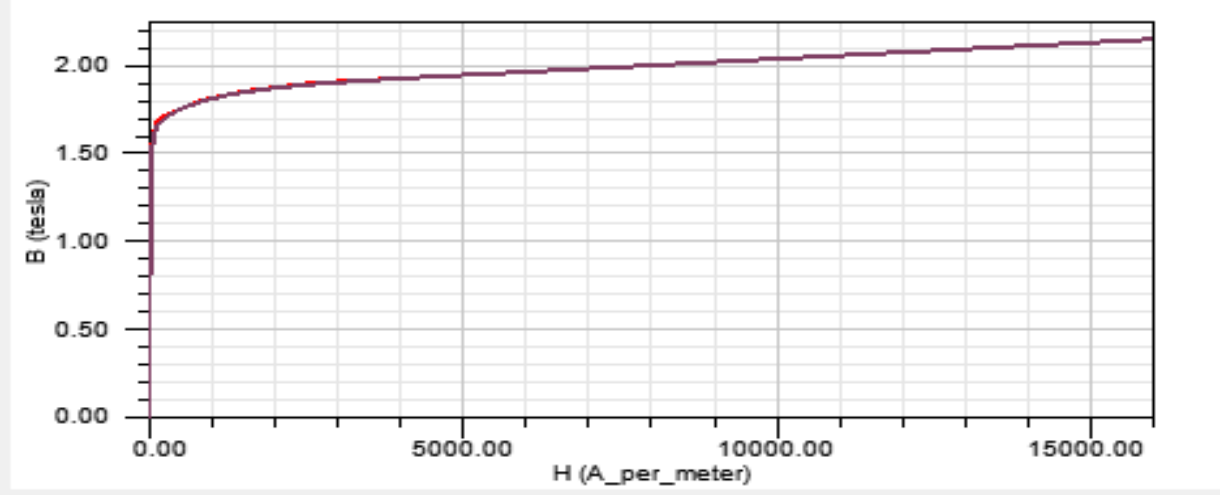


Figure 4. 5: M-5 Material B-H curve

The windings are made of enamel-covered copper wire. The enamel insulation is rated as temperature Class F, i.e. 180ºC. But for longevity sake, temperature rise is limited to 150ºC. The conductor used is 3.55mm diameter drawn ETP copper. The copper cross-sectional area is 9.8976mm$^2$. The design current density is 2.303W/kg.

### 4.7.3 ASSIGN MESH OPERATIONS

The process of representing a physical domain with finite elements is referred to as meshing, and the resulting set of elements is known as the finite element mesh [52]. Figure 4.6 shows a meshed 3p5L transformer model in ANSYS MAXWELL.

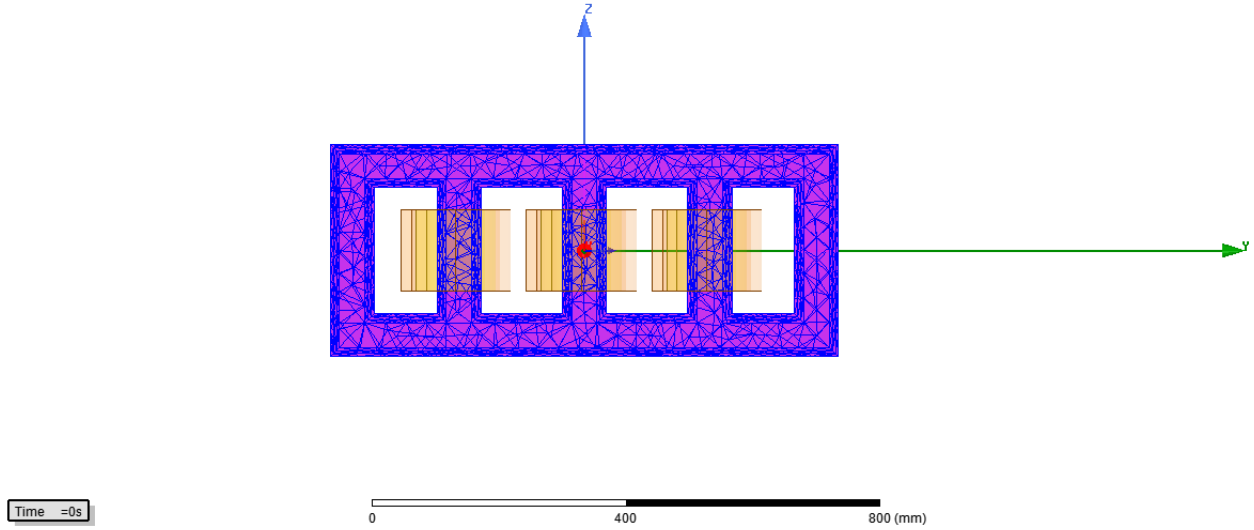


Figure 4. 6: A representation of meshing applied to a 3p5L, 15 kVA transformer

In the transient solvers, there is no automatic adaptive meshing. Therefore, the user must either link the mesh from an identical model solved using the magnetostatic and eddy current solvers, or

alternatively a manual mesh must be created. In this project, a mesh is created manually using "inside selection" to create elements throughout the volume of the transformer.

## 4.7.4 CREATING THE BOUNDARY REGION

Figure 4.7 shows a boundary region (pink) assigned on a 3p5L transformer. The boundary conditions are the specified values of the field variables (or related variables such as derivatives) on the boundaries of the field. Depending on the type of physical problem being analyzed, the field variables may include physical displacement, temperature, heat flux, and fluid velocity to name only a few. In the case of electromagnetic analysis, the boundary condition will be limiting the region in which the electric field extends to. This is done by first defining the region and assigning the vector potential of the boundary region to zero or assigning it a "balloon"- which is a non-conducting region.

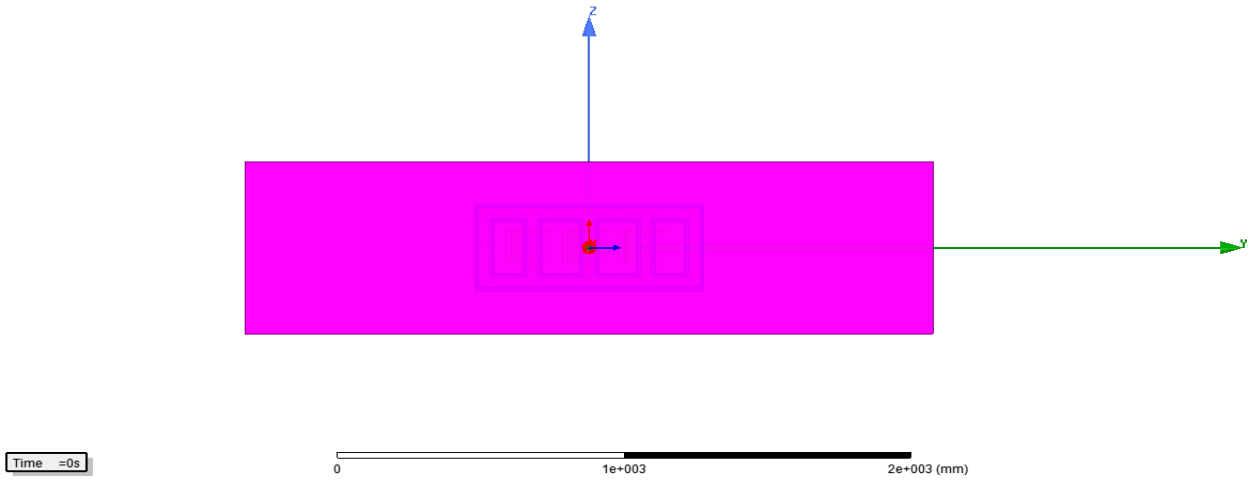


Figure 4. 7: Boundary region (pink) assigned on a 3p5L transformer

### 4.7.5 MODEL VALIDATION

On completion of all the processes, the software allows the user to verify if the problem has been formulated well without any errors by clicking the model validation TAB. The window shown in Figure 4.8 appears, showing that there is no error. If there is an error an X is marked against the operation/command.

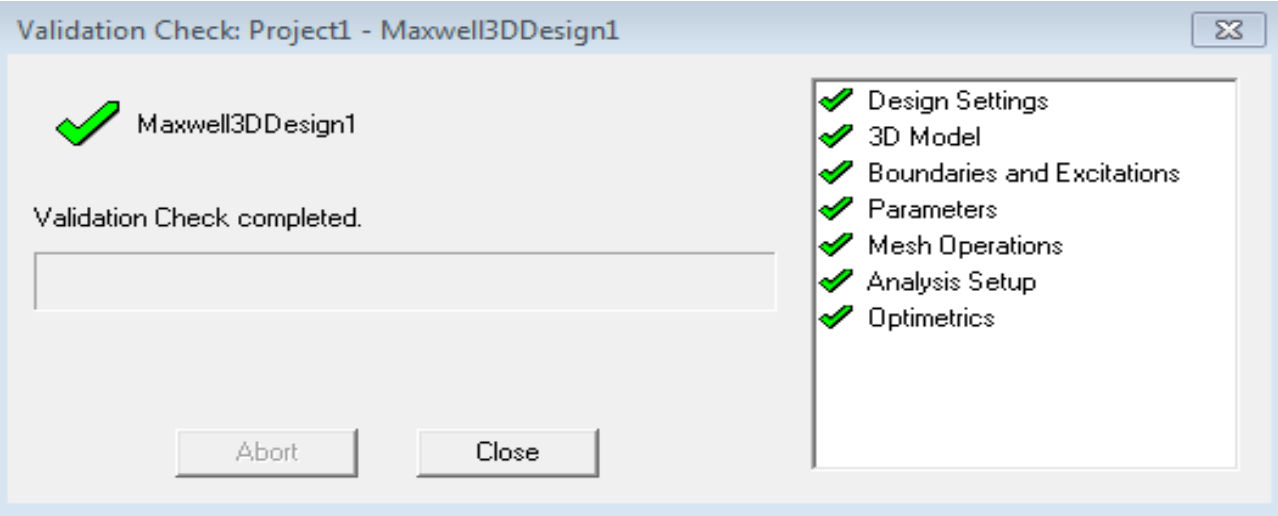


Figure 4. 8: Model validation in FEM software

## 4.8 CONCLUSION

The chapter details the laboratory and simulation protocols that were used in the investigations. The protocol is a powerful mind map that details the step by step approach that was taken to carry out experiments and simulations in this thesis. In addition, an overview of the duality topological model of the 3p5L transformer was described. These models can be used in transient and steady-state investigations. The duality topological model is used for low-frequency electromagnetic transient modelling. Most low-frequency transients are dominated by the behavior of the

transformer’s magnetic core. Their derivation is performed from the core topology and can represent very accurately any type of core design in low-frequency transients if parameters are properly determined.

# CHAPTER 5: PRESENTATION OF RESULTS

## 5.1 INTRODUCTION

This chapter presents the results from the experiments and simulations carried out as part of the investigations of 3p5L transformer responses to GIC. The experiments were carried out on 15 kVA transformers. FEM simulations were carried out on 15 kVA transformers to validate the experimental results.

Transformers Used: Larger transformers

- Source transformer 1:  200 kVA, 0.4/11 kV, 3p3L
- Source transformer 2: 500 kVA, 11/0.4 kV, 3p3L
- Transformer under Test: 15 kVA, 380/380 V, 3p5L

## 5.2 EXCITATION CURVE

A transformer is designed to operate in the linear region below its knee point. If the transformer voltage is increased beyond the operating range which is normally within 10% of its operating range, it begins to saturate. In the laboratory experiment, I excited the transformer until there was no major changes in the input voltage but the current kept on increasing. This determines saturation and a plot of the input voltage versus input current in Figure 5.1 shows the saturation curve obtained. AC voltage was used to excite the transformer in this test. On the other hand, introducing a DC source into the transformer may lead to quick saturation. These ac injection tests established that the magnetization current of the 3p5L transformer is 0.1 A, and this corresponds to the transformer's knee-point voltage.  The knee point voltage is 163 V.

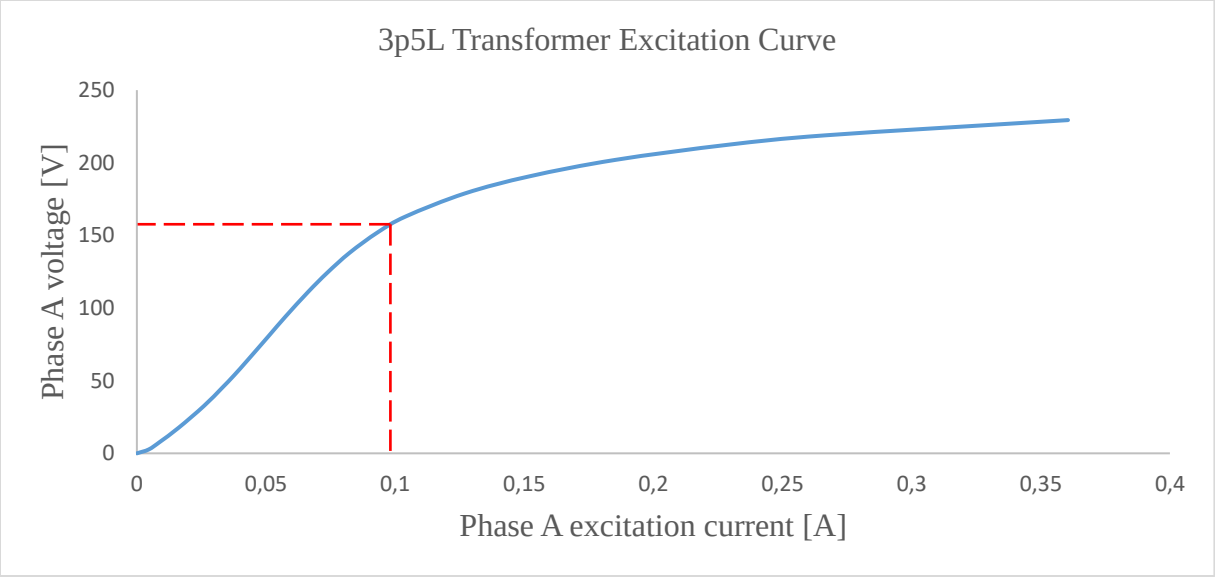


Figure 5. 1: Excitation curve for phase A of a 3p5L, 15kVA transformer

The knee point marks the end of the linear region of the transformer and hence for the purposes of this study, the transformers are going to operate at a de-rated voltage corresponding to the near point. A laboratory protocol that was done at the University of Capetown by Hilary Chisepo established that operating in the non-linear region will affect the validity of the results under DC tests [73]. The magnetization current value was used to determine the values of DC injected, as advised under the laboratory protocol [73]. Introducing geomagnetic induced currents with a transformer may saturate the core, causing it to operate in the non-linear portion of the magnetization curve.

The excitation curve represents the core material characteristic and the core structure [23]. At flux levels below the knee point, the curve is linear, with a very steep slope. This flux level is normally 1.7 T for power transformers. A small exciting current flows when the flux is at or below the rated value. The slope in this range represents the magnetizing inductance. The magnetizing inductance (slope of the curve in the unsaturated region) is determined by both the characteristics of the core steel and the small gaps in the steel at core joints. As the flux level reaches the rated value, the

slope or inductance decreases slightly. This is because the flux is concentrated at the joints, and localized saturation begins to occur. The saturation curve begins with slight saturation just above the knee point. As operating voltage continues to rise, this drives the transformer into deep saturation. Deep saturation causes the core's inductance to drop heavily and it approaches air-core inductance as the GIC continues to increase [74]. As the transformer reaches air-core inductance, the core's permeability reaches that of air. This inductance is commonly called the "air core inductance" because it is typically calculated based on the transformer winding configuration alone, as if that winding is suspended in the air without any magnetic core. In reality, the influence of the tank, structural members, and flux shields will make the final slope of the saturation curve slightly greater than the true "air core" inductance. Despite this difference, the common industry usage applies the term "air-core inductance" to the final slope of the saturation curve.

## 5.3 PHASE TRANSFORMATION LINEARITY (TuT)

Power transformers are designed to operate in their linear regions. The linearity was tested using the results from the open-circuit test and plotting the output voltage against the input voltage. Figure 5.2 shows a linear graph for the transformer phase linearity.

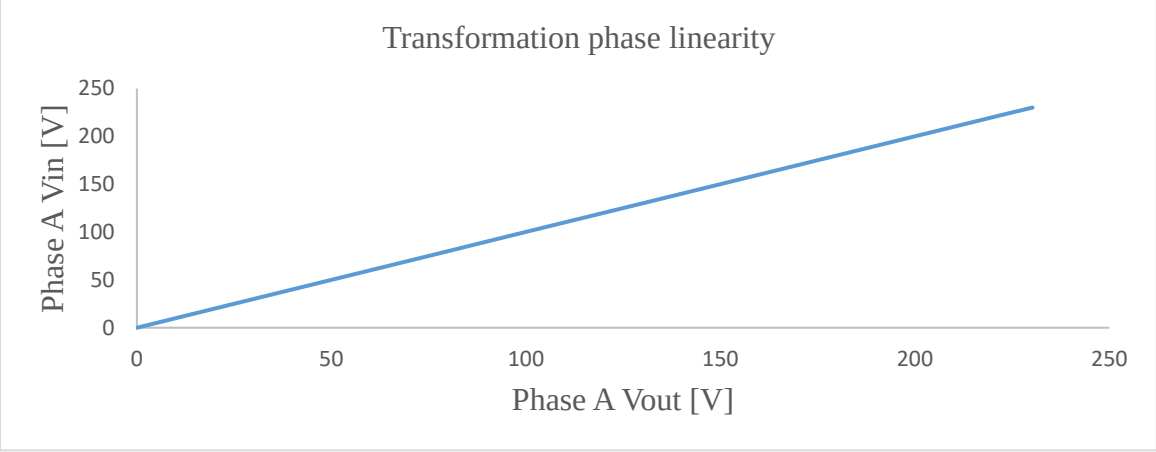


Figure 5. 2: Transformation phase linearity of the 3p5L, 15 kVA transformer

The results show that with AC only the transformer operated in the linear region. The significance of this test is to make sure that the saturation characteristics and subsequent results are solely coming from the DC injected and not from the poor design of the transformer.

## 5.4 MAGNETIZING CURRENT INCREASE WITH DC BIAS

Experimental results in Figure 5.3 show an increase in magnetizing current with an increase in DC injected. A transformer conducting DC undergoes asymmetrical saturation and its inductance drops heavily allowing more magnetizing current to flow [23]. The increase in magnetizing current has an impact of increasing the reactive power flow in the power system.

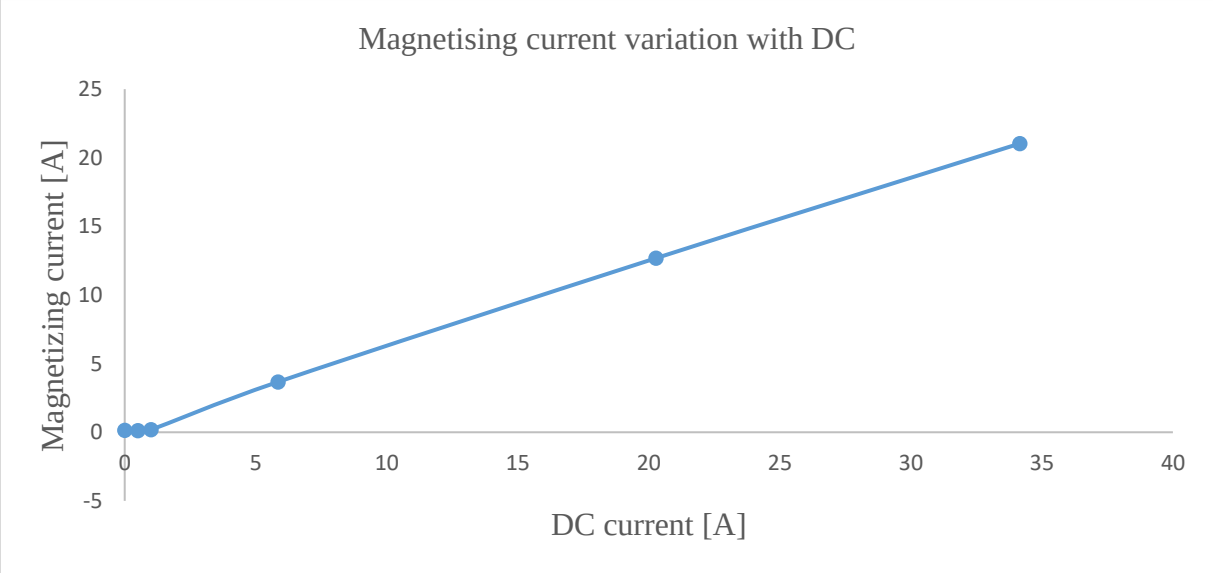


Figure 5. 3: Variation of magnetizing current with DC injection

The magnetization current of a transformer is very small with no DC in the neutral. Magnetizing current increases with several magnitudes in the presence of DC. The increase in magnetization current with increase in injected DC corresponds with simulation results performed by other

researchers [75, 76, 77]. Experimental results from researchers [28, 73] also concluded that there is a linear increase in magnetizing current as more DC is injected in transformer neutrals. Figure 5.4 shows that the magnetizing current of the 3p5L transformer increases a hundred-fold with a DC injection of 6 A in the neutral i.e. 2 A flowing in each phase.

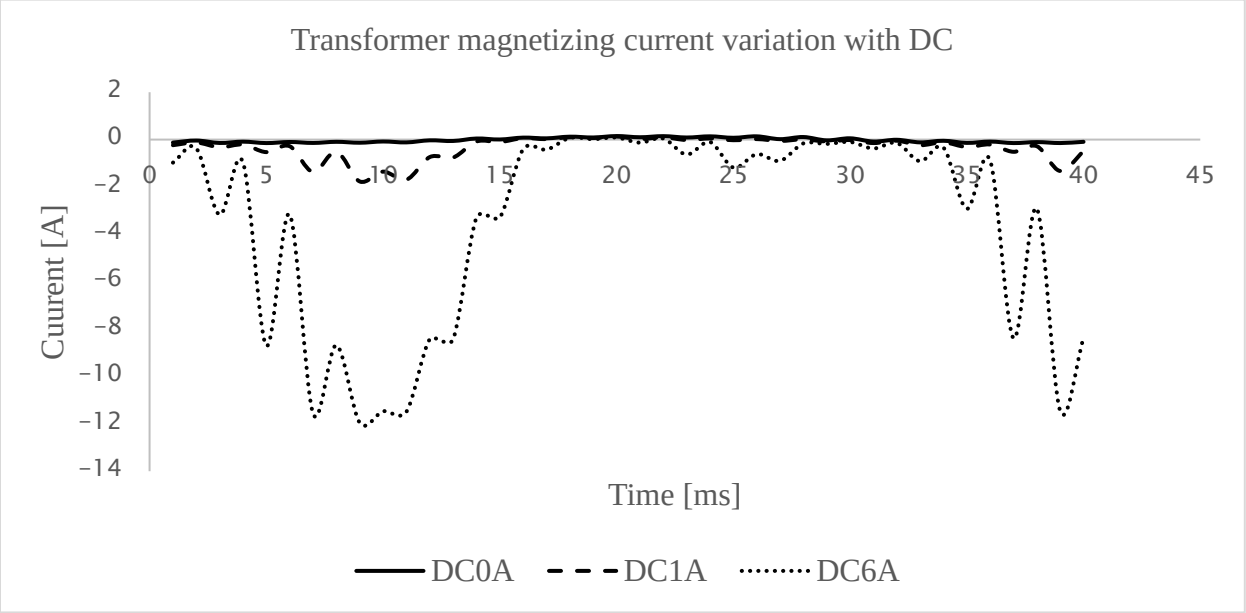


Figure 5. 4: Distortion and increase of the transformer magnetizing current with DC.

The magnetization current is distorted and increases in magnitude. These distortions cause an increase in harmonics that have devastating effects on transformers and the power system. In transformers the distortions give rise to hotspot temperature increase.

Figure 5.5 shows that asymmetrical saturation caused by DC starts at a very low current. The problems associated with DC flowing in the transformer emanates from saturation and distortion of the transformer magnetization current. McLyman in 2004, conducted studies that help to determine saturation analytically from the transformer exciting currents.

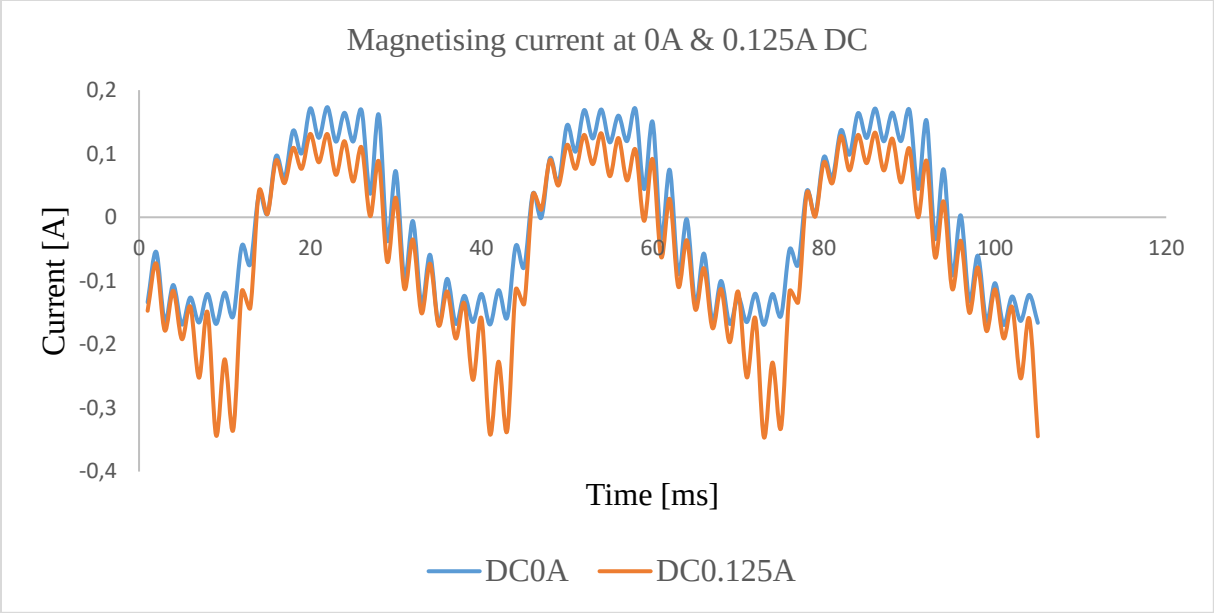


Figure 5. 5: Magnetizing current distortion with 0 A and 0.125 A DC in the neutral

McLyman concluded that saturation occurs when the peak exciting current is twice the average exciting current [70]:

$$I_{peak} = 2I_{avg} \quad 5.1$$

Where $I_{peak}$ is the peak exciting current and $I_{avg}$ is the average exciting current. The equation relates the point at which saturation starts to occur and does not entail full saturation or deep saturation.

## 5.5 REACTIVE POWER AND NON-ACTIVE POWER MEASUREMENT

### 5.5.1 REACTIVE POWER INCREASE WITH DC BIAS

Reactive power increase in transformers conducting GIC is a result of half-cycle saturation [5]. There are two methods of reactive power measurements that have been implemented in this thesis i.e. the IEEE conventional way and the general power theory (GPT). With the later developed at the University of Capetown as explained in section 2.6.1. The instrument used for reactive power measurement uses the IEEE definition of reactive power. It can store instantaneous values of current and voltage that are used to determine general power theory non-active power calculation. Figure 5.6 shows a graph of reactive power against DC in the neutral measured in the conventional way. The power analyzer (Yokogawa WT1800) is a high precision and wide bandwidth, IEC-1992 compliant measuring instrument, with a computational accuracy of ±0.001% for reactive power measurement.

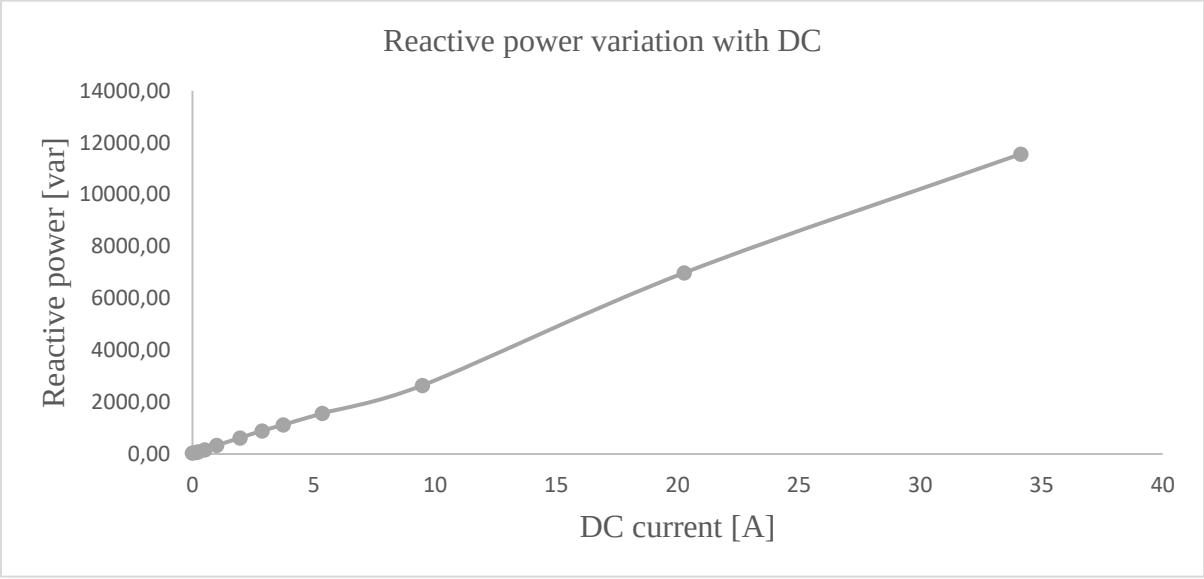


Figure 5. 6: Reactive power against DC in the neutral measured in the conventional way

The conventional methods of calculating power makes use of the power triangle and reactive power Q is obtained from the relationship, $Q^2 = S^2 - P^2$. The results show that there is a linear relationship between the reactive power and DC currents within a 3p5L transformer as shown in Figure 5.6. Hence, power utilities may use this relationship to notice if any potential hazards might result from geomagnetic storms. To ascertain this, the controller on duty must be alert and there is a need for the controllers to access geomagnetic data so that they check if the rise in reactive power is associated with space weather events. Reactive power increase under DC conditions may lead to voltage drop and power loss in a power system [78, 80]. The resulting voltage instability may cause relays to trip the power system due to a momentary disturbance. There is a need for power utilities to study simulate the protection settings under DC conditions to counter tripping that may have been avoided by using the current settings.

Static Var Compensators (SVCs) respond to power swings promptly, but the protection settings need to be carefully chosen to cater for momentary disturbances. This technique of revising protection settings was successfully implemented in the Hydro Quebec power system in Canada after the famous Hydro Quebec blackout of 1989 [79, 80]. The tripping could have been avoided by using suitable protection settings on SVCs that consider the effects of DC flowing in the network.

### 5.5.2 NON-ACTIVE POWER INCREASE UNDER DC BIAS

Several definitions of reactive power under distortion are available [81, 82, 83]. The general power theory (GPT) method is a powerful invention for measuring reactive power under distortions such as DC flow in power transformers and unbalanced load conditions. The Yokogawa WT1800 stores instantaneous values of voltage and current that were used for further computation of non-active power under DC conditions. The results are shown in Figure 5.7.

A linear relationship of non-active power is also exhibited in this method except that the slope has a higher gradient than the IEEE method. This implies an underestimation of reactive power when measured using the IEEE conventional method. A comparative analysis of the reactive power consumption of GIC saturated transformers using two different methods of calculating reactive power is given in Figure 5.8. As can be seen reactive power calculated using the GPT is much higher than in conventional methods. As a precaution, utilities may also consider the GPT when planning their reactive power reserves ahead of a GMD event.

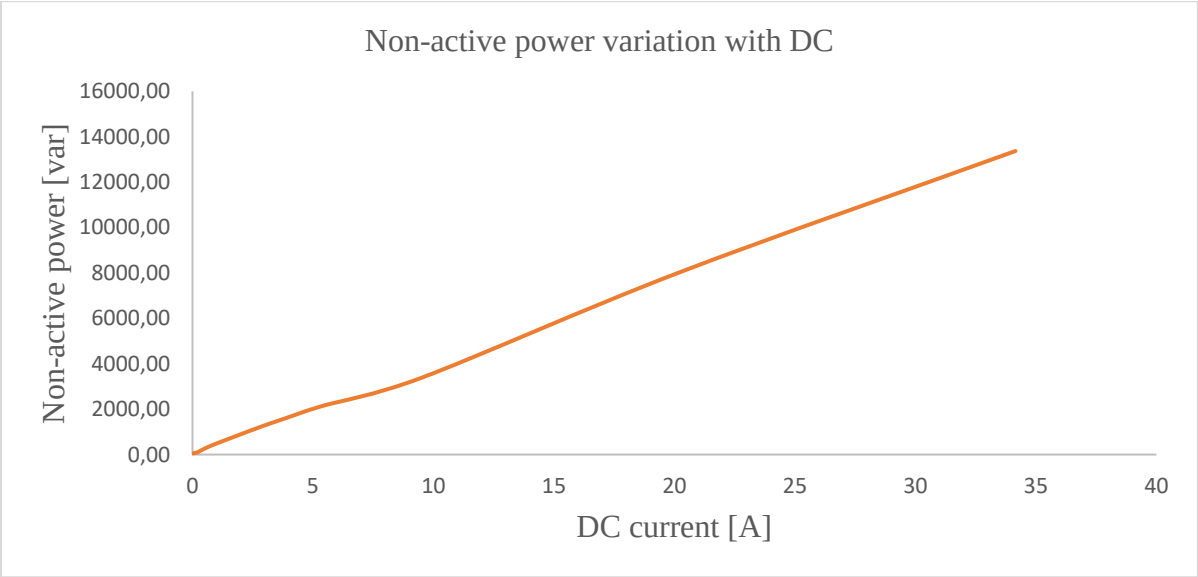


Figure 5. 7: Non-active power increase with DC injected in the neutral.

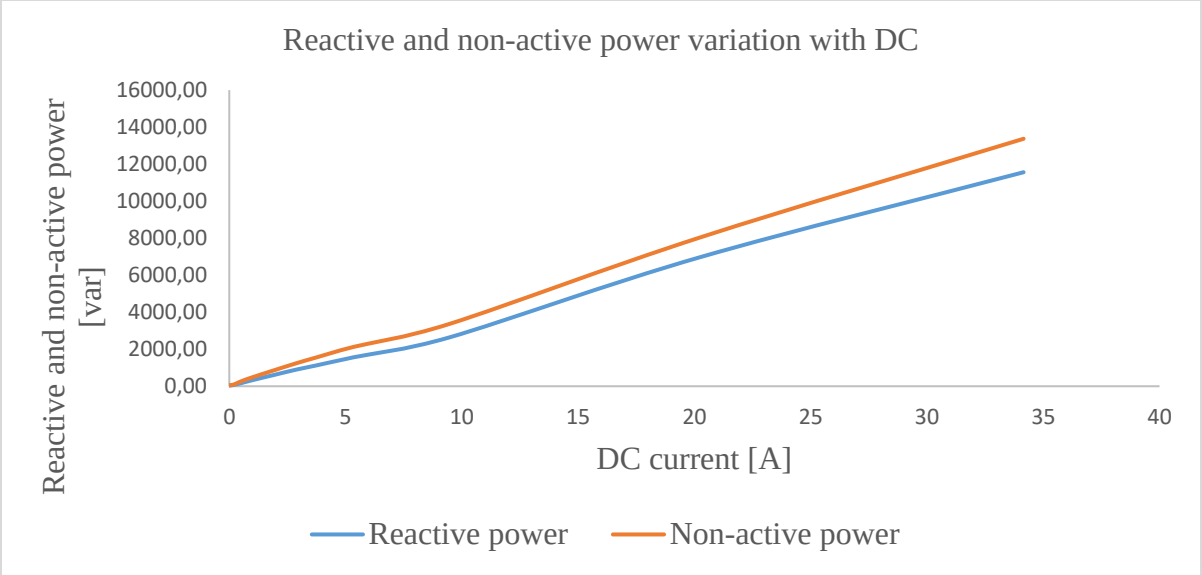


Figure 5. 8: Reactive power comparison of 3p5L, 15 kVA when measured conventionally (blue graph) and according to General Power Theory (brown graph)

The GPT showed much higher increases in non-active power as it takes into consideration the distortions in the line experienced under DC cases. At each instant, the GPT computed reactive power was bigger than the conventionally measured reactive power, with the margins widening with increasing DC injected. Increasing DC enlarges the amount of distortions hence the increase in the difference. The impact of distortions on reactive power is further noticed with the GPT curve being much steeper than the curve from conventional IEEE due to more distortions being present at higher DC injection.

### 5.5.3 REACTIVE POWER AT DIFFERENT LOADS

The effect of load on transformer reactive power consumption was also investigated. The results in Figure 5.9 show that there is not much increase in reactive power consumed when a reactive load is connected. There reactive power consumption at 1.5 kW and 3.0 kW load is almost

constant with a slight increase at higher loading. The difference in reactive power consumed seems to converge at higher DC values for all types of loads.

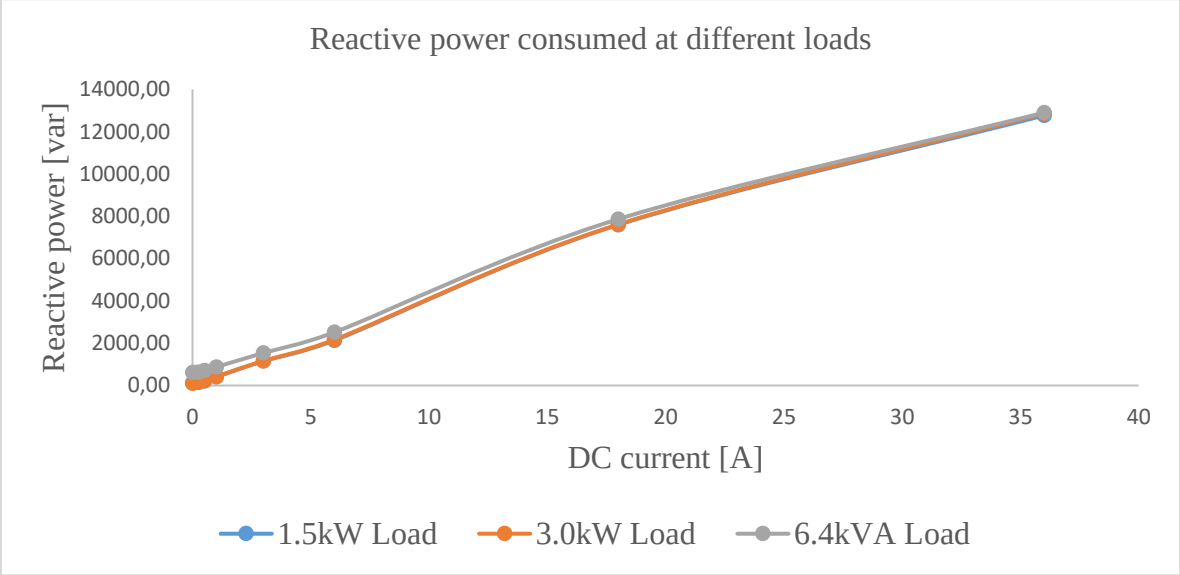


Figure 5. 9: Transformer reactive power increase at different loads.

## 5.5.4 S, P, Q INPUT VARIATION WITH DC BIAS

Figure 5.10a shows the variation of apparent power, real power and active power (S, P, Q) with DC at no load. Active power slightly drops as DC increases. The reason is partly due to the drop in load end voltage and the increase in core losses and magnetostriction [84]. A large increase in reactive power is a major contribution to the increase in apparent power. The drop in active power is minimal and thus its effect is outweighed by the massive increase in reactive power. S, P, Q output variation clearly shows that the apparent power and Q increase linearly with DC. This is the case at no load (Figure 5.10a) and with a 6.4 kVA load as shown in Figure 5.10b. The output power also drops because of drop in output voltage of the transformer as shown in Figure 5.10c.

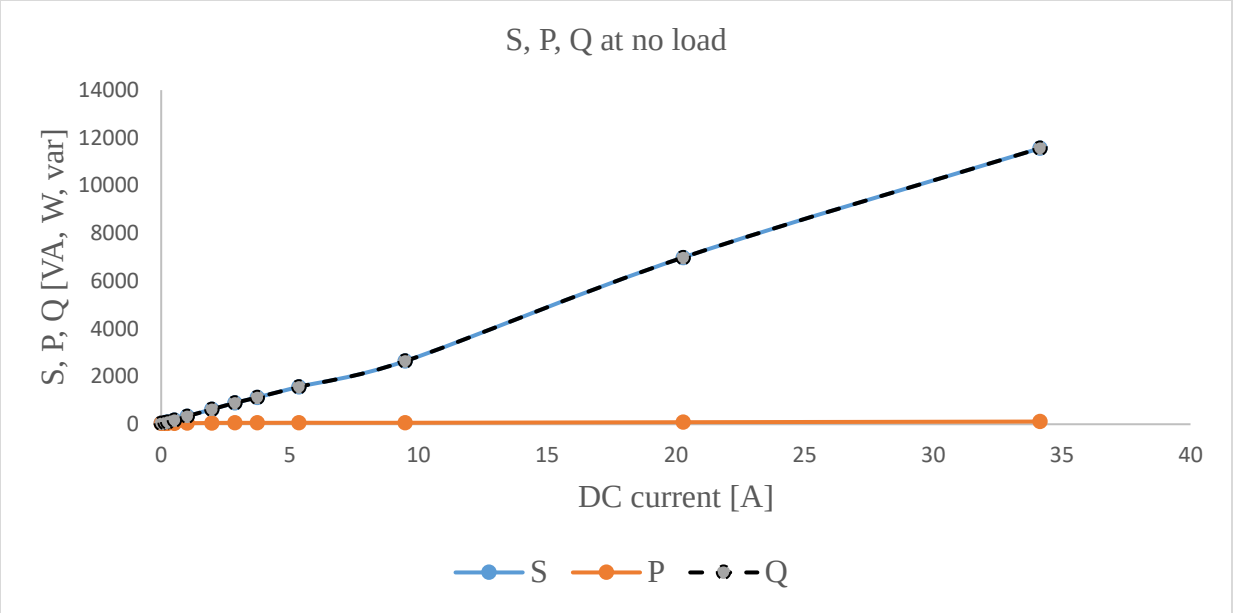


Figure 5. 10a: S, P, Q variation with DC at no load

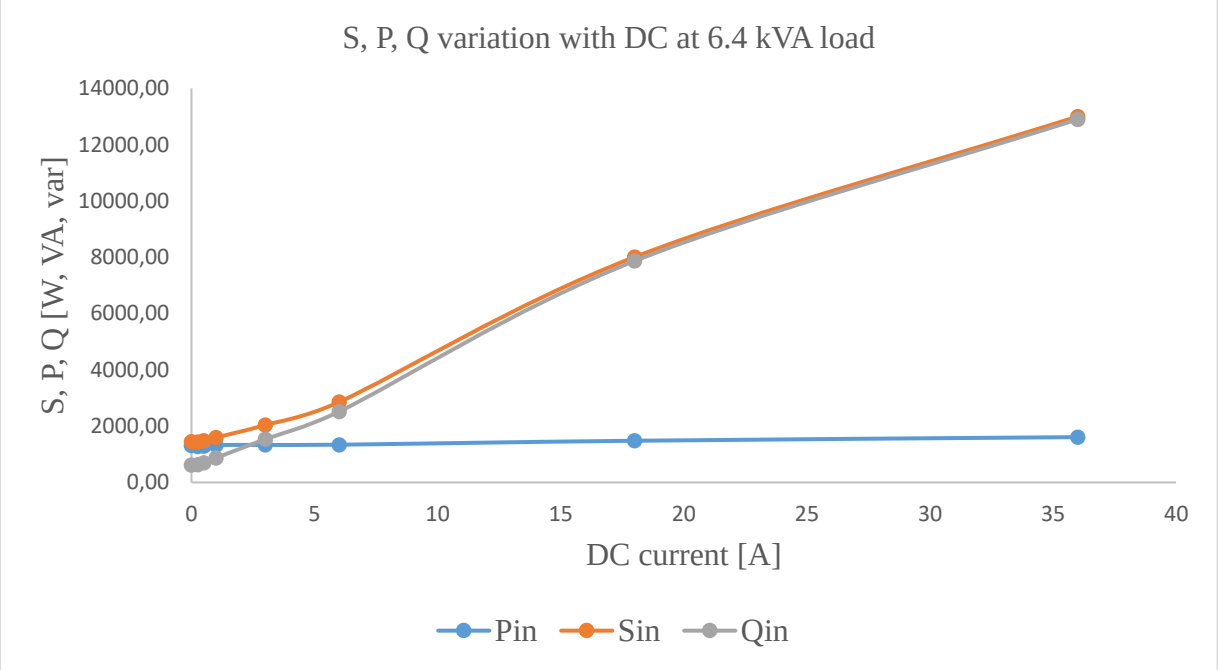


Figure 5.10b: S, P, Q variation with DC at 6.4 kVA

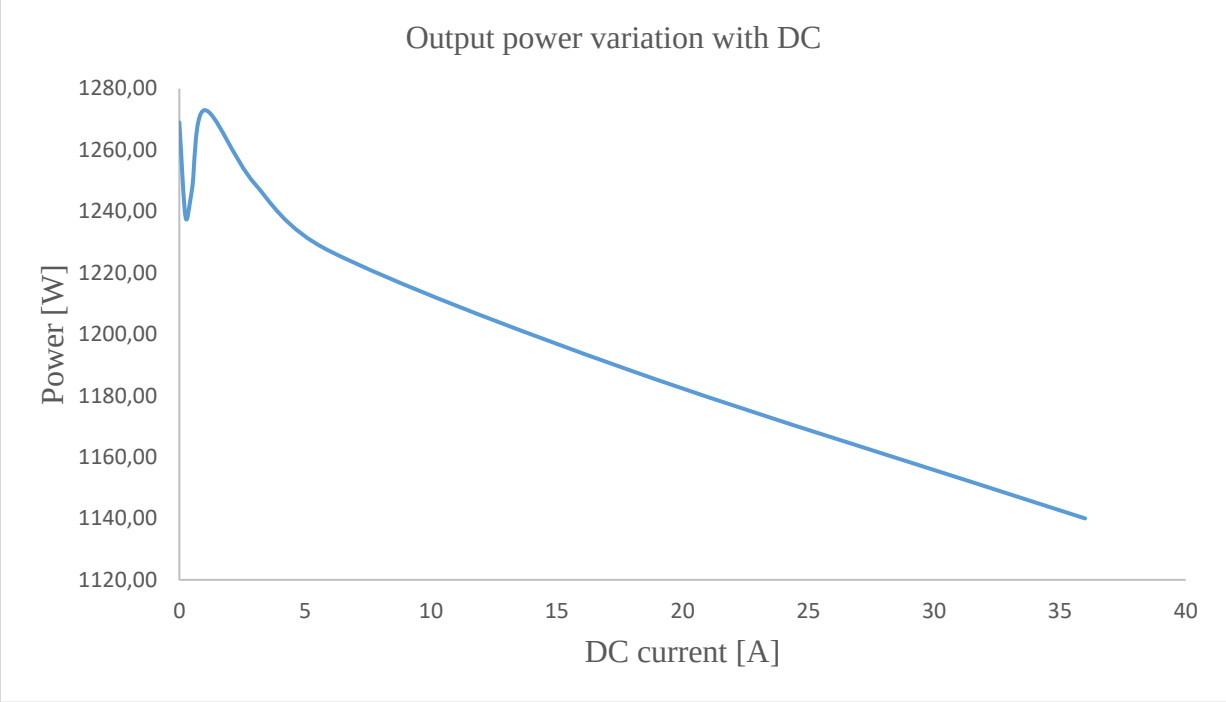


Figure 5.10c: Output power variation with DC at 6.4 kVA load

## 5.6 POWER FACTOR MEASUREMENT

### 5.6.1 POWER FACTOR MEASURED CONVENTIONALLY

Power factor is a good measure for the system performance. An increase in DC current flowing in the transformer reduced the power factor of the system as shown in Figure 5.11. This experiment was carried out with a load of 1.5 kW. The output power factor remains constant at unit power factor through the entire duration of the experiment since the load is resistive.

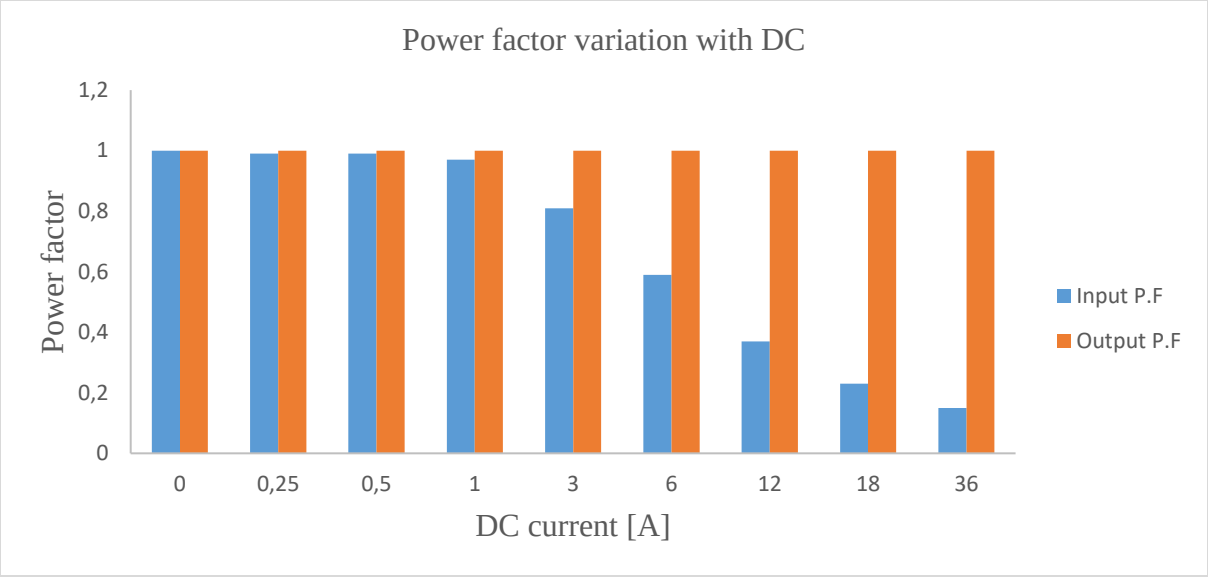


Figure 5. 11: Conventionally measured power factor with 1.5 kW load connected

The input power factor, however, drops hugely with increase in DC. A power factor of 0.8 is considered good for a transformer. It takes 3 A DC in the neutral for the input power factor to drop from unity to 0.8. DC beyond 3 A in the neutral will push the power factor of the transformer into a lower power factor that causes operational costs of supplying electricity to increase. At 6 A in the neutral, the input power factor drops to 0.6. From these results, we can say that 3 A of DC in the neutral is the threshold of DC that does not excessively affect the operational costs of supplying electricity.

## 5.6.2 POWER FACTOR USING CONVENTIONAL AND GPT CALCULATIONS

Power factor is a good indicator of losses in the power system. The flow of DC in a power system reduces the power factor and hence the performance of the system as explained earlier. The power factor calculations using General Power Theory and the IEEE conventional method is shown

below. The experiment was conducted with a 3 kW load connected. The difference exhibited in the power factor in Figure 5.12 is largely due to increased reactive power losses when measured using the general power theory.

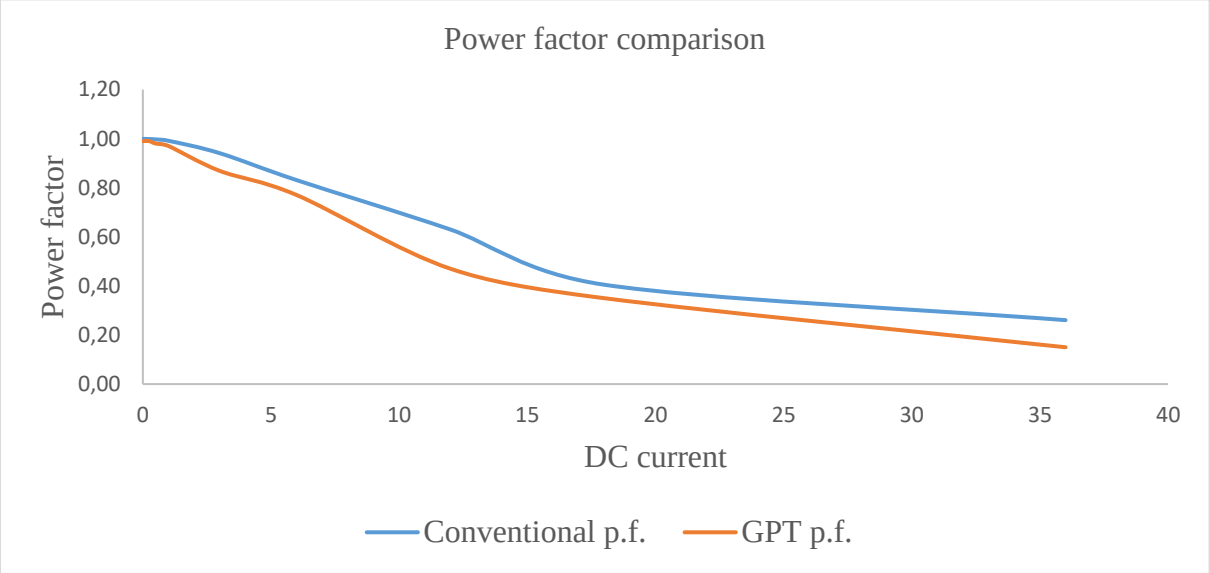


Figure 5. 12: Power factor comparison of 3p5L, 15 kVA when measured conventionally (blue graph) and according to General Power Theory (brown graph)

In both cases the drop in power factor is caused by increased heating, reactive power losses, and increased flow of harmonics when a transformer is subjected to DC flow. Thus, the flow of DC results in poor performance of the system as indicated by power factor measurements.

## 5.7 CORE LOSS INCREASE WITH DC

Figure 5.13 shows the core loss variation in a transformer injected with DC. The core losses increase with an increase in DC injected. Core losses are made up of copper losses, eddy current losses and hysteresis losses. Copper losses increase is attributed to higher magnetization currents

with an increase in DC. The increase in magnetizing current and harmonics causes the flux to increase in the core leading to more eddy currents flowing in the core. On the other hand, hysteresis losses which are a result of the vibrations in core material termed magnetostriction also increase with DC causing an ultimate rise in hysteresis losses.

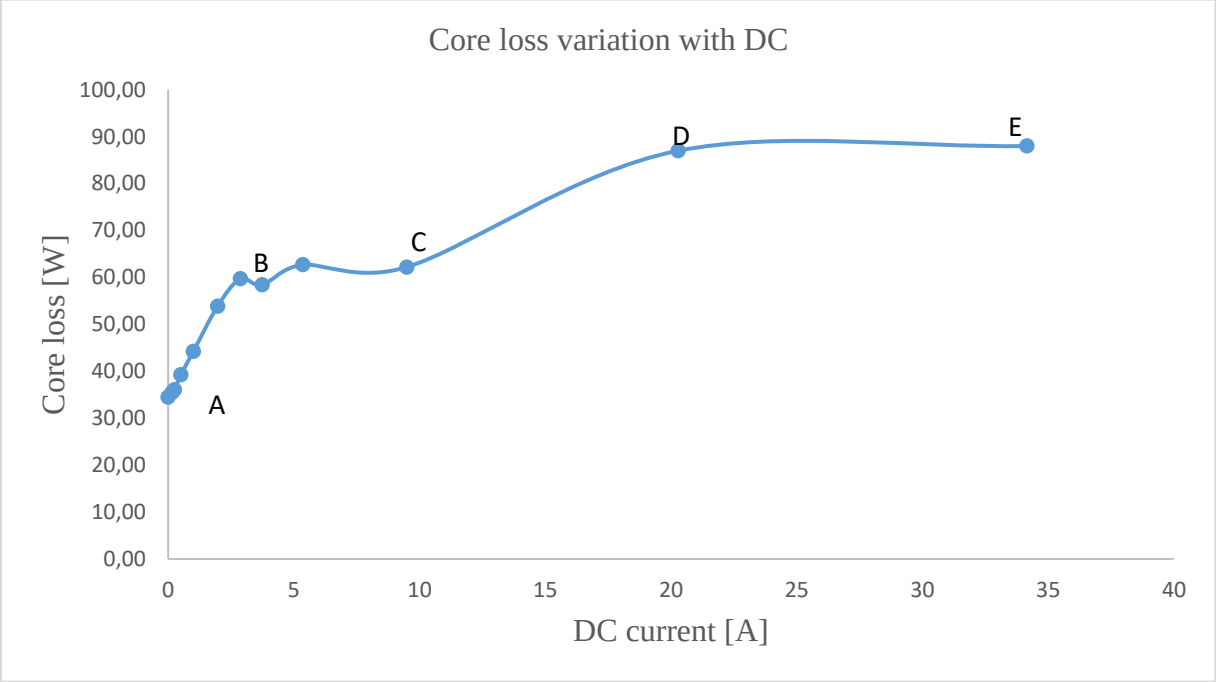


Figure 5. 13: Core losses increase with DC injected in the neutral

The core losses were measured at a de-rated voltage of 160 V in accordance with the laboratory protocol. Above this voltage the transformer will be operating in the saturation region as seen from its excitation curve. The various points on the graph denotes the following changes within the transformer:

- A to B – flux is increasing in the core and core losses gradually increases
- B to C – core losses maintains its value from 3 A to 12 A DC in the neutral as the level of saturation is almost the same.

- D - Between 18 A and 20 A DC in the neutral, the transformer moves into deep saturation and the core losses increase sharply from 60 W to 88 W.
- E – There is no difference between core losses at D and E as the transformer is in deep saturation where there is no further increase in core losses whereas almost double the DC is applied between points D and E.

## 5.8 LOAD END VOLTAGE UNDER DC BIAS

The voltage profile of a power system under severe geomagnetic disturbance normally falls as shown in Figure 5.14. This is due to the increased reactive power consumption of the saturated transformer.

The increased reactive power will add to the existing load of the generators at the power station. A heavy load slows down the speed of the generators and as a result the frequency drops. The relationship below illustrates how frequency depends on the speed of generators;

$$f = \frac{np}{120} \qquad 5.2$$

Where: f=frequency, n=speed in revolutions per minute and p=number of poles

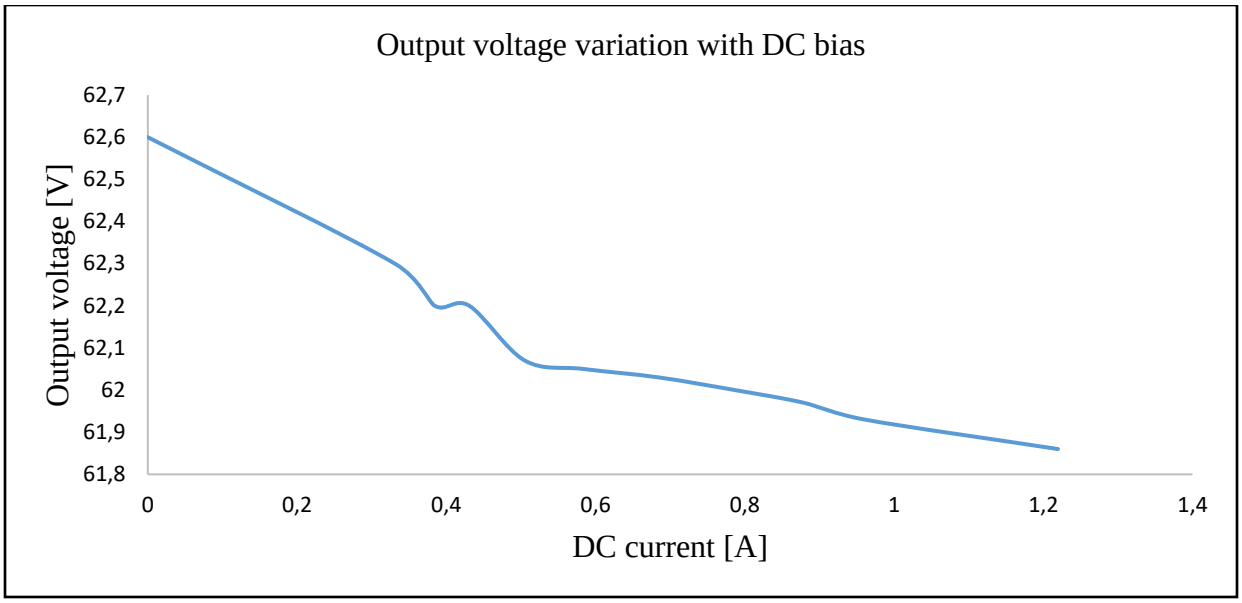


Figure 5. 14: Load voltage profile of 3p5L transformer under DC bias

The excitation system responds by increasing the excitation current and thus boosting the MVAr flow into the system. At the same, the SVC capacitors will also kick in in order to offset to supply the extra demand in reactive power. According to [29], the additional reactive power demand during a geomagnetic disturbance (GMD) event, if not offset by reactive power compensation equipment, can cause a reduction in the system voltage to the point of encroaching secure system limits. In actual sense, the quasi-DC caused by GIC is not unidirectional, therefore the reactive power is fluctuating resulting in power swings.

A closer look at the Hydro Quebec collapse (Figure 5.15) shows that voltage declines during a GMD, and as the voltage reached 0.7 p.u the first line tripped. Lines have under-voltage and overvoltage protection, and in this case the under-voltage relay tripped the line. Also, if the line is protected by distance protection as the voltage drops drastically, the impedance of the line may fall within the tripping zone thus the line is taken out of service. The tripping of the line further worsened the reactive power demand, and the voltage further dropped. The tripping of the last line remaining line separated the La Grande network from the Hydro Quebec network. Complete

isolation of the La Grande network caused frequency to rapidly fall on the Quebec network. In response, automatic load shedding system tripped the load but could still not offset the loss of approximately 9400 MW of generation from La Grande Complex. Complete separation of the network caused the voltage to rise dramatically.

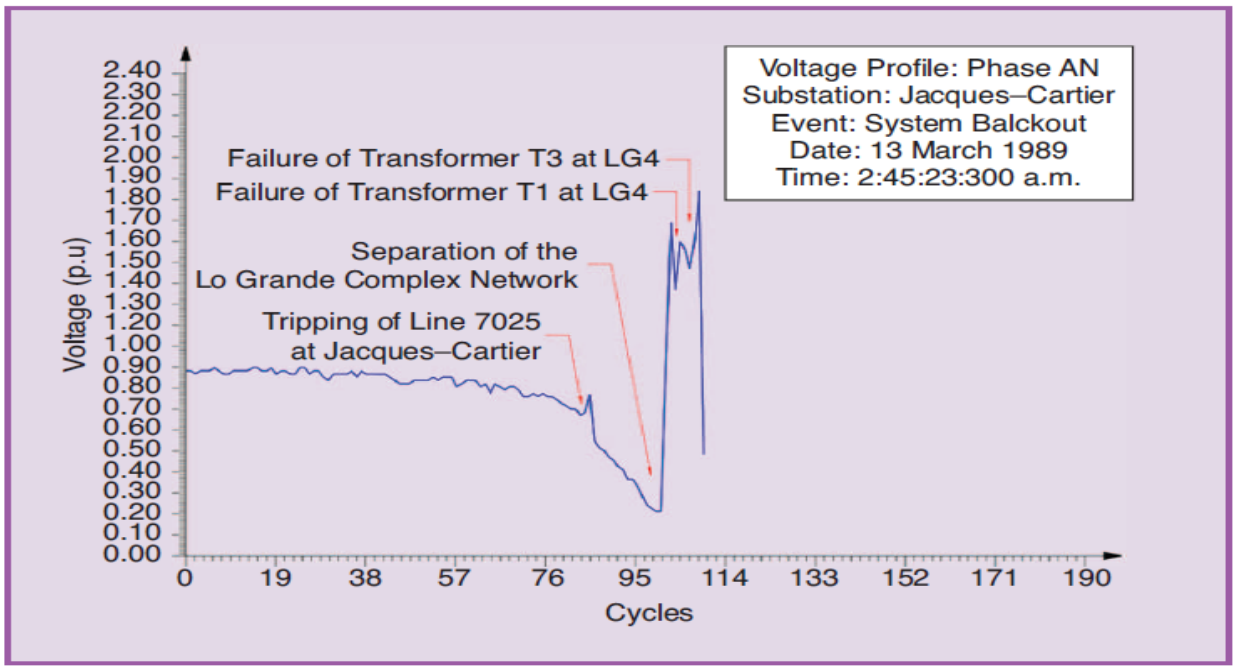


Figure 5. 15: The voltage collapse and over-voltages as observed at the Jacques-Cartier substation [74]

The reason for a sharp increase in voltage is that the generators were running fast and unexpectedly there was no load to supply hence an open circuit condition was created. The no-load voltage is usually very high, the only load to the generator was the transformer and at nearly 1.5 p.u one phase of the transformers permanently failed.

## 5.9 HARMONICS UNDER DC BIAS

The principal threat to electrical infrastructure during a GIC event is spot heating of the transformer core due to harmonic currents. A factor called the total harmonic distortion (THD) is used to quantify the harmonic content of a given voltage or current wave. THD is a measure of the magnitude of all the harmonic components present in the wave as compared to the magnitude of the fundamental component [48]. The THD is expressed as follows:

$$THD = \sqrt{\sum_{h=2}^{N} \left(\frac{I(h)}{I(1)}\right)^2} \quad 5.3$$

A THD of 5% for a voltage wave means that the harmonic content is 5% of the fundamental component. Definitions of THD are given in [60]:

$$V_{THD} = \frac{\sqrt{V_2^2+V_3^2+V_4^2+V_5^2+\cdots}}{V_1} \times 100\% \quad 5.4$$

**Voltage THD**: Total harmonic distortion of the voltage waveform. The ratio of the root-sum-square value of the harmonic content of the voltage to the root-mean-square value of the fundamental voltage.

$$I_{THD} = \frac{\sqrt{I_2^2+I_3^2+I_4^2+I_5^2+\cdots}}{I_1} \times 100\% \quad 5.5$$

**Current THD**: Total harmonic distortion of the current waveform. The ratio of the root-sum-square value of the harmonic content of the current to the root-mean-square value of the fundamental current.

The extent to which harmonic currents cause spot heating, and the impact of that heating on transformer life vary depending on various factors including transformer construction and core type.

### 5.9.1 VOLTAGE HARMONICS ON NO-LOAD

Several researchers have said that triplen or third-order harmonics are predominant in transformers conducting GIC [19, 36, 85]. This research has shown that this is the case at no load only for 3p5L transformers as seen from Figure 5.16. When the transformer is loaded, both even and odd harmonics exist with no specific order being predominant.

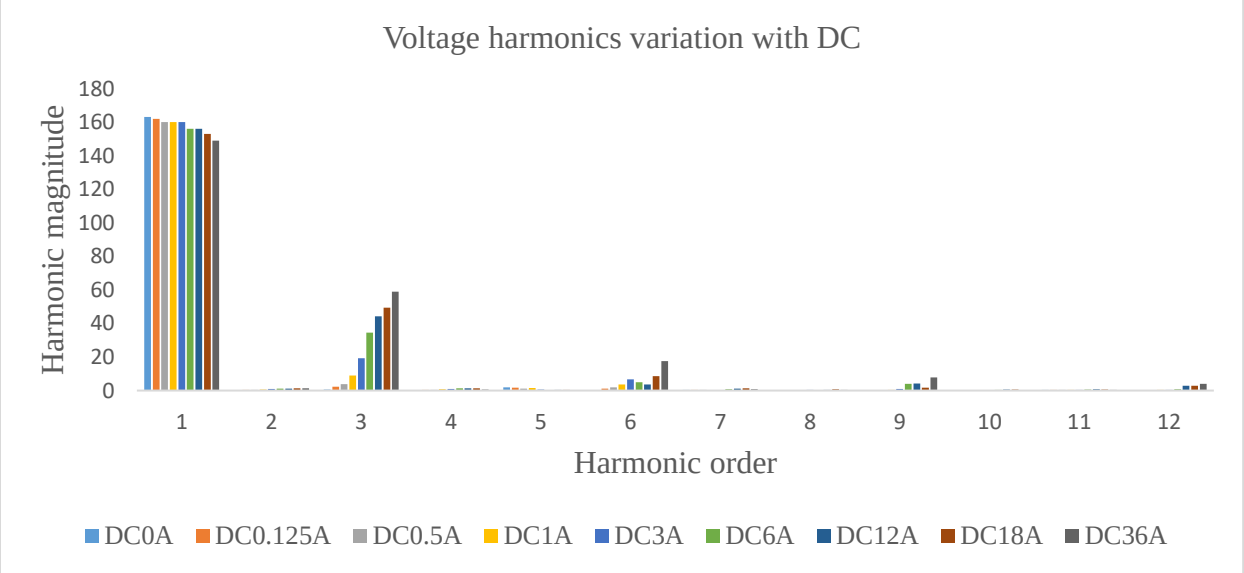


Figure 5. 16: Voltage harmonics on no-load [85]

Triplen harmonics are zero sequence currents that flow in the phases and back into the neutral. That is why a neutral conductor will need to be oversized (compared to phase conductors) to carry out these extra-currents [85]. For example, in the presence of around 10 Amps of 3rd order harmonics in each of the 3 phases will mean an extra current of around 30 Amps in the neutral conductor (at 150 Hz in a 50 Hz installation). Other effects of triplen harmonics are excessive neutral currents, transformer failures, excessive heating of motors, electronic device failures, failed capacitor banks, breakers and fuse tripping, and interference in communication systems [81].

## 5.9.2 CURRENT HARMONICS NO-LOAD

The current harmonics at no load increase as DC is increased as shown in Figure 5.17. Higher-order harmonics seem to diminish at each level of DC injected. First-order harmonics increase slowly from 0 A to 18 A DC and there is a huge rise when the DC is doubled to 36 A in the neutral. The increase of second-order and higher-order harmonics shows an almost linear pattern.

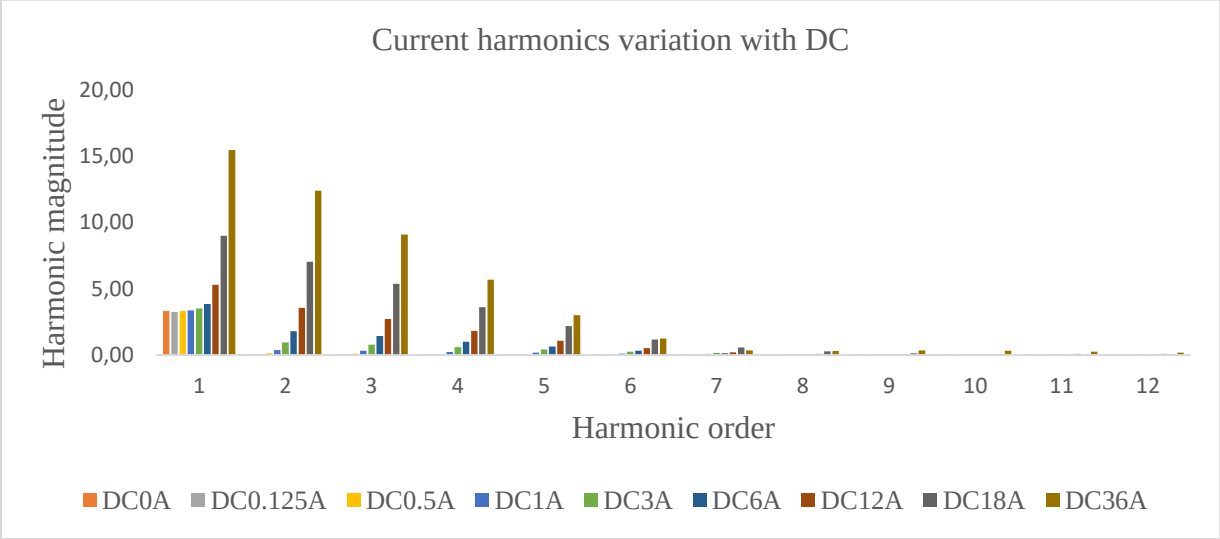


Figure 5. 17: Current harmonics increase with DC in the neutral at no load [85]

### 5.9.3 VOLTAGE THD WITH A LOAD OF 1.5 kW LOAD

The current and voltage THD results at the input side are shown in Figure 5.18. Current and voltage THD with a load of 1.5 kW is 1.2% and 1.1% with no DC injected into the system. A DC approximately 2.2 A is sufficient enough to give a THD rise of current beyond the IEEE threshold of 20% [55]. In contrast, voltage THD needs a much higher current to surpass the IEEE threshold of 5%. It can be seen that there is a very steep rise in current THD between 1 A and 12 A in the neutral. At higher values of DC the THD will stabilize because the inductance of the transformer will be almost constant in deep saturation. It is believed that as more DC is injected, the transformer will reach air-core saturation and that subsequently lead to the THD to drop [85].

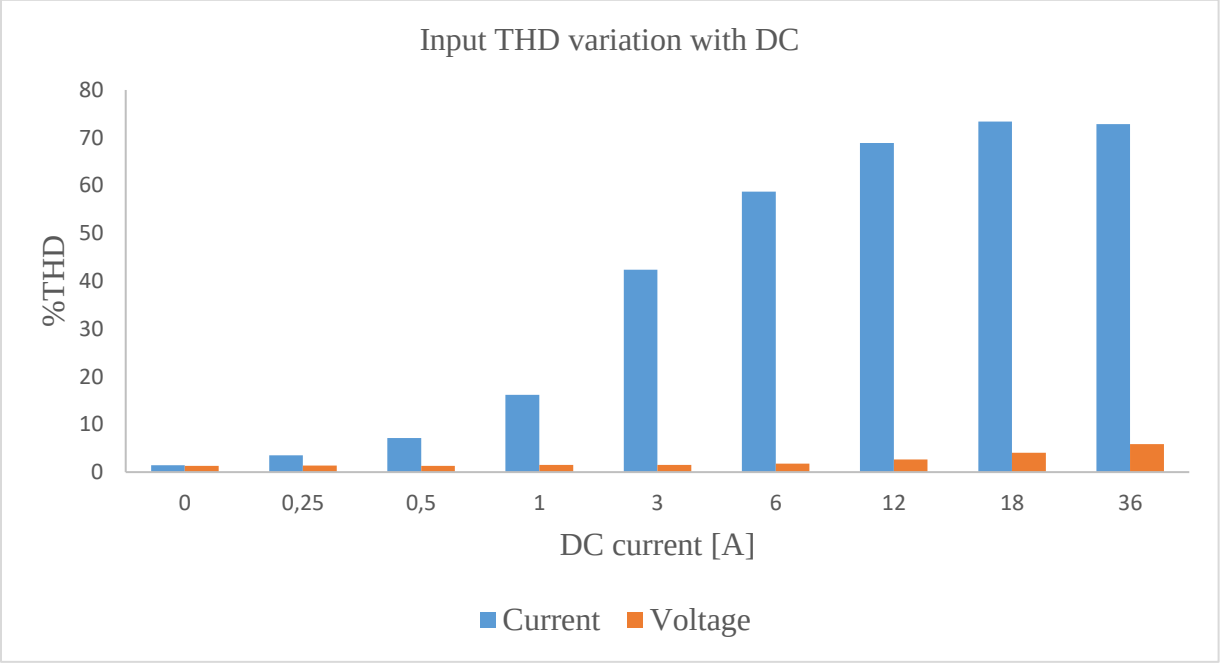


Figure 5. 18: Current and voltage THD as measured from the input side [85]

The input and output THD of voltage is shown in Figure 5.19. As explained earlier, in both cases, a DC of 25A DC in neutral is required to surpass the IEEE threshold of voltage. This current is 36.71 percent of the rated current of the transformer used in the investigations.

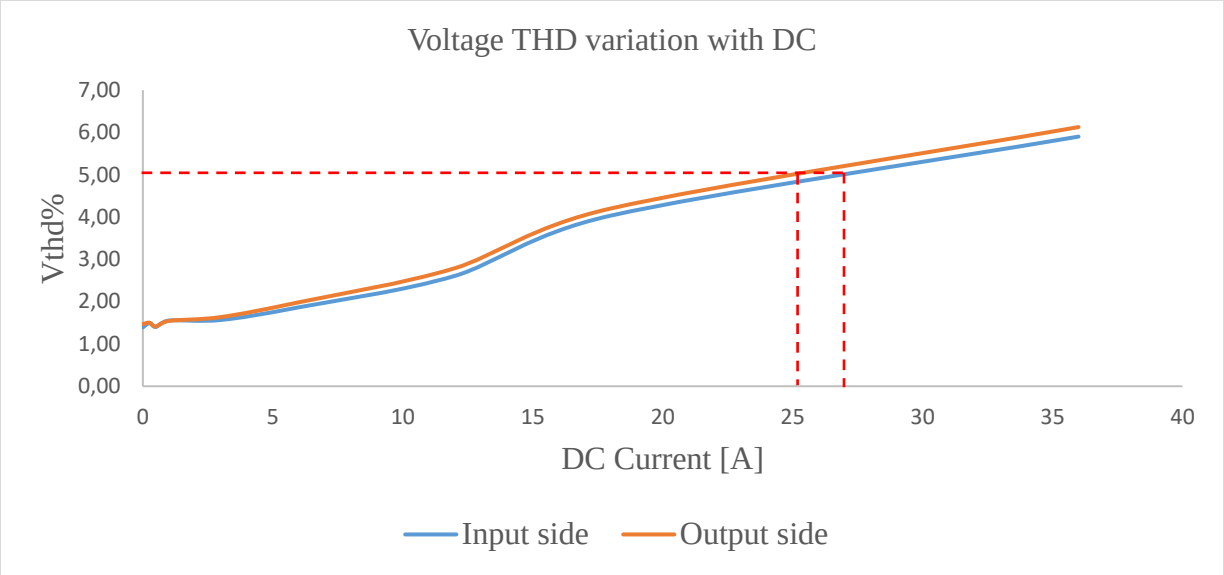


Figure 5. 19: Input and output voltage THD [85]

## 5.9.4 HARMONICS AT DIFFERENT LOADING

The voltage THD at varying loads was also investigated in order to establish the effect of load type on THD. Three different loads that were used are; THD r1 – at 1.5 kW load, THD r2 – at 3 kW load, THD rl3 – at 6.4 kVA. The conclusion is that voltage THD is lower for resistive loads than inductive loads, while it is slightly maintained for resistive loads [83]. This means power utilities will suffer the effects of GIC more when they have inductive loads. Figure 5.20, shows the variation of voltage THD at varying loads.

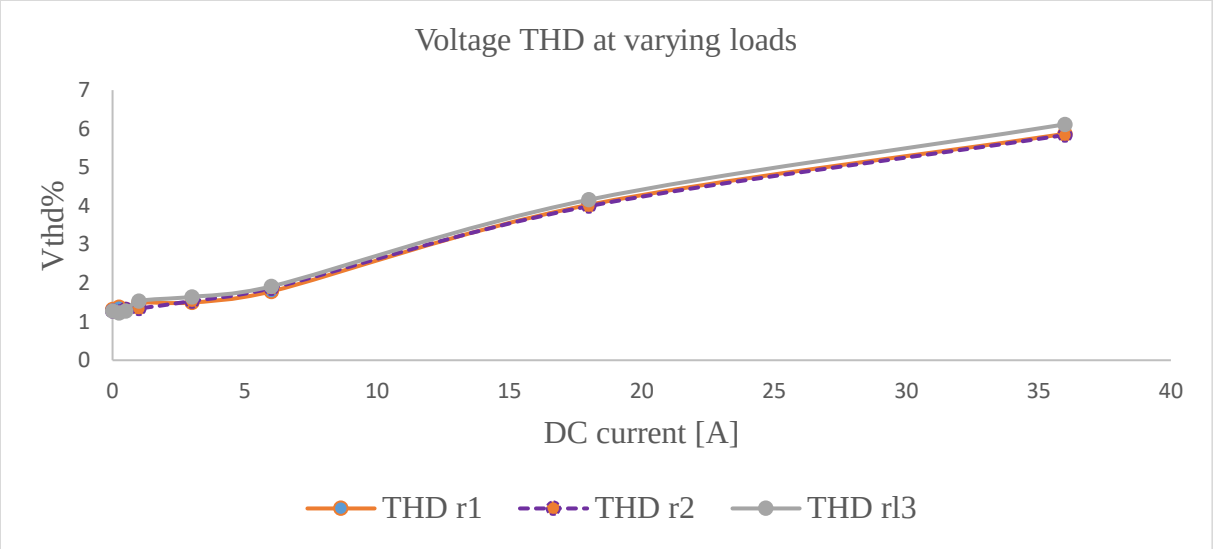


Figure 5. 20: Voltage THD at varying loads [85]

The current harmonics at different types of loads shown in 5.21 also show that the current harmonics are lowest at higher resistive loading i.e. 3.0 kW. The current harmonics THD surpasses the IEEE threshold of 20% at 2.2 A in all cases. This means that the operational conditions of equipment are likely to be affected by harmonics at very low DC currents.

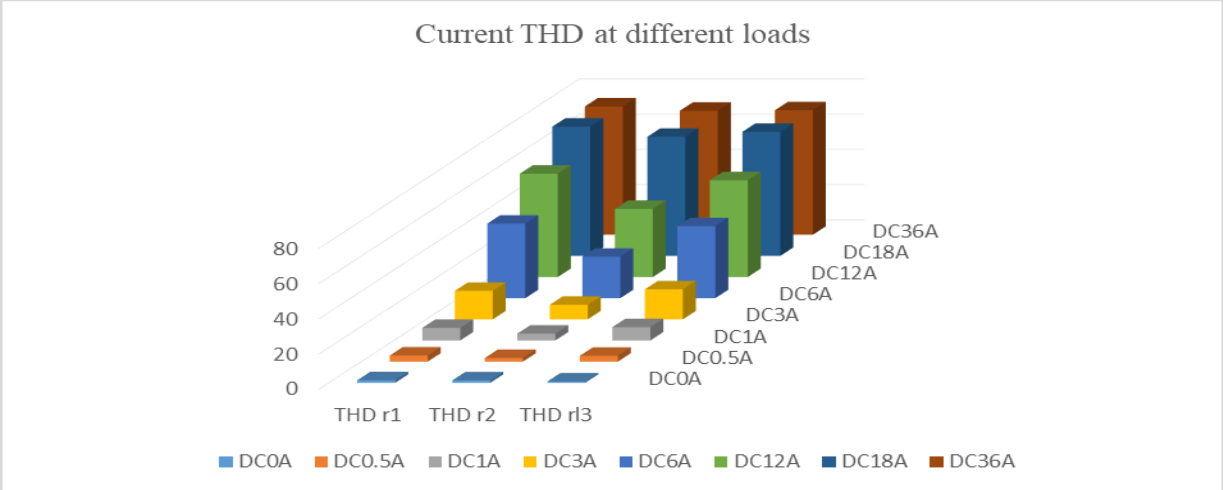


Figure 5. 21: Current THD at 1.5 kW, 3 kW and 6 kVA.

## 5.10 FLUX MEASUREMENT AND ANALYSIS

### 5.10.1 CORE FLUX ANALYSIS

Search coils were implemented as a way of measuring the behavior of flux under DC conditions. Figure 5.22 shows the positioning of search coils around the core to monitor flux in the limbs and yoke.

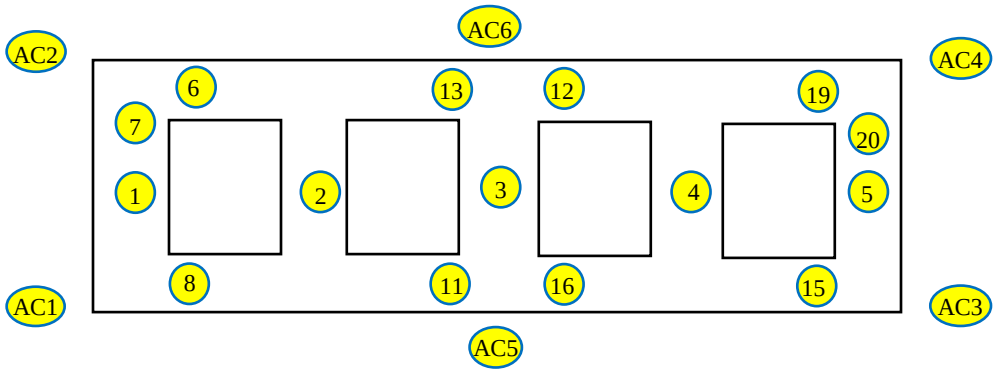


Figure 5. 22: Positioning of search coils around the core.

Air search coils to monitor stray flux out of the core are denoted AC1, AC2, AC3, AC4, AC5 and AC6. There was no flux measured in these search coils up to 36 A of DC injected in the transformer neutral. Twenty search coils were tied around the core and these were named SC1 to SC20. Some of the search coils are symmetrical and would read the same value: SC6=SC8; SC11= SC13; SC12=SC16; SC15=SC19. Figure 5.23 shows the variation of measured search coil voltage against increasing DC values.

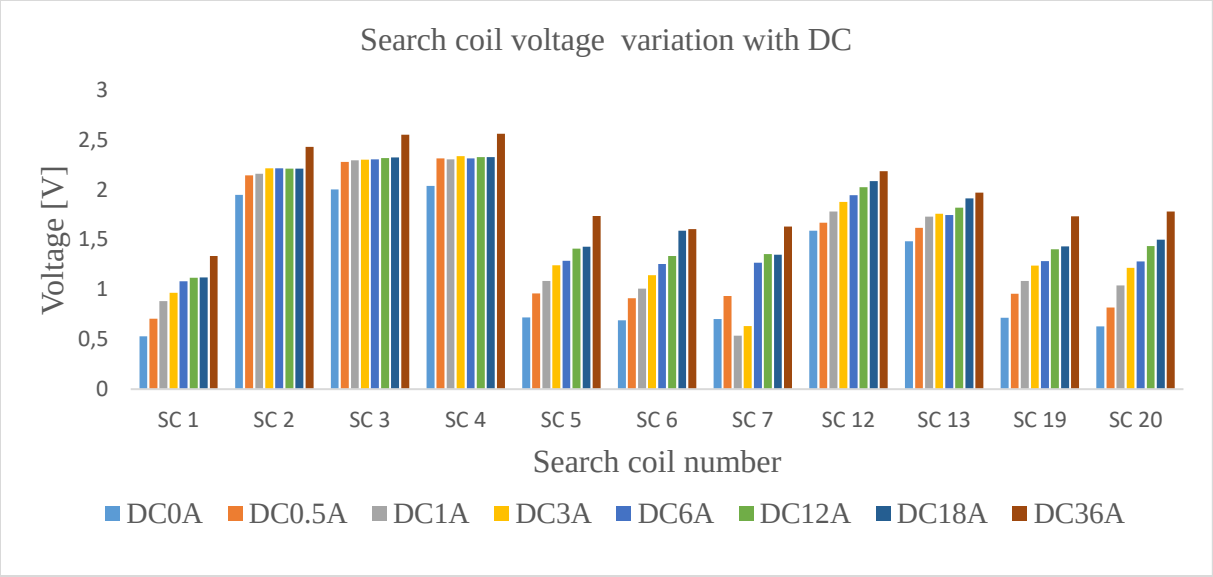


Figure 5. 23: Flux variation in the core

There is a general increase in the search coil voltage i.e. flux in the core as DC is increased. The flux measurements in the phase limbs SC2, SC3 and SC4 are the same and they were all increasing with DC and the greatest increase can be seen when the DC was doubled from 18 A to 36 A. The return limbs also shared the return flux equally with an almost linear increase exhibited in the measured search coil output voltage.

## 5.10.2 AIR SEARCH COILS WITH DC (STRAY FLUX)

The 3p5L transformer is mostly used in European networks but it is also available in the South African network. The transformer has two return paths for flux, this is not the case in a three-phase three-limb (3p3L) transformer. In a 3p3L transformer conducting GIC, the flux must travel through a high reluctance path outside the core to complete its circuit. The stray flux is believed to cause heating of the tank and other structural parts of the transformer. Most studies have reported that there is no stray flux outside the core in a five-limb transformer. Thus, it is envisaged that, heating of the tank in the five-limb transformer cannot occur as a result of GIC flow. However, this does

not dismiss that heating of other structural parts of the transformer does not occur. There was a fast rise in the flux in the core as measured using search coils tied around the core in the investigation that we carried out in the laboratory. This rise in flux may cause heating of the core, tie plates and core bolts in power transformers. A DC of 12 A per phase was injected in the five-limb transformer and air search coils were installed in the positions shown in Figure 5.24.

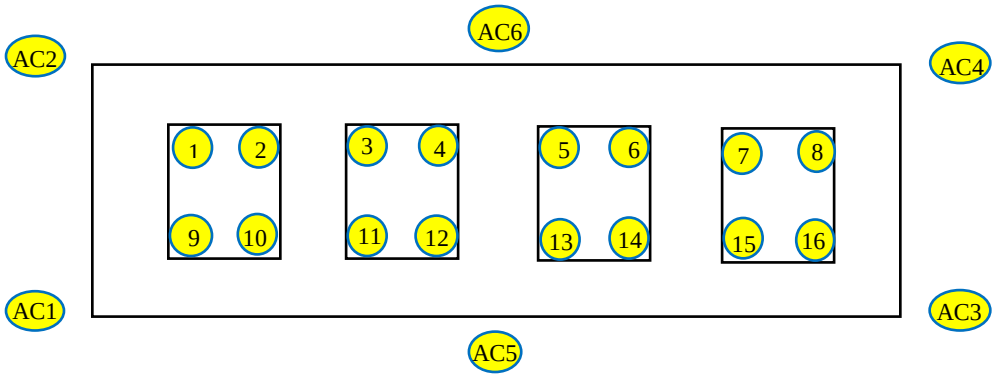


Figure 5. 24: Positioning of air search coils around the 3p5L, 15 kVA transformer

The search coils outside the core (AC1-AC6) did not show any leakage flux – which is widely reported in literature. Taking a different approach, we decided to install search coils (1-16) in the inner windows and the results show that leakage flux can be measured starting from 0.33 A per phase of DC. None of the papers that discuss the effects of DC were able to figure out that while there is no outward leakage flux, some leakage flux can be found in the inner windows of the five-limb transformer. Figure 5.25 shows the inner search coil voltage against DC.

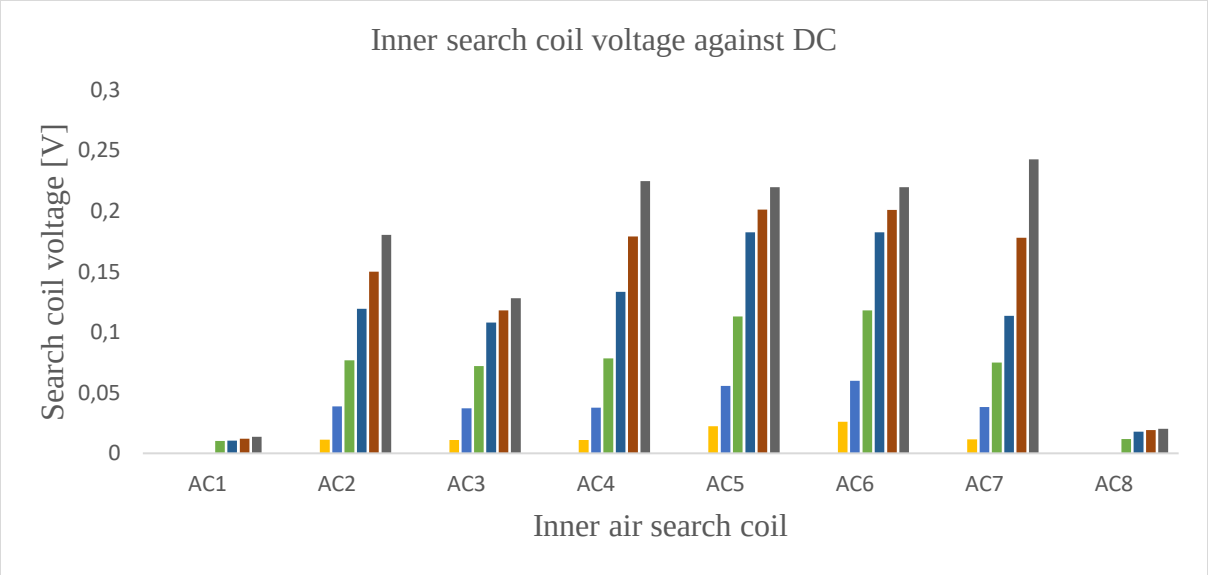


Figure 5. 25: Leakage flux in the inner windows of the 3p5L, 15 kVA transformer.

## 5.11 TRANSFORMER TIME RESPONSE

There is a difference between GIC measured and calculated values that flow in a power network. Modelling and calculation of GIC is imperative in the analysis of the effects of GIC to a network. Models of calculating GIC that have been formulated, have been improved from time to time. Despite these improvements, there were still differences between the modelled and actual GIC. A comprehensive method that improved the calculation was presented in [86], introduced transformer time response as a factor that improved the differences between measured and calculated GIC. The transformer time response is however different among transformer cores. It implies that the calculated GIC values depends on the transformer core types inherent in the network.

Figure 5.26 shows that the transformer time response of a 3p5L transformer decreases with increasing DC. This implies that the transformer will react quickly and the changes that occur as a result of DC in a transformer will occur almost immediately. As the transformer is driven into deep

saturation by the DC, the response time of the 3p5L continues to drop whereas that of the 3p3L remains steady as reported in [86]. Measurement and simulations performed in [86] show that the transformer core structure with the shortest response time is the 3p3L, followed by the 3p5L and the single-phase transformer.

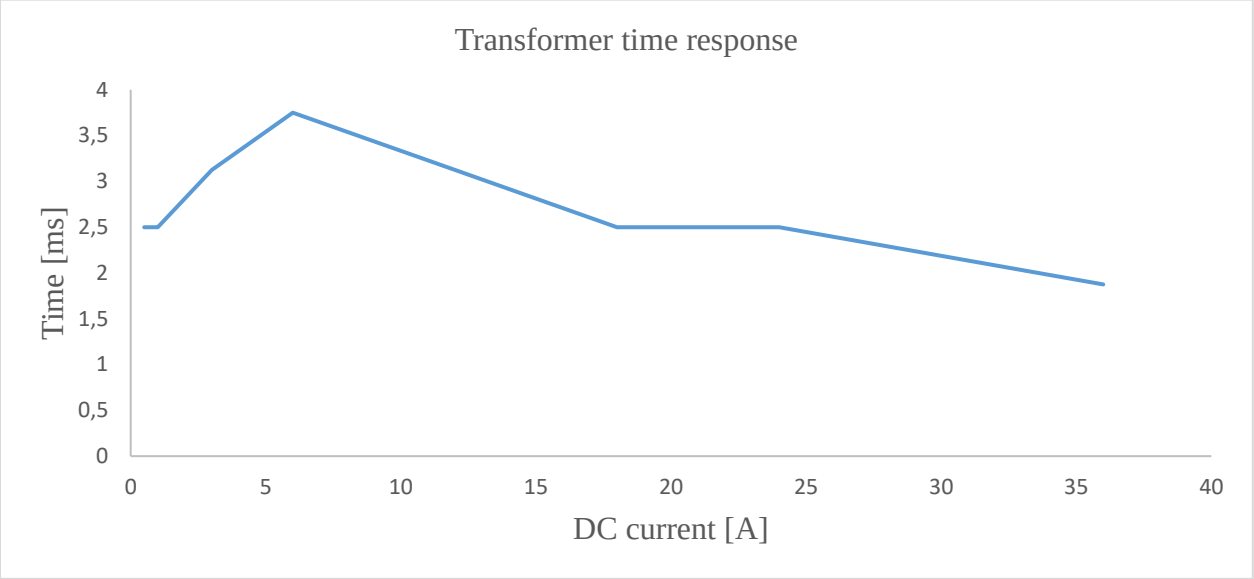


Figure 5. 26: Transformer time response for a 3p5L, 15kVA transformer

The transformer time response affects the flow of GIC in a transformer. The fact that the transformer falls within the path of a GIC, and thus contributes as the resistive path makes it worthwhile to include transformer time response in calculating GIC. Including transformer time response has indeed led to an improved correlation between measured and calculated GIC.

## 5.12 FINITE ELEMENT SIMULATION RESULTS

Finite element simulations are accurate in performing simulation of reactive power and non-active power, harmonic analysis and computation of losses in electromagnetic devices such as

transformers. FEM using ANSYS MAXWELL package was chosen as the simulation platform to investigate the effects of DC in power transformers in this thesis. A three-dimensional model that was used in the simulation is shown in Figure 5.27a. It was built based on actual measurements and materials used in the real transformer to improve the accuracy and validity of the results.

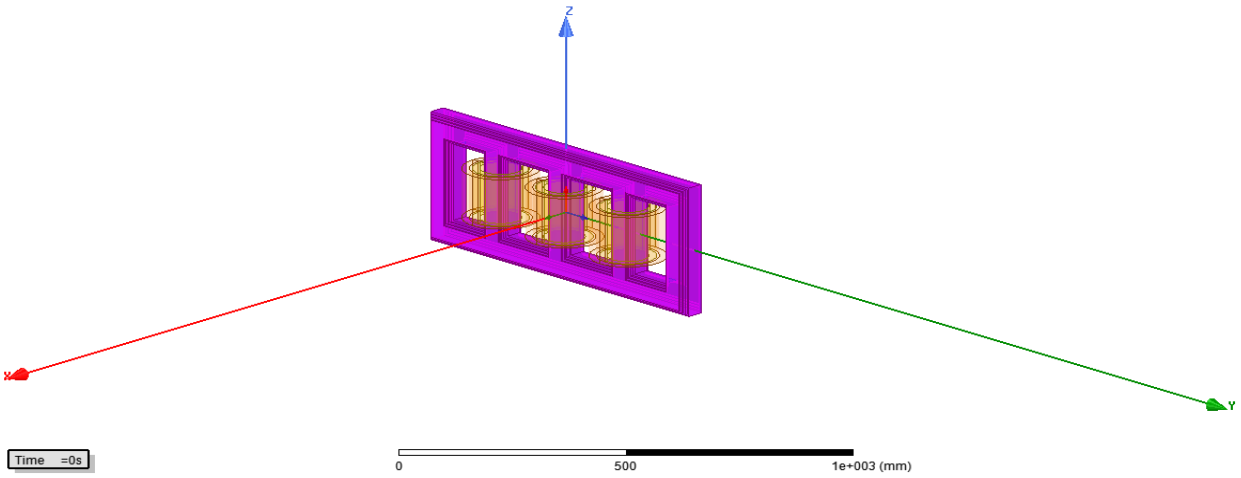


Figure 5. 27a: 3p5L Finite Element Model used for GIC studies

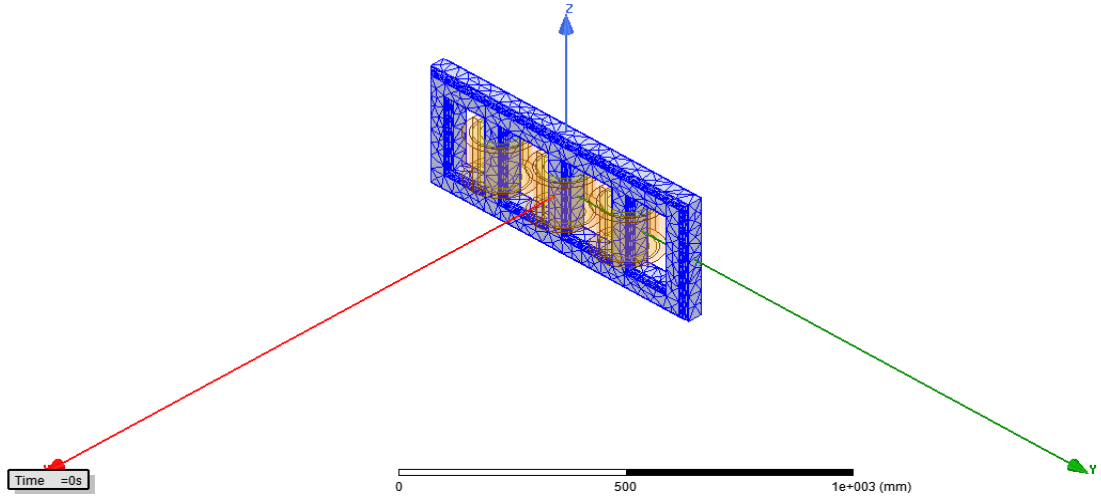


Figure 5.27b: Meshing performed on the 3p5L model used for GIC simulations

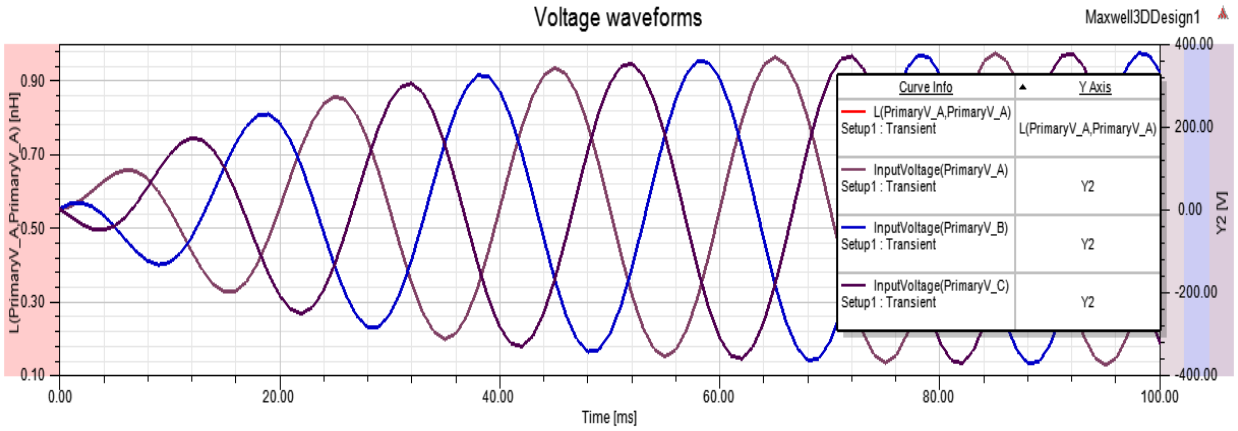


Figure 5.27c: The input voltage at 50Hz

## 5.12.1 REACTIVE POWER AND NON-ACTIVE POWER

Simulations confirmed the experimental results showing a linear increase in reactive and non-active power measured by the conventional and general power theory respectively. High magnetization currents were also noticed with an increase in DC. Figure 5.28 shows a comparison of simulated reactive power and measured reactive power. The simulation results are close to the practical results, implying that the model was implemented correctly. Furthermore, there is a guarantee that FEM can estimate reactive power consumed by transformers under DC conditions, hence the extension of the results to large power transformers using equivalent circuit parameters can be done accurately.

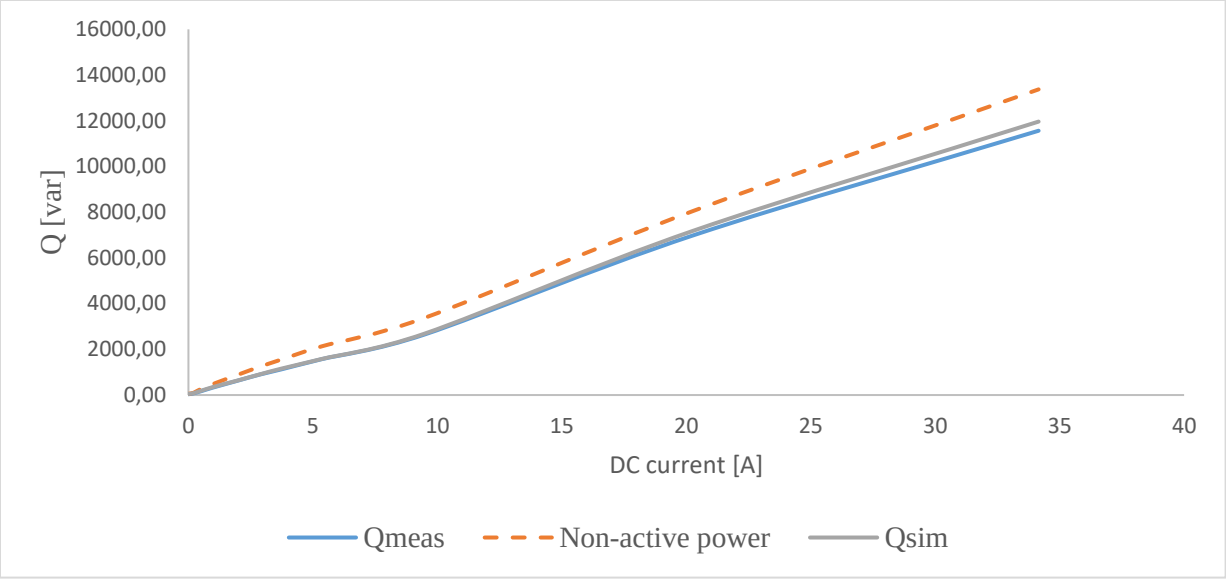


Figure 5. 28: Practical and simulated reactive and non-active power comparison

## 5.12.2 FLUX ANALYSIS USING FEM

Core saturation was also investigated in FEM under DC injections. To assess the flux, the magnetic field is plotted. Figure 5.29 explains what the colors that appear in the simulated transformer core stands for on the B-H curve. Figure 5.30a shows the flux map with no DC hence no saturation as indicated by most regions being blue and on the other hand Figure 5.30c shows a fully saturated core within the windings and the joints as indicated by most portions of the core turning yellow.

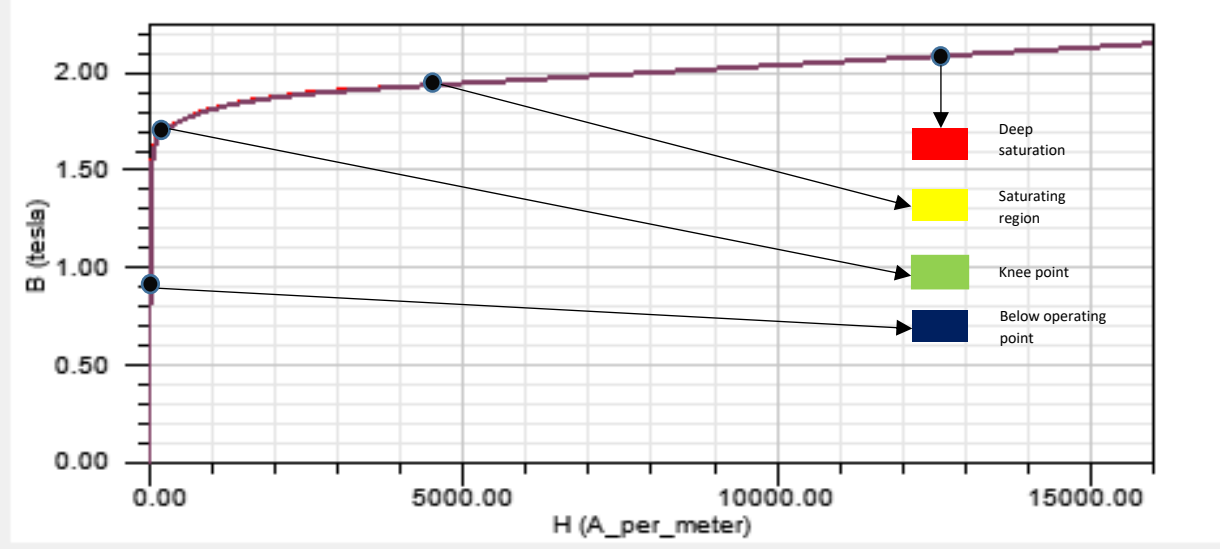


Figure 5. 29: FEM color code to denote different points on the B-H curve

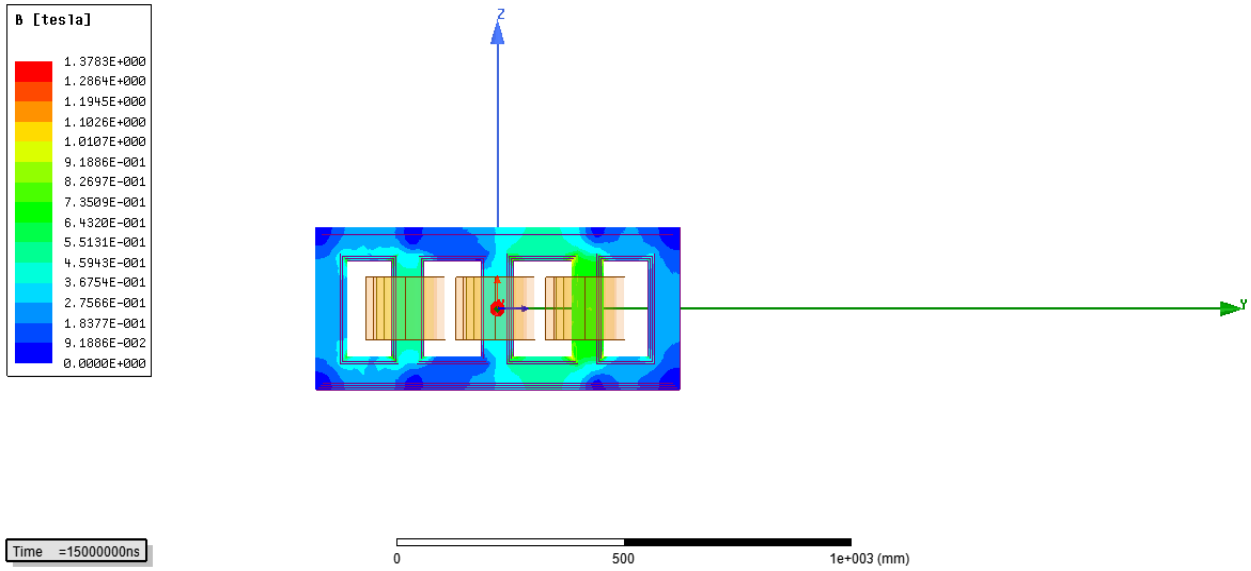


Figure 5. 30a: Unsaturated five limb transformer core with no DC injection

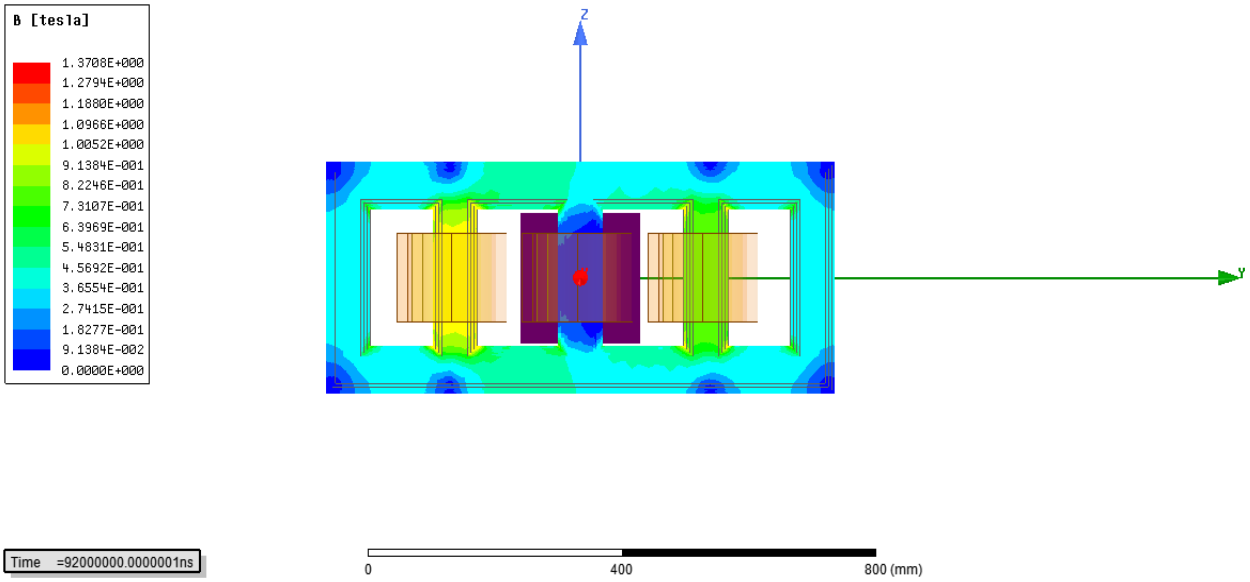


Figure 5.30b: Saturation starts to show in A and C phases with 0.125 A DC injected

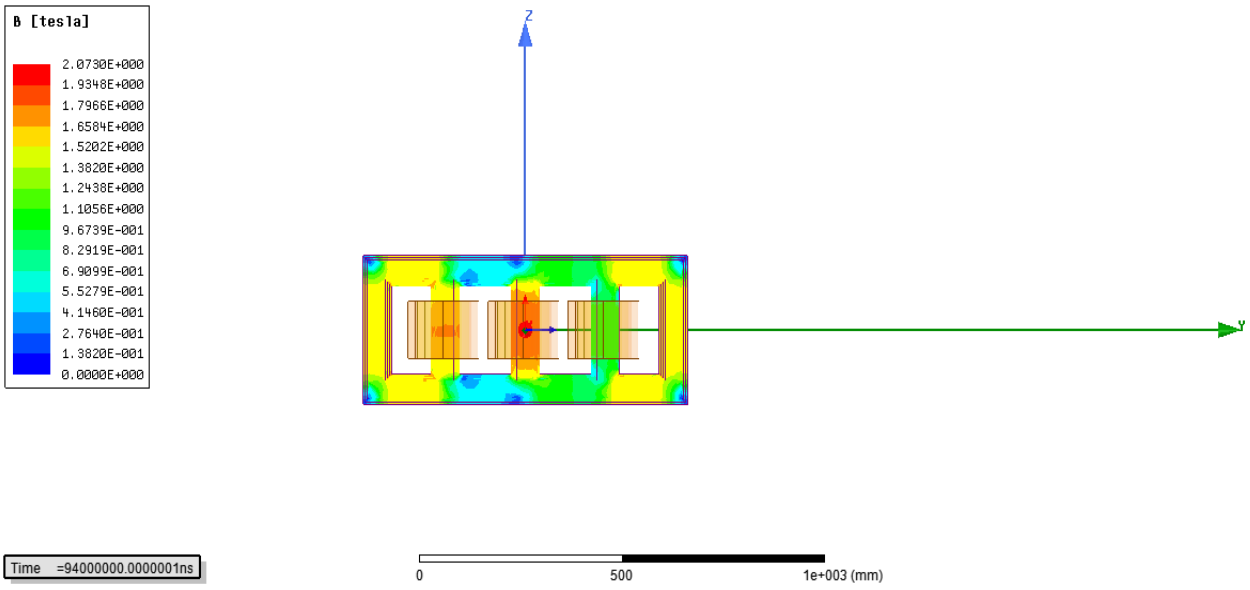


Figure 5.30c: Saturated five limb transformer core

The magnetic flux density values plotted below show an increase in flux computed with ANSYS and these show the early saturation with a DC value of 0.125 A. These results are in line with the waveforms from practical tests shown in section 5.4.

### 5.12.3 CORE LOSSES

The results show that FEM is an accurate tool to estimate transformer core losses. The percentage error is that I obtained is comparable to other researchers who have used FEM to estimate core losses in transformers [87, 88]. The average accuracy obtained in calculating core losses in FEM is 2.52%. Simulation and practical results together show an increase in core losses with an increase in DC injected. Figure 5.31 shows the simulation results showing an increase in core losses with DC. The increase in core losses is due to the increased flux in the core under DC condition as illustrated earlier with the search coil measurements.

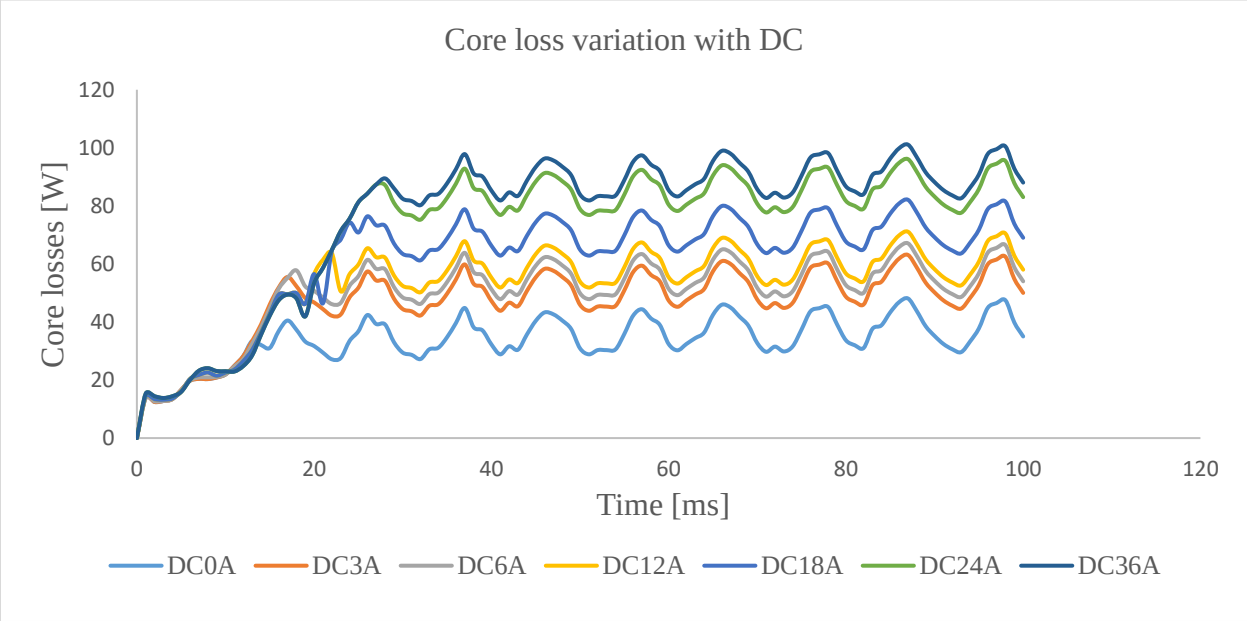


Figure 5. 31: Simulated core loss variation with DC

Core losses are made up of static hysteresis losses, classic eddy current loss and excess eddy current losses. [45]. FEM calculates the core losses using the following equation [89]:

$$P_t = P_h + P_e + P_{exc} = K_1 B_m^2 + K_2 B_m^{1.5} \quad 5.6$$

where $P_t$ represents the total losses, $P_h$ is static hysteresis losses, $P_e$ is classic eddy current loss and $P_{exc}$ is excess eddy current losses.

The eddy current losses are calculated as:

$$P_e = k_c (f B_m)^2 \quad 5.7$$

The hysteresis losses are:

$$P_h = k_h (f B_m)^2 \quad 5.8$$

And the excess losses are:

$$P_{excess} = K_e (f B_m)^{1.5} \quad 5.9$$

Hence:

$$K_1 = K_h f + K_c f^2 \quad 5.10$$

$$K_2 = k_e f^{1.5} \quad 5.11$$

The eddy current coefficient is calculated as:

$$k_e = \pi^2 \sigma \frac{d^2}{6} \quad 5.12$$

Where $\sigma$ is the conductivity and $d$ is the thickness of one lamination sheet and f is the frequency. Coefficients $K_1$ and $K_2$ are obtained from the minimization of function:

$$f(K_1 K_2) = \sum \left[ P_{vi} - (K_1 B_{mi}^2 + K_2 B_{mi}^{1.5}) \right]^2 \quad 5.13$$

Static hysteresis losses represent that part of the hysteresis cycle obtained at very low frequencies and they are independent of the magnetization rate [90, 91]. Hysteresis losses are a result of the vibrations in core material termed magnetostriction and this increases with DC causing an ultimate rise in hysteresis losses. On the other hand, the eddy current losses depend on the magnetizing current flowing in the transformer and as it increases with DC so does these losses. Eddy currents are a result of the change in flux in the core. At a constant flux they are maintained. An increase in magnetizing current causes a rise in flux change in the core, ultimately increasing the eddy current losses. Figure 5.32 shows asymmetrical saturation of the hysteresis loop caused by DC/GIC. Hysteresis losses are represented by the area of the hysteresis loop and as a result the asymmetrical increase in the hysteresis loop under DC influence causes these losses to rise in the transformer.

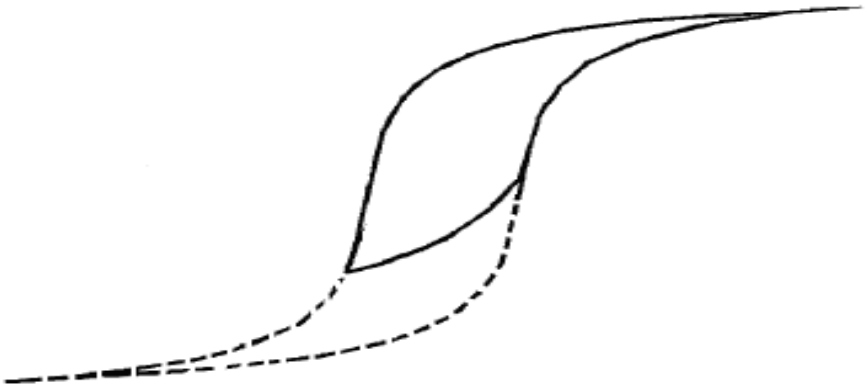

Figure 5. 32: Asymmetric hysteresis loop caused by DC [90]

## 5.13 EXTENSION OF RESULTS TO MVA RANGE

FEM simulations were used to extend the results to MVA range. A 500 MVA, 330/220 kV transformer was arbitrarily chosen to simulate the effects of DC on power transformers. Table 5.1 shows the parameters of the transformer used to extend the results to MVA range transformers. This section begins with the design specifications for the transformer leading to the simulation results.

### 5.13.1 500 MVA TRANSFORMER DESIGN SPECIFICATIONS

Power rating: 500 MVA Phase: 3

Voltage ratio: 330kV/220 kV Connection: Delta-Star

Frequency: 50 Hz

Table 5. 1: shows the parameters of the transformer used to extend the results to MVA range transformers

| Parameters | A | B | C |
|---|---|---|---|
| *Voltage ratio* [V] | 330 kV | 330 kV | 330 kV |
| *HV current* [A] | 874.77 A | 874.77 A | 874.77 A |
| *LV current* [A] | 1312.16 A | 1312.16 A | 1312.16 A |

## 5.13.2 REACTIVE AND NON-ACTIVE POWER

Figure 5.33 shows the simulation results of reactive and non-active power under varying DC conditions. The values of DC injected ranges from 0 to 100 A/phase.

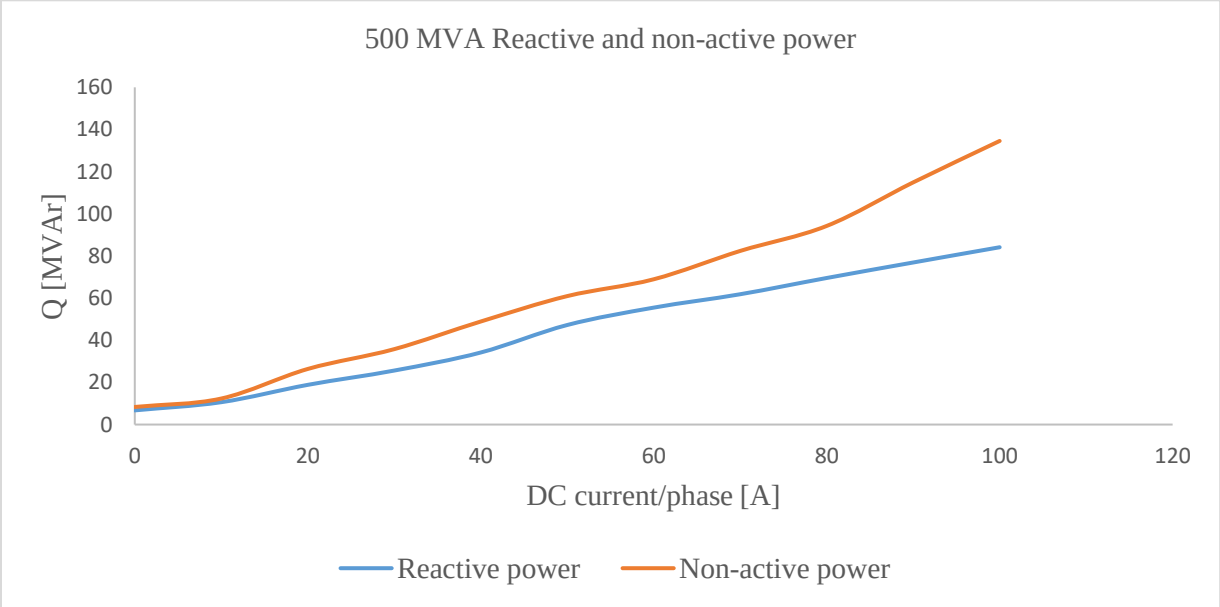


Figure 5. 33: Reactive and non-active power variation with DC for a 500 MVA transformer

There is a very small difference between calculated values at DC values below 10A/phase but the difference gradually widens as more DC is injected. This proves that conventional methods of calculating power may be misleading under distorted conditions such as when DC is flowing in the network.

FEM simulation performed using a 500 MVA transformer under varying DC showed that the reactive power and non-active power absorbed by a transformer conducting GIC is linear. As seen from the practical results, conventional methods of calculating reactive power underestimate power calculations.

## 5.14 CONCLUSION

This chapter presented results from practical tests and FEM simulations. There is consistency in the measured and simulated results showing that FEM simulations are accurate in simulating transformer responses to GIC. The results have shown an increase that the 3p5L transformer saturates with very low values of DC injected. This increases the magnetizing current, no-load losses, reactive power and non-active power.

# CHAPTER 6: CONCLUSION

## 6.1 INTRODUCTION

This chapter summarises the findings of this research. Furthermore, the two major effects of GIC events; increased reactive power absorption and harmonic currents were thoroughly investigated. Two methods of measuring power were implemented. Both methods were verified with FEM simulations and yielded comparable results with practical tests performed on transformers. The literature survey played a phenomenal part in answering the research questions, and in validating the hypothesis.

## 6.2 ACHIEVEMENT OF OBJECTIVES

This project has sought to investigate the effects of GIC on 3p5L power transformers. A comprehensive review of literature was conducted providing a summary of the effect that direct current has on power transformers. The saturation phenomenon has been fully explored and the theory behind its occurrence elaborated upon. Experiments and simulations were rigorously done to investigate the response of 3p5L to geomagnetic induced currents. Investigations on the thresholds of GIC initiating damage was done, and the research identified key areas that were neglected in similar previous researches in coming up with the thresholds. Answers to the research questions that formed the backbone of this research are given below.

## 6.3 ANSWERS TO RESEARCH QUESTIONS

The following research questions have been set up to assess the project hypothesis:

a) How does reactive power increase in transformers saturated by the flow of GIC affect power system stability?

The research has shown that a transformer conducting GIC will saturate causing it to become a harmonic source and drawing large amounts of reactive power. Simulations and practical tests have shown the rapid increase in the transformer's magnetizing current which leads to more reactive power being drawn by the transformer. An increase in reactive power of the system will destabilize the grid by causing power swings, reduction in system voltage and ultimately increasing the system frequency as generators try to compensate for lost power [2, 90]. This was experienced in the famous Hydro Quebec blackout that was a result of GICs. Power swings may cause relays to trip the power system due to a momentary disturbance. The extent to which the reactive power increases was investigated using two methods namely the conventional and general power theory. A linear relationship between Geomagnetically Induced Current flowing through a transformer's windings and the reactive power absorbed by that transformer's core was noticed for the 3p5L transformer. Many other researchers [73, 74, 92] achieved the same results experimentally. However, the two methods yielded different results despite showing the same linear relationship. Conventional methods of reactive power measurement underestimate the reactive power absorbed by the transformer. These methods neglect distortions and losses in the neutral. This underestimation of consumed reactive power may have implications of unexpected blackouts, which can be avoided by using a more accurate method; the general power theory.

The problems of increased reactive power on the system may be avoided by installing reactive power compensation equipment, implementing GIC blocking equipment on transformer neutrals that are earthed and conducting careful studies on protection settings to avoid spurious relay tripping due to momentary power swings. An example of reactive power compensation equipment that is commonly used in national grids is the SVC. Static var compensators respond to power swings promptly, but their protection settings need to be carefully chosen so that they don't trip due to momentary disturbances. This technique

of revising protection settings was successfully implemented in the Hydro Quebec power system in Canada [78]. Enough reactive power reserves is often a better solution to counter reactive power variations but the capital costs of installing these are very high.

b) What is the role of installing GIC monitoring devices in order to fully understand the phenomenon behind the risk of quasi-DC current to transformers?

The national hazard registers and regulatory rules [93, 94] have included space weather as a threat to power systems. This is due to a high rise in GIC events and the potential risks that they pose on the power system network. In that regard, monitoring GIC should become a very crucial consideration for many power systems operators. Many power system operators are unaware of the effects of GICs on the grid. In South Africa and Namibia, the installation of GIC monitoring devices began after the Halloween Storm of 2003 that devastated several transformers at Ruacana, Matimba and Grassridge substation. A list of equipment that was damaged by GIC in South Africa is given in Table 2.1. Monitoring GIC currents will help power system operators to identify problems associated with GIC and this will allow them to create a risk register that identifies the problems associated and have mitigation strategies. Further, trends of GIC flowing in particular seasons of the year can be identified and clear and accurate planning can be done beforehand.

c) How does the different structure of transformers affect their response to GIC?

Literature has established that the 3p3L is more tolerant of GIC currents than any other transformer core, followed by 3p5L and the single-phase transformer is most susceptible to GIC [95]. The reason being the existence of zero sequence flux return paths in single-phase and 3p5L transformers, as illustrated in section 2.4. Practical tests conducted have proved that the 3p5L transformer saturates more quickly that the 3p3L transformer. This is

an indication that the transformer is more susceptible to GIC since all problems associated with GIC emanate from transformer saturation.

d) What are the different levels of GIC that cause noticeable degradation in power transformers?

Studies performed by NERC suggests that the GIC threshold that causes degradation in power transformers is 75 A. Thermal analysis alone was used to arrive at this threshold. L Marti 2016 [59] has argued that the method used by NERC has loopholes because it does not include the other operating limits for transformers set by IEEE such as harmonic thresholds. He further explained that simulations confirm that the THD harmonic threshold for large power transformers such as the one used by NERC is 1.5% which is exceeded within a range of (2 A-5 A). R Walling [23] also conducted experiments that showed the harmonic threshold for large power transformers is less than 10 A. In addition, NERC did not consider saturation which causes a transformer to become a harmonic source. Harmonics may cause heating and relays tripping which is a threat to the transformers within the grid. Several researchers have shown that DC currents as low as 2 A may cause a large power transformer to saturate. This research has also shown that the five limb transformer (distribution transformer size) will saturate with a DC of 0.125 A flowing in its neutral.

Case studies presented in section 3.6 suggested that transformers have failed when GIC currents that were flowing in their neutral did not exceed 5 A during the Halloween Storm in South Africa and Britain. This could be because the power system response to the transformer saturating contributed to the failure of these transformers. The changes in reactive power caused by GIC can cause power system instability that may result in damage to transformers. Post-event analysis in the famous Hydro Quebec event suggested that adjustment to the SVC overcurrent setting would have prevented damage to transformers.

This research has brought some highlights on the considerations that must be taken into account in determining thresholds. These are saturation, harmonic thresholds, power factor and thermal analysis since all these factors contribute to transformer failure or degradation. For instance, this research has shown that the IEEE harmonic threshold of distribution transformers of 5% is exceeded when a DC of 25 A in the neutral is flowing through the transformer and that saturation begins at a very low current of 0.125 A. Putting all these facts together proves that careful considerations need to be taken when even small amounts of GIC are flowing in the network as transformers may saturate, and generate harmonics that might harm the transformer.

e) How does the reactive power consumed by a power transformer vary with respect to GIC?

Numerous researchers found a linear relationship between reactive power increase and induced DC. Two methods of computing reactive power used in this research proved that the relationship is truly linear. However, a unique research [75] suggested that the relationship is non-linear. Using the linear relationship, power system operators can predict the reactive power reservations required for a known amount of DC would have been predicted in space weather reports.

f) What is the implication of general power theory in determining reactive power absorbed by the transformer as opposed to conventional methods of calculating power?

Both the IEEE and the general power theory show a linear relationship in reactive power absorbed under DC bias in neutral. A key difference is the amount of reactive power measured. Huge underestimation is seen in the IEEE conventional way. The result of underestimation may lead to poor system response to GIC events, failure of operators and power system planners to put in place mitigation measures. As a result, unexpected blackouts may occur.

## 6.4 VALIDITY OF HYPOTHESIS

In the beginning of the thesis, a hypothesis was formulated, and it is stated as:

- Tests on model transformers and extension of the results to power transformers with suitable transformer equivalent circuit and FEM simulations will improve the conventional models of the reactive power requirement in transformers conducting GIC.

Thorough research carried out showed that the hypothesis is valid. Practical tests and FEM simulations on power transformers were conducted. Application of general power theory to measure reactive power on these transformers yielded different results from conventional methods of measuring reactive power in both simulation and practical tests. As elaborated earlier, GPT is a better method of measuring non-active power under distortion such as DC flowing in transformer neutrals. Thus, conventional models of the reactive power requirement in transformers conducting GIC can be improved by applying GPT. The results were extended to utility power transformers using the exact transformer equivalent model.

A comprehensive literature survey was conducted on thresholds of GIC that may cause noticeable degradation in power transformers. Tests were also performed to identify thresholds of GIC initiating damage in power transformers. The results show that DC currents below 3 A lowers the operational efficiency of the transformer and causes harmonics sufficient to cause transformer heating and insulation failure.

## 6.5 LIMITATION OF STUDY

Geomagnetic induced currents are low-frequency AC currents. In this research, direct current from batteries was used as in most researches linked to the topic. Over the years, researchers have considered transformer responses to GIC to be typical to that produced by injecting DC through the neutrals of transformers. In recent times, researchers have proposed that a more realistic quasi-DC should be injected into the neutrals of transformers instead of DC [96]. Although a low-frequency current was not used in this research due to practical limitations, this is currently been investigated in a separate project by the research group where a new protocol for low-frequency AC has been developed. Further to this, a recent publication highlighted the scope of frequency components that may be considered [96] noted that the results may be different as listed below:

- The relationship between GIC and reactive power has been considered
- Voltage stability within networks may be different from current models

# 7. REFERENCES


1. P. R. Price, “Geomagnetically Induced Current Effects on Transformers,” IEEE Transactions on Power Delivery, 2002.
2. J. Koen, C. T. Gaunt, “Geomagnetically Induced Currents in the Southern African Electricity Transmission Network,” IEEE Bologna Power Tech Conference, Italy, 2003.
3. S. MacMillan, “Earth’s Magnetic Field in Geophysics and Geochemistry,” 2004.
4. N. Homeir, L. Wei, “Solar Storm Risk to the North American Grid,” Atmospheric and Environmental Research, 2013.
5. R. Pirjola, “Geomagnetically Induced Currents during Solar Storms,” IEEE Transaction on Plasma Science, December 2000.
6. K. P. Arun Babu, “Coronal Mass Ejection from the Sun,” PhD Thesis, Indian Institute of Science and Research, Pune, 2014.
7. E. Matandirotya, “Measurement and Modelling of Geomagnetically Induced Currents in power lines, Doctor of Technology, Cape Peninsula University of Technology, 2015.
8. K. O. Akpeji, A. O. Olasoji, C. Gaunt, D. T. O. Oyedokun, K. O. Awodele and K. A. Folly, "Economic impact of electricity supply interruptions in South Africa," in SAIEE Africa Research Journal, June 2020.
9. L. Bolduc, “GIC Observations and Studies in the Hydro-Quebec Power System,” Journal of Atmospheric and Solar-Terrestrial Physics 64, 2002.
10. R. Baker, R. Balstad, J. M. Bodeau, E. Cemron, J. F. Fennell, and G. M. Fisher, “Severe space weather events-understanding societal and economic impacts,” Report, 2008.
11. R. Thorberg, “Risk analysis of geomagnetically induced currents in power systems,” Report, 2012.
12. Q. Liu, Y. Xie, N. Dong, Y. Chen, M. Liu and Q. Li, "Uncertainty Quantification of Geo-Magnetically Induced Currents in UHV Power Grid," in IEEE Transactions on Electromagnetic Compatibility, 2019.
13. N. B. Trivedi, I. Vitorello, W. Kabata, S. L. G. Dutra, A. L. Padilha, et al, “Geomagnetically induced currents in an electric power transmission system at low latitudes in Brazil: a case study,” Space Weather, 2007.

14. C. S. Barbosa, G. A. Hartmann, and K. J. Pinheiro, “Numerical modeling of geomagnetically induced currents in a Brazilian transmission line,” Adv. Space Res., 2015.
15. J. Koen, C. T. Gaunt, “Preliminary Investigation of GICs in the Eskom Network,” Report to Eskom, University of Cape Town, December 1999.
16. E. Matandirotya, P. J. Cilliers, R. R. Van Zyl, “Modeling geomagnetically induced currents in the South African power transmission network using the finite element method”, Space Weather, 13, 2015.
17. R. Zhang, Transformer modelling and influential parameters identification for geomagnetic events,” Ph.D. Thesis, University of Manchester, 2012.
18. J. Koen, “Geomagnetically Induced Currents and its Presence in the Eskom Transmission Network,” MSc Thesis, University of Capetown, 2000.
19. J. Koen & C. T. Gaunt, “Disturbances in the Southern African Power Network due to Geomagnetically Induced Currents”, Paris, 2002.
20. N. Takasu, F. Miyawaki, S. Saito, Y. Fujiwara, “An Experimental Analysis of DC Excitation of Transformers by Geomagnetically Induced Currents,” IEEE Transactions on Power Delivery, 1994.
21. L. Bolduc, A. Gaudreau, A. Dutil, “Saturation Time of Transformers under DC Excitation,” Electric Power Systems Research, 2000.
22. I. Babaeiyazdi, M. Rezaei-Zare and A. Rezaei-Zare, "Wind Farm Operating Conditions under Geomagnetic Disturbance," in IEEE Transactions on Power Delivery, 2019.
23. R. Walling, “Analysis of Geomagnetic Disturbance (GMD) Related Harmonics”, EPRI, Palo Alto, CA: 2014.
24. T. S. Molinski, “Why Utilities Respect Geomagnetically Induced Currents,” Journal of Atmospheric and Solar-Terrestrial Physics, 2002.
25. R. Girgis, K. Vedante, “Methodology for evaluating impacts of GIC and capability of transformer design,” IEEE Transaction on power delivery, 2013.
26. Nahayo E, Kotzé PB, Cilliers PJ, Lotz S. Observations from SANSA’s geomagnetic network during the Saint Patrick’s Day storm of 17–18 March 2015, South Africa Journal of Science, 2019.
27. P. Hurlet, F. Berthereau, “Impact of Geomagnetic Induced Currents on Power Transformer design,” JST Transformateurs, France, 2007.

28. J. Berge, R. K. Varma and L. Marti, "Laboratory Validation of the Relationship Induced Current," in IEEE Electrical Power and Energy Conference, 2011.
29. A. Vitols, F. Faxvog, “GIC Neutral Blocking System,” IEEE Meeting in Augusta, Maine, July 2015.
30. T. Ngnegueu, F. Marketos, F. Devaux, T. Xu, R. Bardsley, S. Barker, J. Baldauf, J. Oliveira, “Behaviour of transformers under DC/GIC excitation: Phenomenon, Impact on design/design evaluation process and modelling aspects in support of Design,” CIGRE, 2012.
31. R. Girgis and K. Vedante, “Effects of GIC on Power Transformers and Power Systems,” Transmission and Distribution Conference and Exposition (T&D), 2012.
32. Q. Liu, Y. Xie, N. Dong, Y. Chen, M. Liu and Q. Li, "Uncertainty Quantification of Geo-Magnetically Induced Currents in UHV Power Grid," in IEEE Transactions on Electromagnetic Compatibility, 2019.
33. J. Gilbert, J. Kappenman, W. Radasky, E. Savage, “The Late-Time (E3) High-Altitude Electromagnetic Pulse (HEMP) and Its Impact on the U.S. Power Grid,” Metatech Corporation, January 2010.
34. D. J. Fallon, P. M. Balma, W. J. McNutt, “The Destructive Effects of Geomagnetic Induced Currents in Power Transformers,” Doble Clients Conference, 1990.
35. L. L. Grisby, Electric Power Generation, Transmission, and Distribution,” 3rd Edition. 2016
36. E. B. Savage and W. A. Radasky, "Overview of Geomagnetic Storm Coupling to a Power Grid," 2019 Joint International Symposium on Electromagnetic Compatibility, Sapporo and Asia-Pacific International Symposium on Electromagnetic Compatibility (EMC Sapporo/APEMC), Sapporo, Japan, 2019.
37. X. Dong, Y. Liu, J. G. Kappenman, “Comparative Analysis of Exciting Current Harmonics and Reactive Power Consumption from GIC Saturated Transformers,” IEEE Power Engineering Society Winter Meeting, 2001.
38. K. DiZheng, Z. Yun, “Analysis and Processing of the Impact of DC Power transmission Grounding Current to the Network Equipment”, Automation of Electric Power Systems, 2005.

39. I. Y. Zois, “Solar Activity and Transformer Failures in the Greek National Electric Grid”, EDP Sciences, 2013.
40. X. N. Pan and X. L. Yu, “Discussion on Abnormal Noise of Transformer,” EDP Sciences, 2006.
41. C. Liu, R. Pirjola, “Geomagnetically Induced Currents in the High-Voltage Power Grid in China”, IEEE Transaction on Power Delivery, October 2009.
42. Q. Lin and Y. F. Gao, “On the October–November 2003 giant storms,” Seismol. Geomagn. Observation Res., November 2006.
43. L. Y. Liu and X. W. Xie, “Analysis of increase of noise of 500 kV transformer,” High Voltage Eng., 2005
44. D. Z. Kuai, C. M. Liu, and D. Wan, “Experiment and Research of the Influence of Direct-Current Magnetic Bias on Transformer,” Jiangsu Elect. Eng., 2004.
45. S. A Mousavi, G. Engdahl, E. Agheb “Investigation of GIC effects on core losses in single-phase power transformers”, Norwegian University of Science and Technology (NTNU), 2011.
46. C. T. Gaunt and M. Malengret, “Why we use the term non-active power, and how it can be measured under non-ideal power supply conditions,” IEEE PES PowerAfrica, Johannesburg, 2012.
47. International Electrotechnical Commission. Technical Committee No. 25, Working Group 7, Report: “Reactive power and distortion power”, No. 25, December, 1979
48. C. T. Gaunt, M. Malengret, “True power factor metering for m-wire systems with distortion, unbalance and direct current components,” Electric Power Systems Research 95, 2013.
49. M. Malengret, C. T. Gaunt, “General theory of instantaneous power for multi-phase systems with distortion, unbalance and direct current components,” Electric Power Systems Research 81, 2011.
50. D. Emad, “A simplified iron loss model for laminated magnetic cores,” IEEE Transactions on Magnetics, 2008.
51. D. A Hutton, “Fundamentals of Finite Element Analysis,” McGraw-Hill Companies, 2004.
52. Introduction to ANSYS MAXWELL, ANSYS Inc., 2013.

53. K. Mukesh, “Study of stray losses reduction through Finite Element Method,” Annual IEEE India Conference (INDICON), 2013.
54. IEEE Std. C57.91-1995, “IEEE Guide for loading mineral-oil-immersed transformers and step-voltage regulators”, 1995.
55. E. B. Savage and W. A. Radasky, "Overview of Geomagnetic Storm Coupling to a Power Grid," 2019 Joint International Symposium on Electromagnetic Compatibility, Sapporo and Asia-Pacific International Symposium on Electromagnetic Compatibility (EMC Sapporo/APEMC), Sapporo, Japan, 2019.
56. IEEE Std. 519-1992, “IEEE Recommended Practices and Requirements for Harmonic Control in Electrical Power Systems, New York, NY: IEEE, 1992.
57. A. Vitols, F. Faxvog, “GIC Neutral Blocking System,” IEEE Meeting in Augusta, Maine, July 2015.
58. C. T. Gaunt, “Notice of Proposed Rulemaking on Reliability Standard for Transmission System for Transmission System Planned Performance for Geomagnetic Disturbance Events,” 2015.
59. L. Marti, “Assessment of the effects of GIC in power systems”, FERC Meeting, 2016
60. J. G. Kappenman, Geomagnetic Storms and Their Impacts on the U.S Power Grid, Goleta, California: Metatech Corporation, 2010.
61. Q. Qiu, D. R. Ball and J. A. Fleeman, R. Girgis and K. Vedante, “Effect of GIC and GIC Capability of EHV Power Transformers - A Case Study on an AEP 765 kV Power Transformer Design,” CIGRE US National Committee: Grid of the Future Symposium, 2013.
62. P. Marketos, A. J. Moses, J. P. Hall, “Effect of DC Voltage on AC Magnetization of Transformer Core Steel,” Journal of Electrical engineering, 2010.
63. NERC, “Transformer Thermal Impact Assessment white paper,” Developed by the Project 2013-03 (Geomagnetic Disturbance) standard drafting team, 2013.
64. J. Verner, G. Hoffman, W. Bartley, R. Ahuja, J. Arteaga et.al., “IEEE Guide for Establishing Transformer Capability while under Geomagnetic Disturbance”, September 2015.
65. Siemens, “GIC Effects on Power Transformers,” NERC Taskforce Meeting”, November 2013.

66. R. Zareand, L. Marti, “Generator Thermal Stress during a GMD”, IEEE PES, Vancouver, Canada, July 2013.

67. S. E Zirka, Y. I Moroz, D. Bonnman, “Topological transient model of three-phase five-limb transformer,” IEEE Trans. Power Delivery, 2017.

68. S. E. Zirka, Y. I. Moroz, C. M. Arturi, Member, IEEE, N. Chiesa, and H. K. Hoidalen, “Topology-Correct Reversible Transformer Model,” IEEE Trans. Power Delivery, October 2012.

69. P. S. Moses, “Operation and Performance of Three-Phase Asymmetric Multi-Leg Power Transformers Subjected to Nonlinear and Dynamic Electromagnetic Disturbances,” Ph.D. Dissertation, Curtin University, 2012.

70. C. W. McLyman, “Transformer and inductor design handbook,” Marcel Dekker, Inc. 3rd edition, 2004.

71. S. E. Zirka, Y.I. Moroz, H. K. Hoidalen, A. Lotfi, N. Chiesa, C. M. Arturi, “Practical experience in using a topological model of a core-type three-phase transformer - No-load and inrush conditions. IEEE Trans. Power Delivery, 2017.

72. H. K. Chisepo, “The Response of Transformers to Geomagnetically Induced-like Currents”, MSc Dissertation, University of Cape Town, 2014.

73. J. Yao, M. Liu, C. Li and Q. Li, “Harmonics and Reactive Power,” Power and Energy Engineering Conference (APPEEC), 2010, Asia-Pacific, IEEE, 2010.

74. C. Bergsaker, “Impact of transformer core size on the reactive power requirement of power transformers due to GIC,” ed, 2014.

75. L. Liu; Zebang Yu; X. Wang and W. Liu, “The Effect of Tidal Geoelectric Fields on GIC and PSP in Buried Pipelines, in IEEE Access, vol. 7, 2019.

76. Ming Yang; Digvijay Deswal and Francisco De Leon, “Mitigation of Half-Cycle Saturation of Adjacent Transformers during HVDC Monopolar Operation - Part I: Mitigation Principle and Device Design, in IEEE Transactions on Power Delivery, 2019.

77. A. Rezaei-Zare, “Three-Phase Transformer Response due to GIC using an Advanced Duality-Based Model”, IEEE Transactions on Power Delivery, 2016.

78. S. Guillon, P. Toner, L. Gibson, and D. Boteler, “A Colorful Blackout: The Havoc Caused by Auroral Electrojet Generated Magnetic Field Variations in 1989”, IEEE Power and Energy Magazine, 2016
79. S. Mkhonta, T.T. Murwira, D.T.O. Oyedokun, K.A. Folly and C.T. Gaunt, “Investigation of Transformer Reactive Power and Temperature Increases Under DC,” IEEE PES/IAS PowerAfrica, 2018.
80. A. E Emanuel, Power in Non-sinusoidal situations – A review of Definitions and Physical Meanings”, IEEE Trans. On Power Delivery, Vol. 5, No. 3, July 1990.
81. J. Arrillaga, D. A. Bradley, P. S. Bodger, Power system Harmonics (John Wiley & Sons, New York, 1985.
82. W. Shepherd, P. Zand, “Energy Flow and Power Factor in Nonsinusoidal Circuit,” Cambridge University Press, 1979.
83. R. Girgis, K. O. Chung-Duck, “Calculation Techniques and Results of Effects of GIC Currents as Applied to Two Large Power Transformers,” IEEE Transactions on Power Delivery, April 1992.
84. T.T. Murwira, S. Mkhonta, D.T.O. Oyedokun, K.A. Folly and C.T. Gaunt, “Three-Phase Five-Limb Transformer Harmonic Analysis under DC-bias,” SAUPEC/RobMech/PRASA Conference, 2019.
85. D. T. Oyedokun, “Geomagnetically induced currents (GIC) in large power systems including transformer time response,” Ph.D. Dissertation, University of Cape Town, 2015.
86. N. Bhatt, S. Kaur, N. Tayal, “Transformer loss calculation and L.V. winding loss reduction using Finite Element Method”, International Journal of research in engineering and applied sciences, July 2016.
87. S. A. Jain, A. A. Pandya, “Three-Phase Power Transformer Modeling Using FEM for Accurate Prediction of Core and Winding Loss”, International Conference on Research and Innovations in Science, Engineering & Technology, 2017.
88. S. Vasilija, “FEM 2D and 3D design of the transformer for core losses computation”, Scientific proceedings XIV international congress machines technologies materials, 2017.
89. E. Barbisio, F. Fiorillo, C. Ragusa, “Predicting loss in magnetic steels under arbitrary induction waveform and with minor hysteresis loops”, IEEE Transaction on Magnetics, 2004.

90. H.K Chisepo, C.T Gaunt, L.D Borill, “Measurement and FEM analysis of DC/GIC effects on transformer magnetization parameters, IEEE Milan Powertech, 2019.
91. R. Siti, S. Hassan, and M. Anuar, “Study the harmonic characteristics of DC bias on the single-phase power transformer," in Power Engineering and Optimization Conference (PEDCO) Melaka, Malaysia, 2012.
92. North American Reliability Corporation (NERC), "Order on GMD Research Work Plan,” ed, 2017.
93. Cabinet Office, "National Risk Register of Civil Emergencies 2015 Edition,” ed. London Cabinet Office, 2015.
94. 70. A. Rezaei-Zare, L. Marti, A. Narang, and A. Yan, “Analysis of Three-Phase Transformer Response due to GIC Using an Advanced Duality-Based Model,” IEEE Transactions on Power Delivery, 2016.
95. D. Oyedokun, M. Heyns, P. Cilliers and C. Gaunt, "Frequency Components of Geomagnetically Induced Currents for Power System Modelling," 2020 International SAUPEC/RobMech/PRASA Conference, Cape Town, South Africa, 2020.
96. P. Jankee, H. Chisepo, V. Adebayo, D. Oyedokun and C. T. Gaunt, “Transformer models and meters in MATLAB and PSCAD for GIC and leakage DC studies”, 2020 International SAUPEC/RobMech/PRASA Conference, Cape Town, South Africa, 2020.

# 8. APPENDICES

## APPENDIX A: EXPERIMENTAL RESULTS: 3P5L, 15 KVA, 380/380 V TRANSFORMER

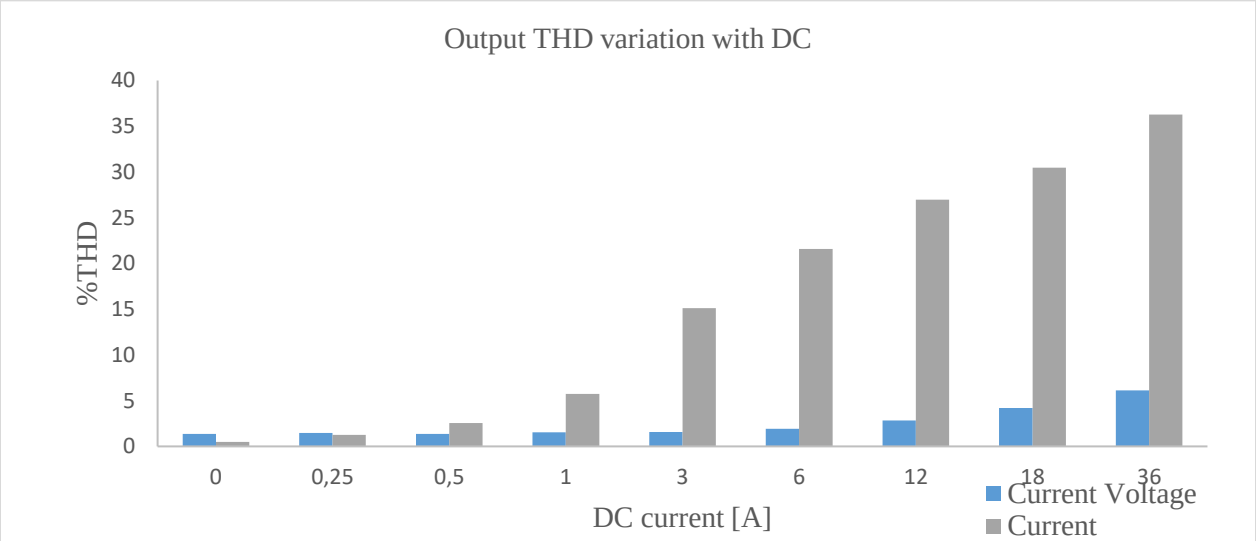


Figure A.1: Output current and voltage THD at 1.5kW load

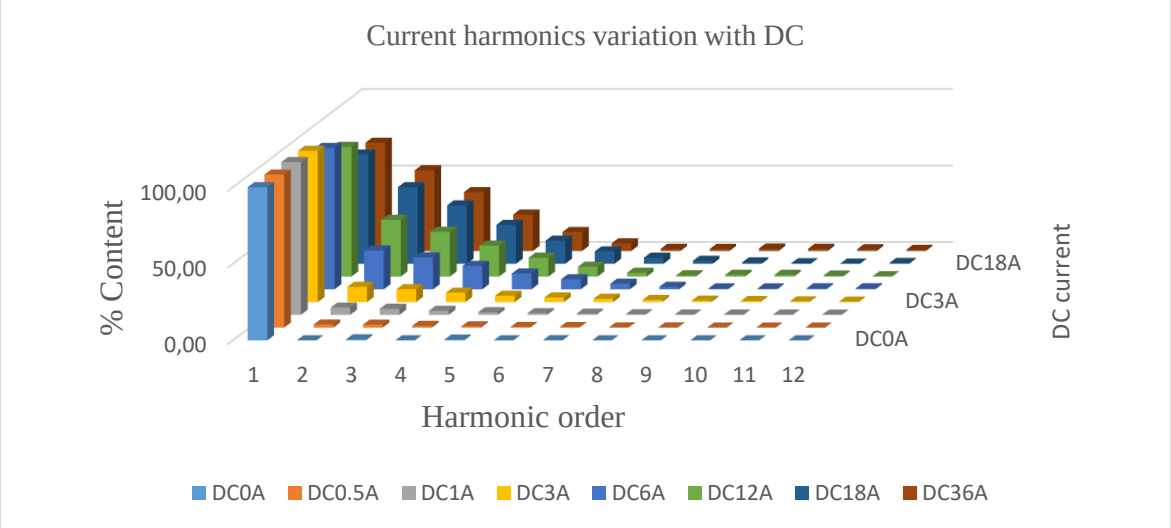


Figure A.2: Current harmonics THD at 6.4 kVA load

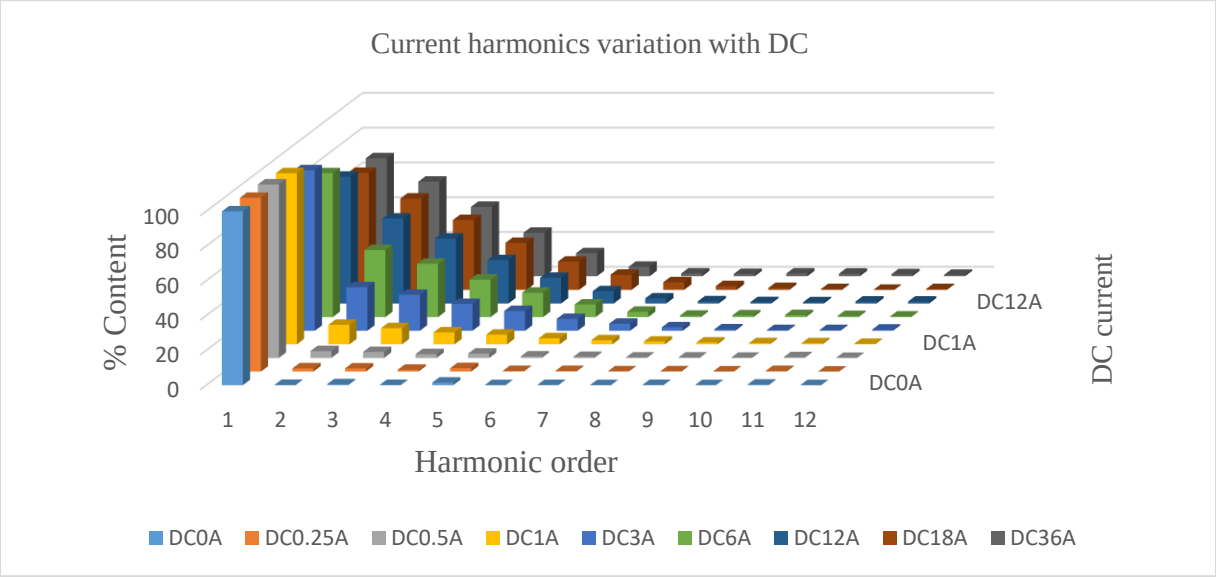


Figure A.3: Current harmonics THD at 1.5 kW load

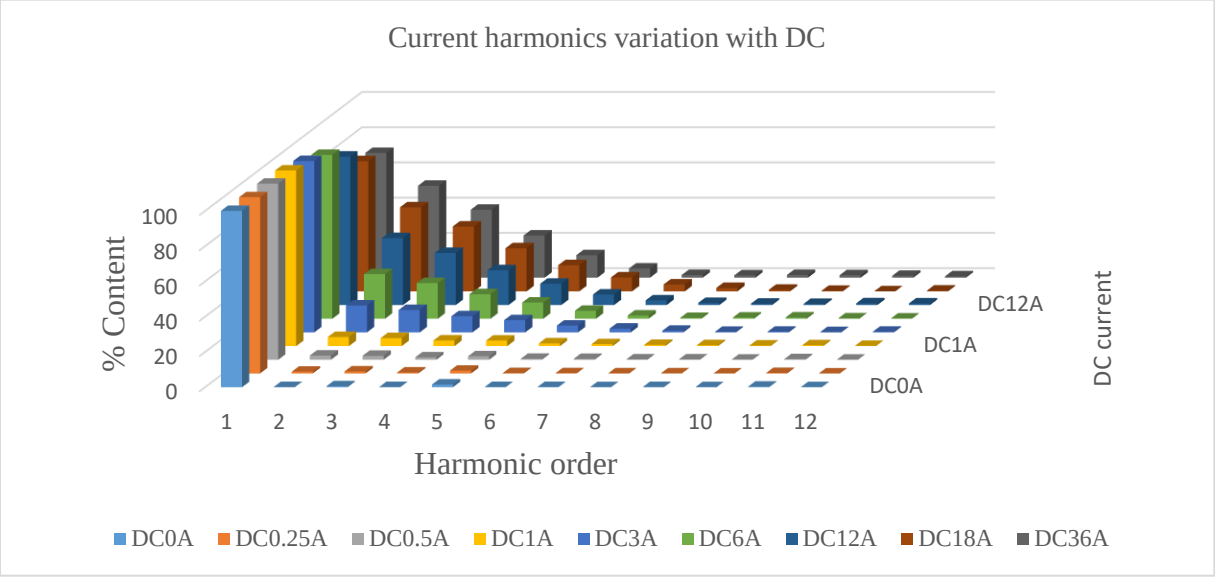


Figure A.4: Current harmonics THD at 3.0 kW load

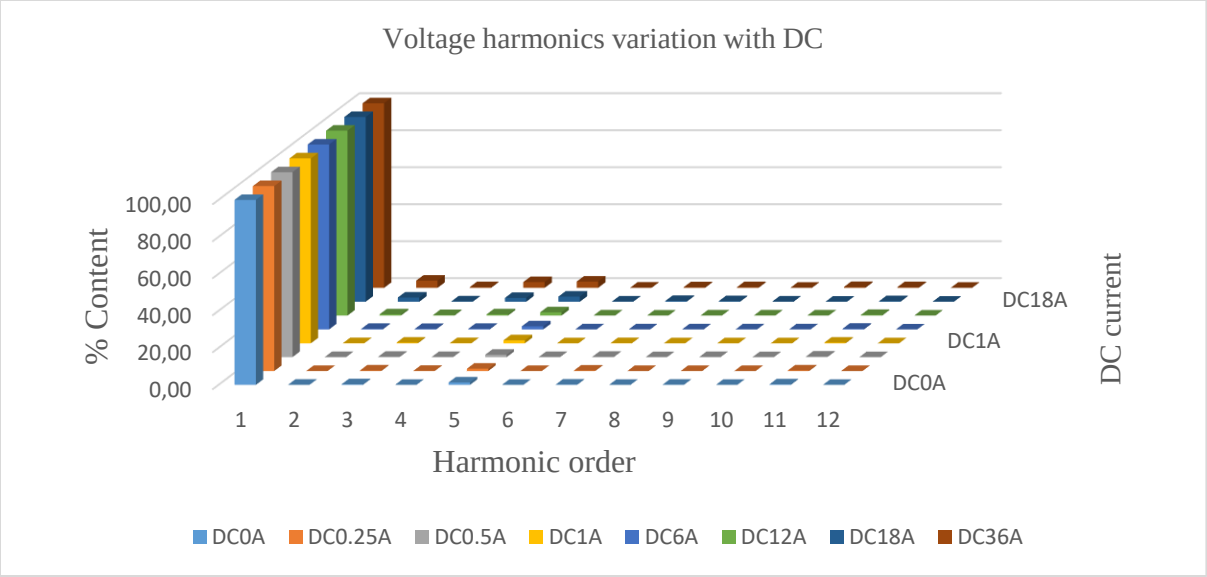


Figure A.5: Voltage harmonics THD at 6.4 kVA load

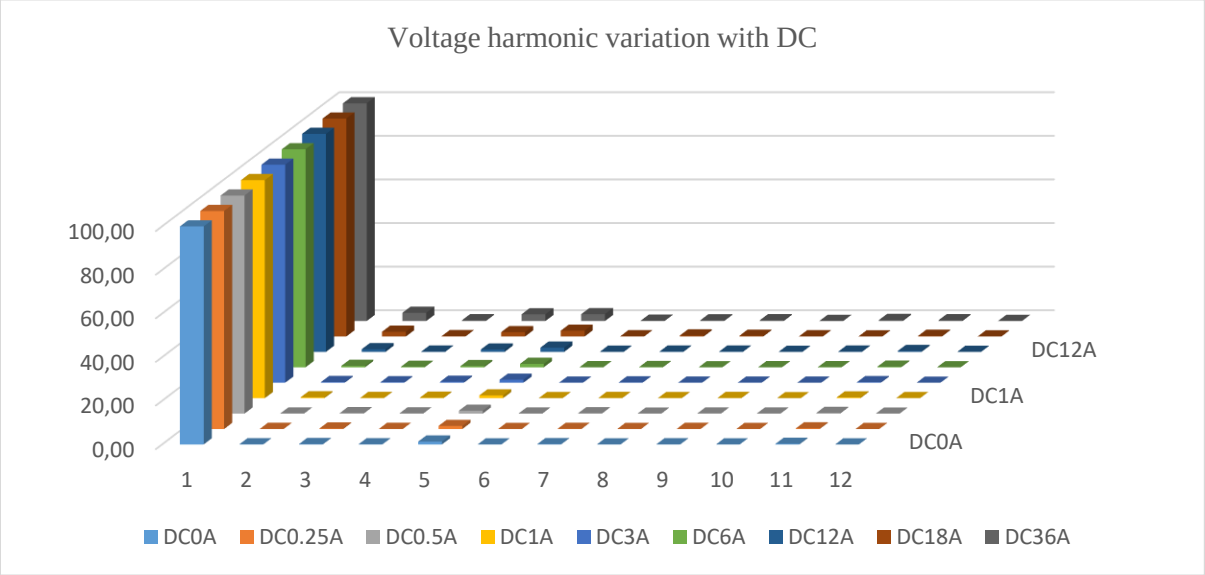


Figure A.6: Voltage harmonics THD at 1.5 kW load

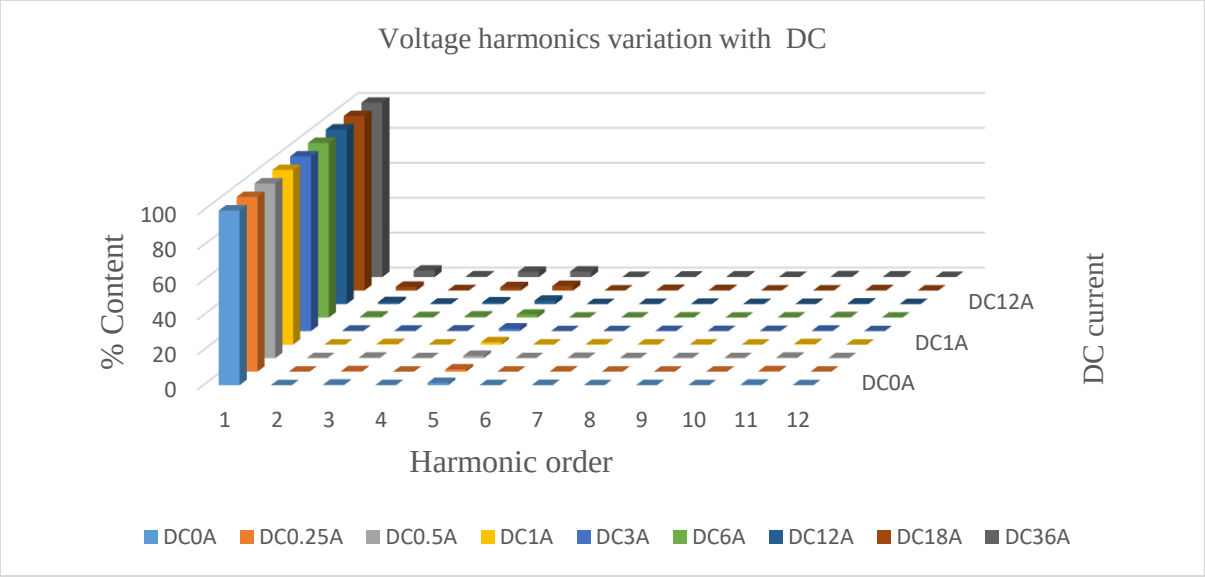


Figure A.7: Voltage harmonics THD at 3.0 kW load

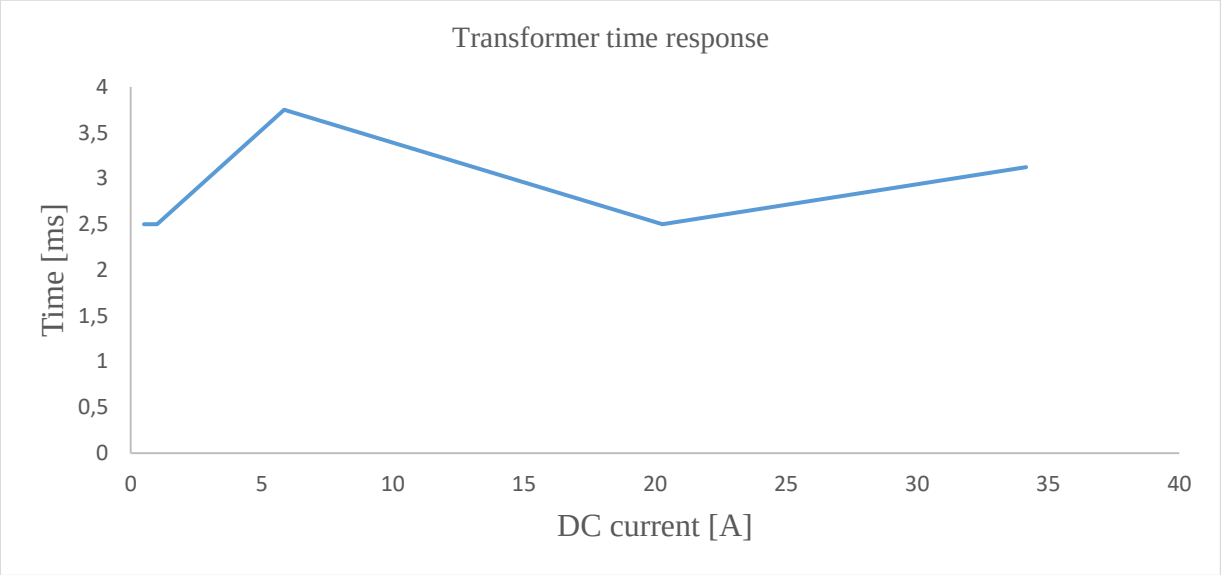


Figure A.8: Transformer time response

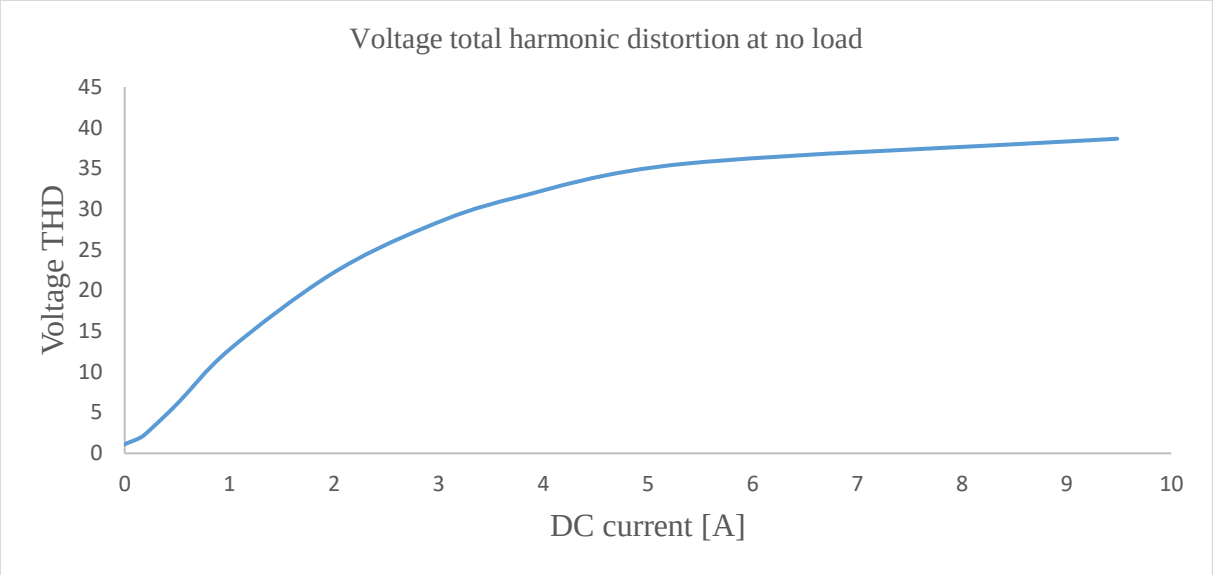


Figure A.9: Total harmonic distortion at no load

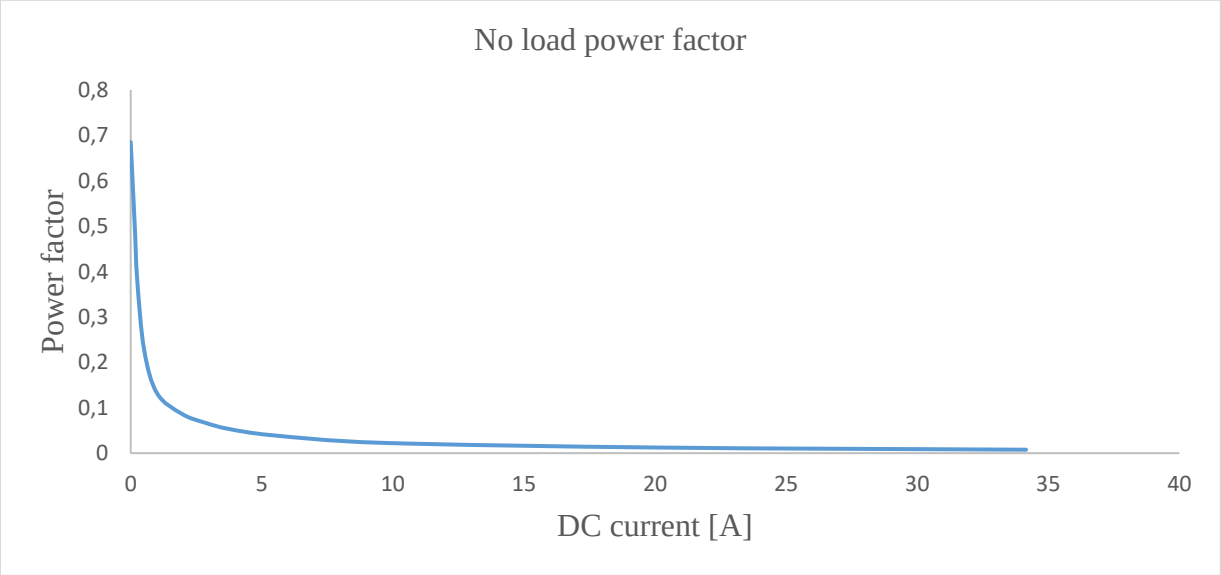


Figure A.10: No load power factor

Table A.1: Open circuit test results

| Parameters | A | B | C | Average |
|---|---|---|---|---|
| $V_{oc}$ [V] | 219.0 | 217.93 | 219.11 | 218.69 |
| $I_{oc}$ [A] | 0.2920 | 0.2408 | 0.2658 | 0.2662 |
| $P_{oc}$ [W] | 32.44 | 26.75 | 20.51 | 26.57 |

Table A.2: Short circuit test results

| Parameters | A | B | C | Average |
|---|---|---|---|---|
| $V_{sc}$ [V] | 8.874 | 8.91 | 9.1 | 8.961 |
| $I_{sc}$ [A] | 21.245 | 21.357 | 21.794 | 21.465 |
| $P_{sc}$ [W] | 106.5 | 107.4 | 111.9 | 108.6 |

## APPENDIX B: EXPERIMENTAL RESULTS: 3P5L, 300 VA, 120/230 V TRANSFORMER

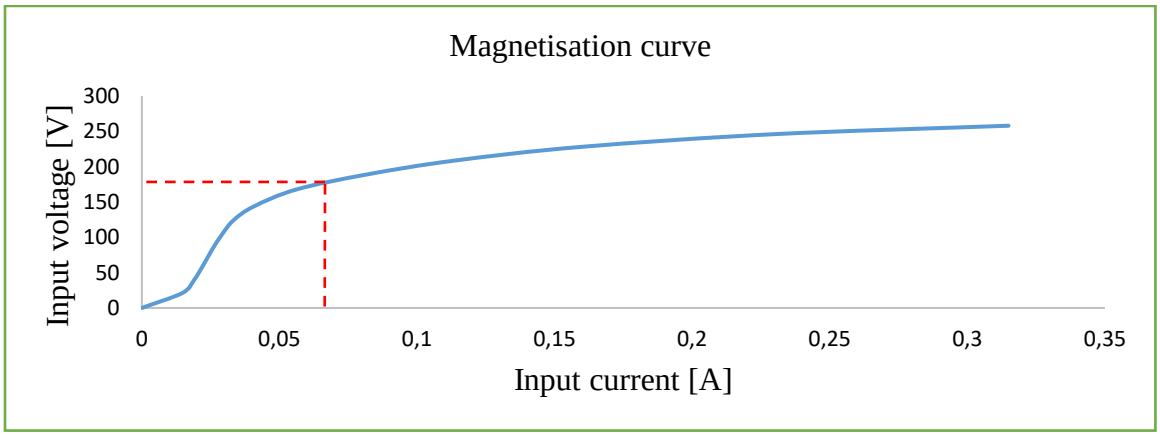


Figure B.1: Excitation curve

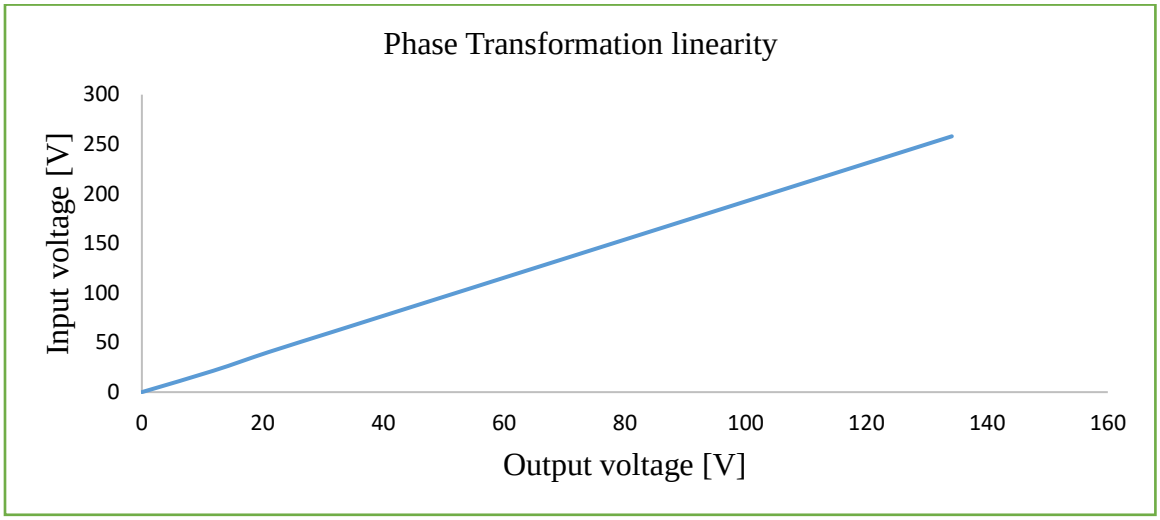


Figure B.2: Phase transformation linearity (TuT)

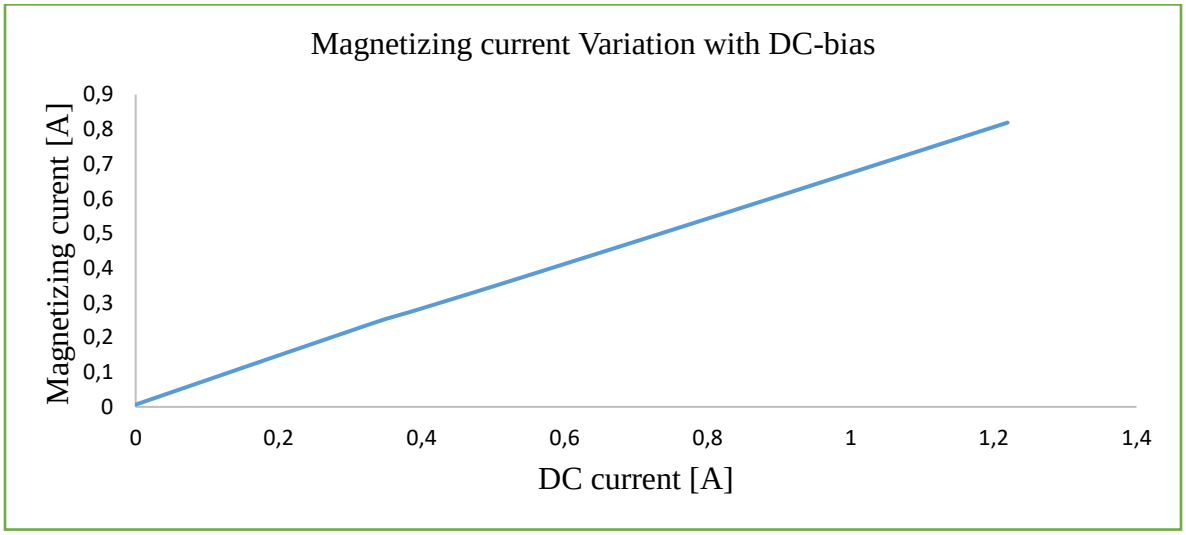


Figure B.3: Magnetizing current increase with DC bias

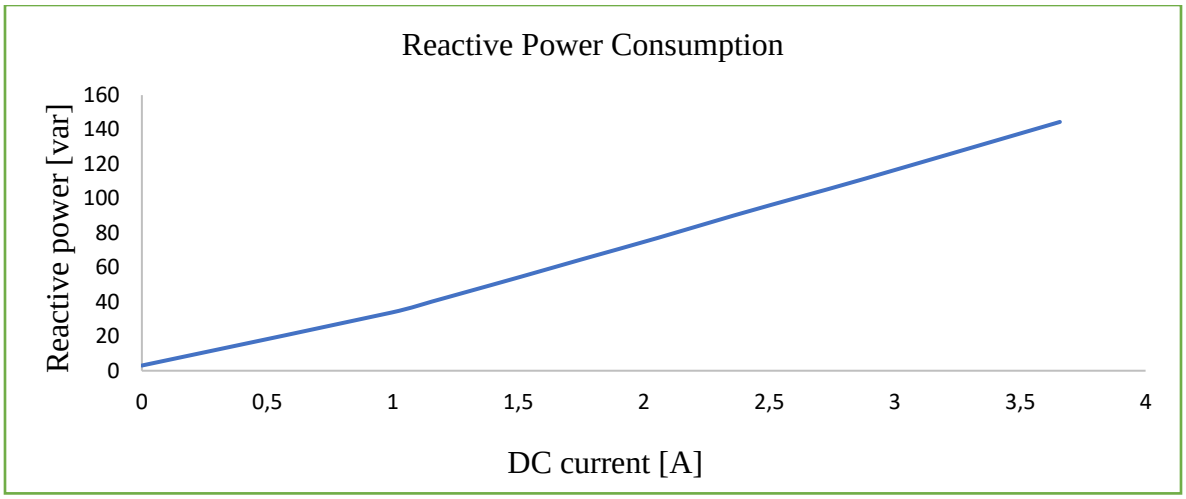


Figure B.4: Reactive power increase with DC-bias

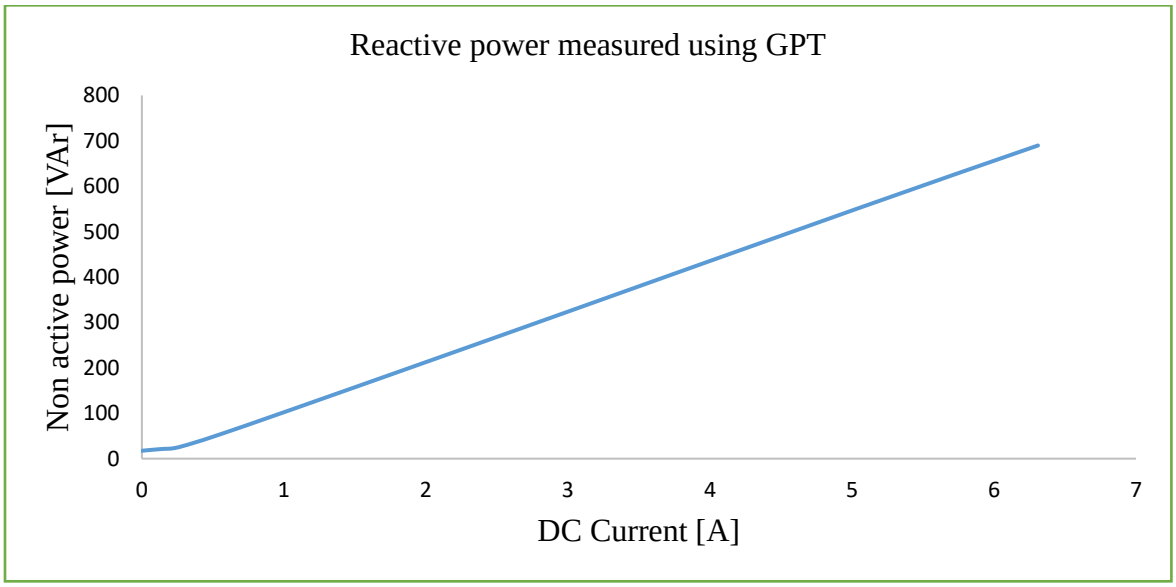


Figure B.5: Non-active power increase under DC-bias

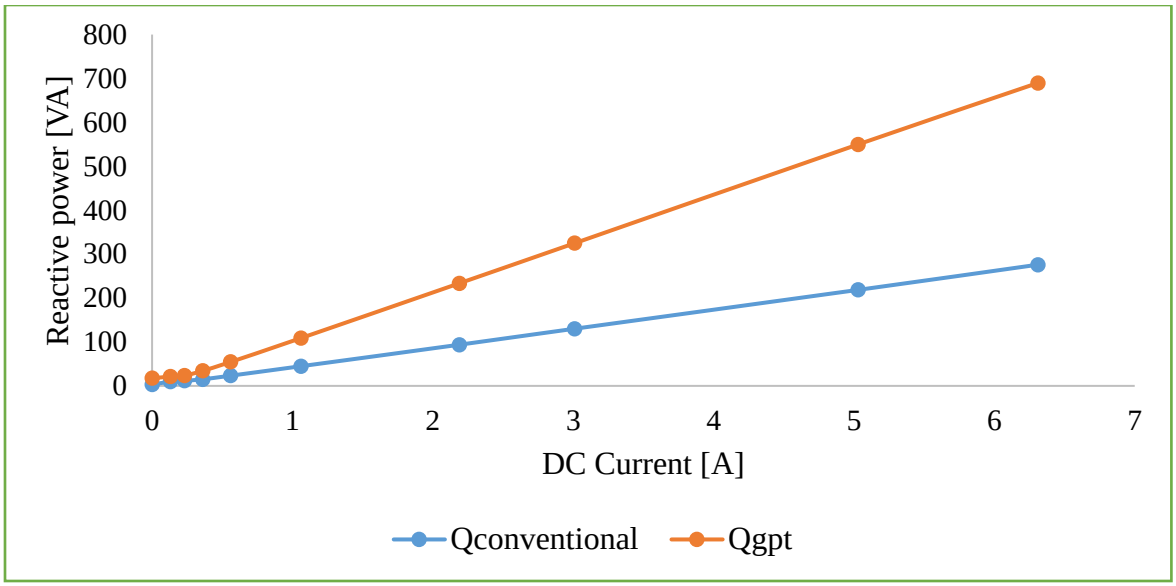


Figure B.5: Reactive power comparison of 3p5L, 300 VA when measured conventionally (blue graph) and according to General Power Theory (brown graph).

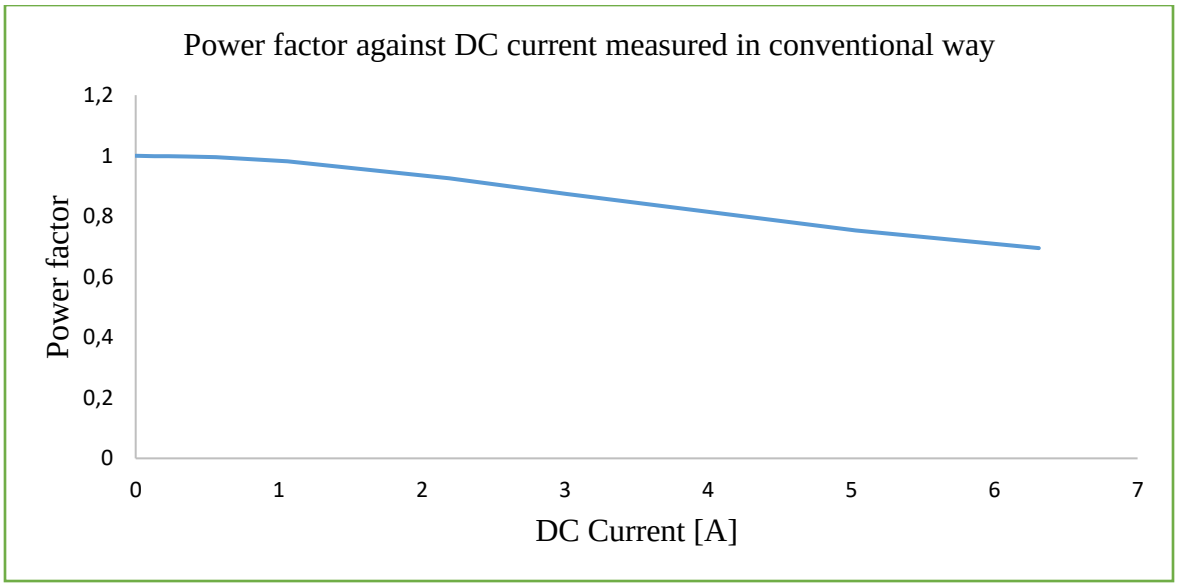


Figure B.6: Power factor measured conventionally

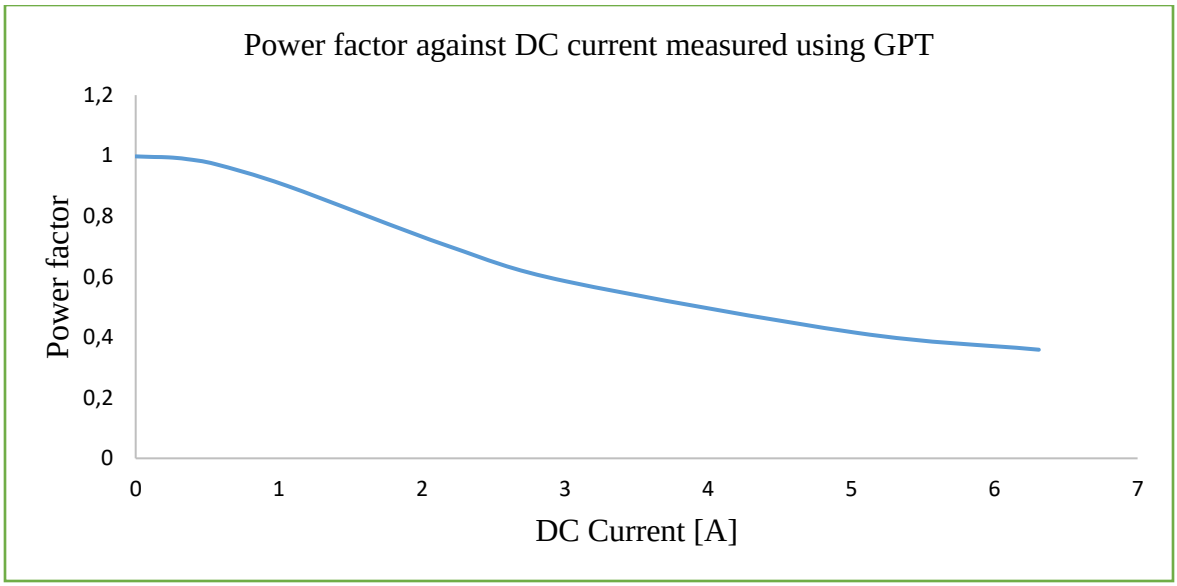


Figure B.7: Power factor measured using GPT

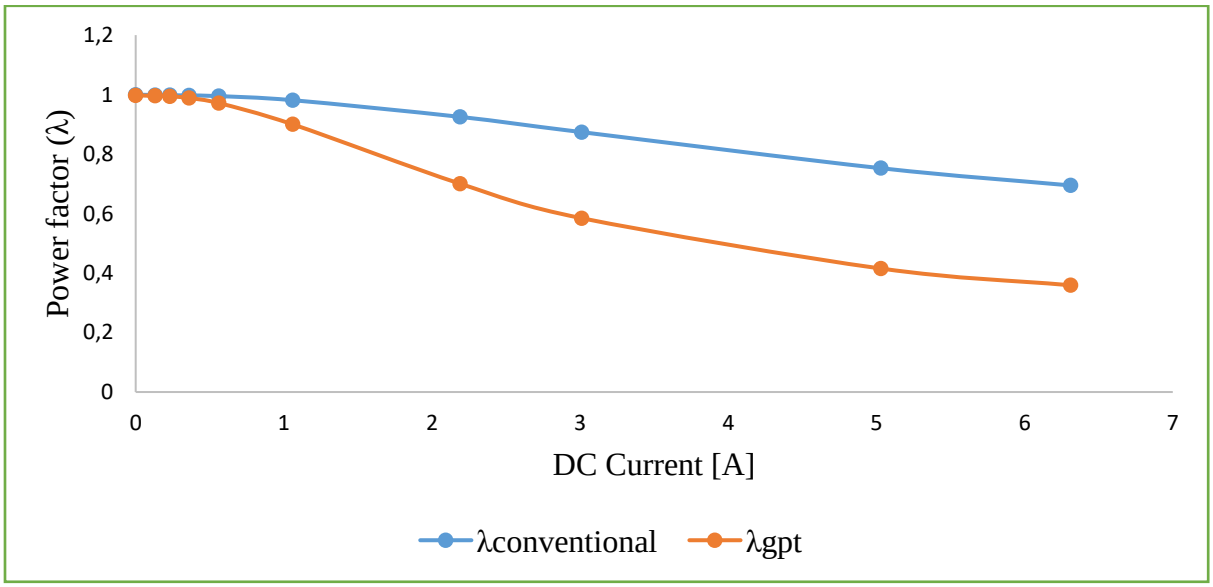


Figure B.8: Power factor comparison of 3p5L, 300 VA when measured conventionally (blue graph) and according to General Power Theory (brown graph).

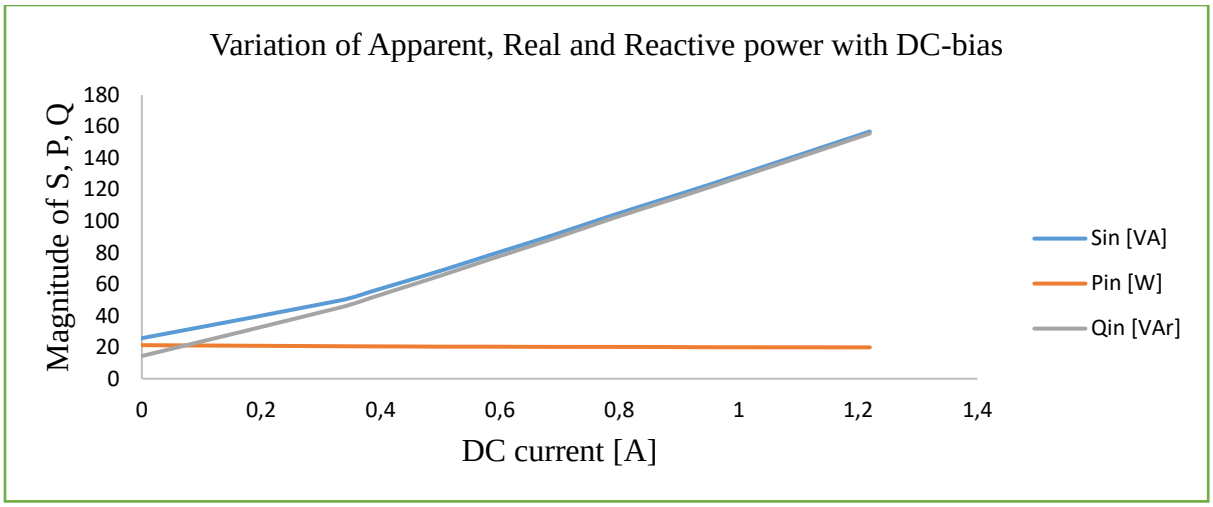


Figure B.9: S, P, Q input variation with DC-bias

## APPENDIX C: FINITE ELEMENT SIMULATION

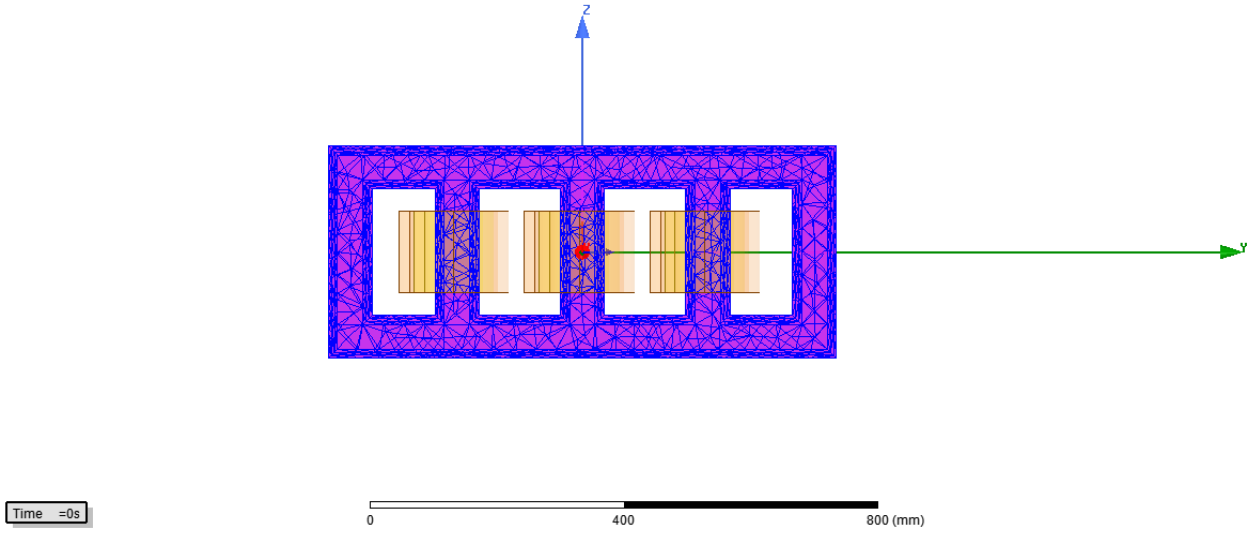


Figure C.1: 3p5L meshing

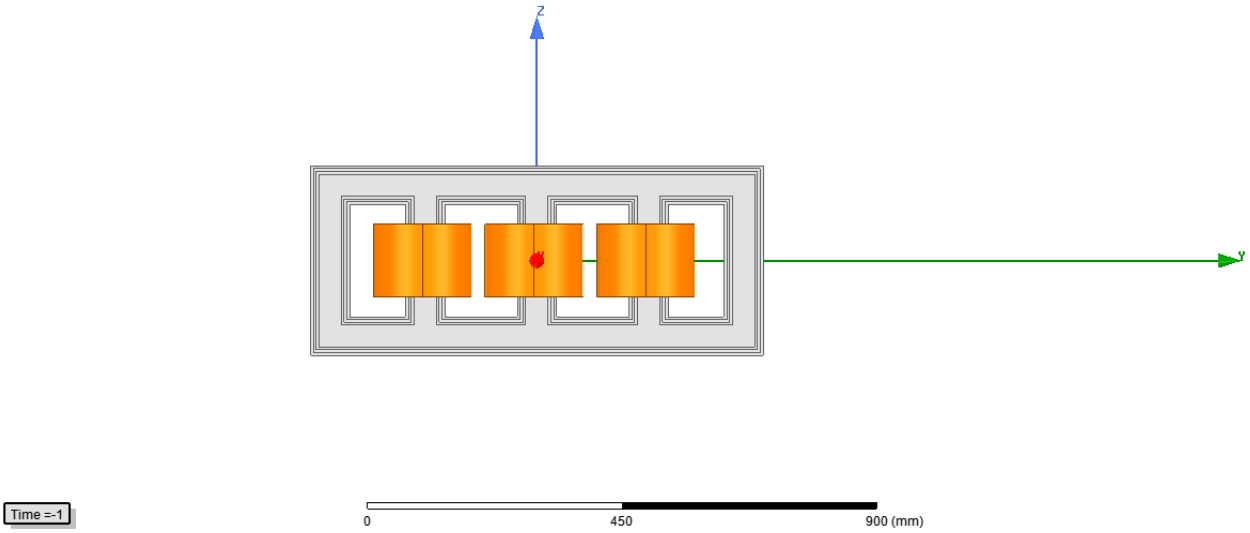


Figure C.2: Front view of 3D model

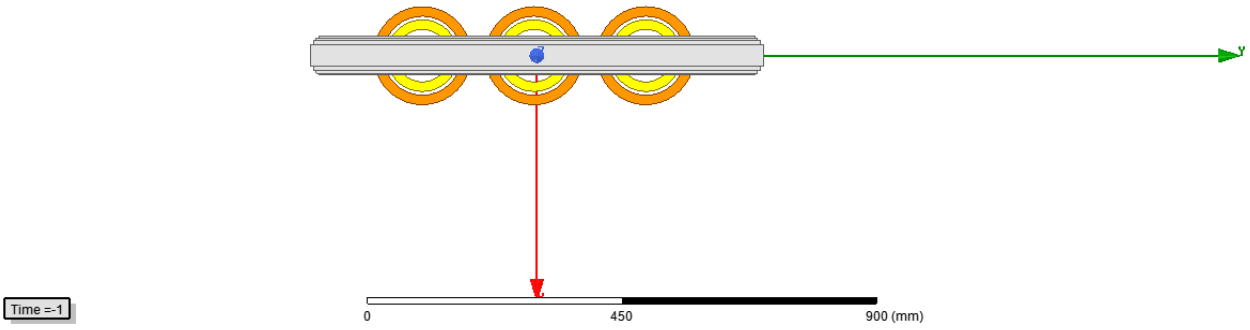


Figure C.3: Plan view of the 3D model

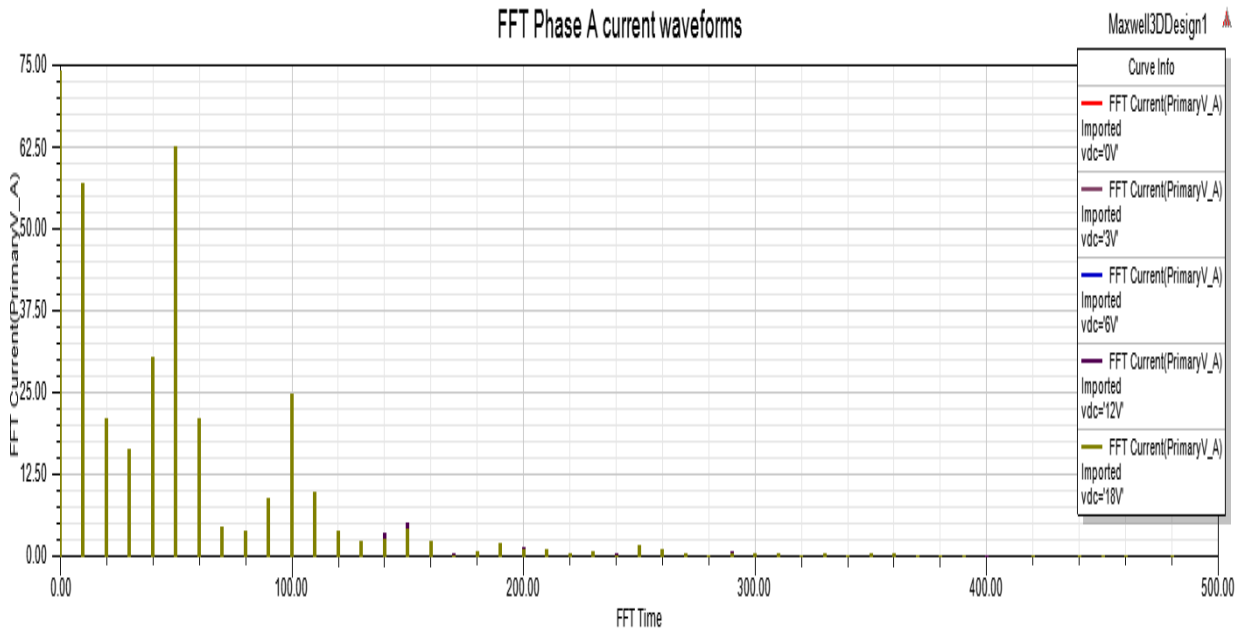


Figure C.4: Current harmonics in phase A

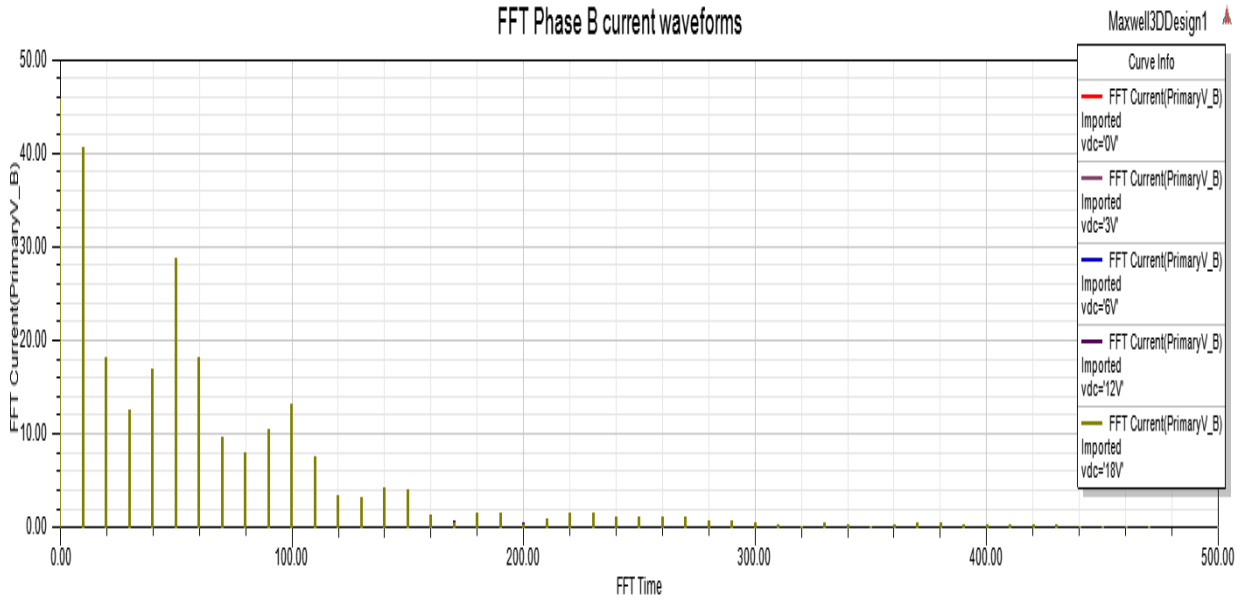


Figure C.5: Current harmonics in phase B

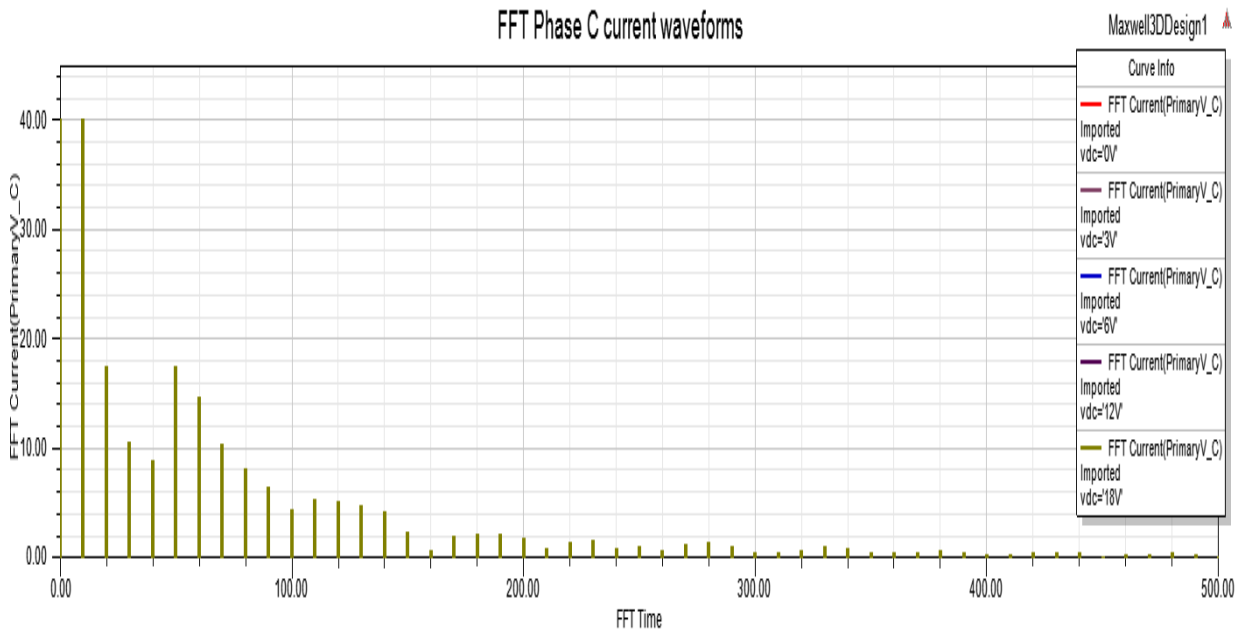


Figure C.6: Current harmonics in phase C